Journal of
Water Resource
and Protection

Editor-in-Chief : Jian Shen

Scientific
Research

❖❖ Scientific Research

TABLE OF CONTENTS

Volume 1 Number 4   **October 2009**

Journal of Water Resource and Protection (JWARP)

Journal Information

SUBSCRIPTIONS

SERVICES

COPYRIGHT

PRODUCTION INFORMATION

◆◆ Scientific
◆◆ Research

Using MODIS Images and TRMM Data to Correlate Rainfall Peaks and Water Discharges from the Lebanese Coastal Rivers

Amin SHABAN[1], Crodula ROBINSON[2], Farouk EL-BAZ[3]

[1]*CRS, National Council for Scientific Research, P. O. Box 11-8281, Beirut, Lebanon*
[2]*SPCS, Department of Earth and Environmental Sciences, Northeastern University, MA, USA*
[3]*Center for Remote Sensing, Boston University, 685 Commonwealth Avenue, Boston, MA. USA*
E-mail: geoamin@gmail.com
Received June 8, 2009; revised July 22, 2009; accepted July 31, 2009

Abstract

Water flows from rivers into the sea (plumes) is a common phenomenon in many coastal zones. The hydrologic behavior of plumes differs from one river to another depending on rainfall rate and intensity, as well as it is influenced by the hydrologic characteristics of river basin. In order to investigate the precipitation regime in a drainage basin versus the flow into the sea, sequential data must be available. Remotely sensed data can fulfill this scope, thus it can provide climatic and hydrologic data. The scope of this study is to monitor the behavior of water input in the catchments versus the output from rivers in the Lebanese coastal zone using remote sensing data. For this purpose, TRMM (Tropical Rainfall Mapping Mission) data and MODIS satellite images were used. Hence, rainfall data from TRMM was compared with the areal extent of water plumes from rivers. This enables establishing interpolation between water input/output for each river basin. In addition, the lag time and residence time of plumes into the sea can be measured and compared between the issuing rivers. The extracted data from remote sensing was compared with terrain measures and shows its reliability and accordance. The used approach proved to be creditable, non-invasive and cost effective and can be applied to other costal river basins.

Keywords: Plume, Rainfall, MODIS Image, Coastal Rivers, Lebanon

1. Introduction

Water runoff into the sea has been received substantial attention in several coastal zones worldwide, in time many of these zones experience water shortage. This is well pronounced in arid and semi-arid regions, like the case of the Middle East.

The Eastern Mediterranean is typical example for this the hydrologic phenomenon. Hence, studies carried out in this regard include the coast of Lebanon, Arabian Sea and the Arabian Gulf [1–9] The discharged freshwater into the sea occurs either as direct surface runoff (i.e., from rivers and streams), or as groundwater discharge, which is commonly called "submarine springs " and sometime as "invisible rivers".

In Lebanon, high precipitation rate (i.e., averaging 950-1100 mm) results large amounts of surface water that rapidly flows towards the sea due to steep terrain.

Also, there is groundwater seeps from coastal aquifers to the sea along the bedding planes of rocks, which encompass often with acute dip. Additionally, the intensive fracture systems increase the flow regime of groundwater seaward.

The coastal zone of Lebanon (33° 03′ 17"; 34° 40′ 00" N, and 35° 06′ 11"; 36° 19′ 16" E) is mountainous, with narrow coastal plain (<5km). It has an area of about 5000 km^2. The width of this area is less than 50km and extends from the sea to mountain crests to the east. The length of the area is about 225 km (Figure 1).

The area of concern is a good example for surface and subsurface water flow to the sea, which is considered as losses. There are many studies in Lebanon tackled this hydrologic phenomenon. Many of these studies have been performed to identify the sources of groundwater discharges in the sea, such as those by [1,2], [10–13] and [8]. Besides, studies to utilize rivers water and their

quantitative assessment are negligible, which is often attributed mainly to the lack of data.

In Lebanon, there are fourteen major rivers. Three of them are inner ones and originate from the Bekaa plain (i.e. a depression located between the major two mountain chains of Lebanon). The coastal rivers flow directly to the Mediterranean Sea. One of the inner rivers (the Litani River), is originates from the plain and flow southward, then diverts to the west where it also outlets in the sea (Figure 1); therefore, it was not included in this study because the threshold of its basin located outside of the study area. Also, El-Kabir River, which is a coastal one in the north, was not involved in this study, since the large part of its basin is located in Syria.

According to the available hydrologic records, the maximum reported average discharge from the Lebanese coastal rivers is approximately 408 million m^3/year,

which in Ibrahim River and the minimum discharge is 55 million m^3/year in Siniq River [14]. The large variance in discharge between these rivers is not related to the catchment area or to the river's length, etc. [15].

In the study area, the largest catchment is 480 km^2 for Abou Ali River [16], with an average discharge of about 269 million m^3/year. The hydrologic characteristic differs from one river to another. This is obvious in the drainage density, relief gradient, meandering ratio and width/length ratio [9]. It can be attributed to the existence of different rock lithologies and intensive structures (e.g. faults and fractures).

Filed observations and available data from rainfall records show direct relationship between rainfall intensity and flow regime of surface runoff to the sea (i.e., plumes), but the mechanism and dynamics of flow are still undefined.
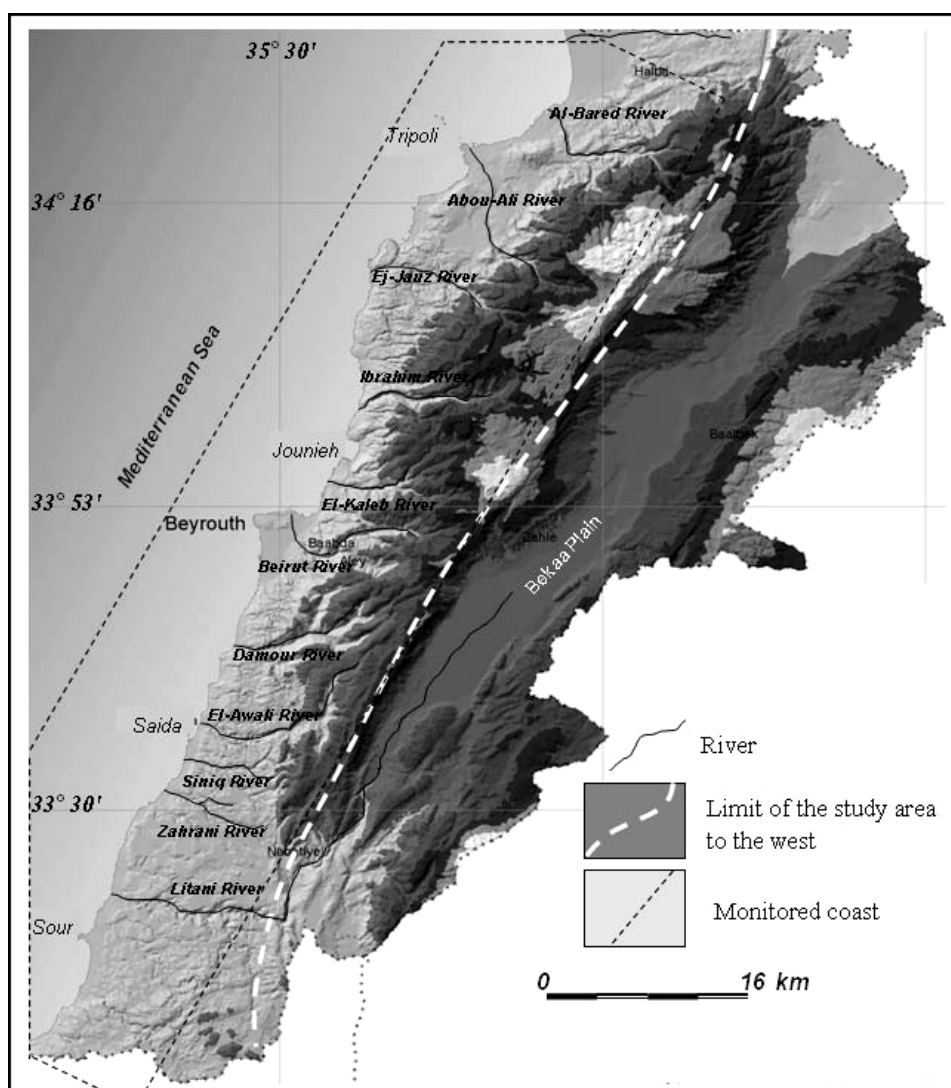

Figure 1. Location map of the study area

In Lebanon, most instruments used to measure rivers discharge (i.e. hydrographs and flow-meters) were destroyed during the past three decades, and only a limited number of them remains operational. This decreases the availability of data, notably in a sequential time series. Therefore, the use of remote sensing techniques, combined with field surveys, could compensate the lack of data and fill gaps in hydrologic and climatic records, like the case in the area of concern.

In this study, two types of remotely sensed data were utilized. The first is the TRMM (Tropical Rainfall Mapping Mission) data, which illustrates rainfall amounts and peaks. The second one is the satellite images of MODIS-Terra, which enable detecting sea surface temperature, thus observing the areal extent of water plumes from rivers, and consequently estimating the volume of discharged water in the sea.

The main objective of this study is to use remote sensing data as a monitoring system between rainfall and water flow from rivers, thus applying comparative analyses for each river basin separately. Also, assuring the creditability of remotely sensed data as a supporting tool to ground measuring stations. It is a cost-effective approach to monitor and assess the hydrologic regime of rivers and the relation to their basins. Also, it interprets a number of hydrologic criteria, such as the existing of small-scale plumes (i.e. low discharge) from river basins with high rainfall and vise versa. The used approach also reflects the hydrologic characteristics of basin terrain.

2. Method and Data Sources

The main implication of this research is a monitoring approach of water flow from rivers versus rainfall peaks. Fresh water flow in the sea can be monitored using thermal data from MODIS-Terra images. These images are acquired on daily basis. While, sequential series of rainfall data are also available from TRMM data daily. In this study, data comparison was carried out for the period from January 2002 till February 2003, in total 396 days. The selection of this year based on the availability of ground measures from gauge stations and flow-meters. This enables obtaining comparison between data from remote sensing and ground data.

The emphasis was on rainfall peaks, after which monitoring the areal extent of water flow in the sea (plumes) starts for each river basin. With this premise, the time period between the date of rainfall peak and the appearance of water plumes in the sea (i.e. lag time) was calculated, as well as the residence time of the plume in the sea (i.e., time the plume remains on sea surface). This allows assessing of the hydrologic dynamics of flowing water and the terrain characteristics

for each basin that captures rainfall water and diverts it seaward.

2.1. TRMM Data

Operational meteorological stations in Lebanon are insufficient, and in some regions rare. In addition, the existing stations are not evenly distributed and are not closely spaced to present a comprehensive figure on rainfall.

In this study, a continuous rainfall record was adopted from TRMM rainfall data. TRMM is a joint mission between NASA and the Japan Aerospace Exploration Agency (JAXA) and was primarily designed to study and monitor tropical rainfall. This data is acquired globally, and is free of charge. It can be retrieved either as graphic illustrations/ or as contour maps for any area worldwide and to any selected time interval.

Also, in this study the creditability of TRMM data was investigated by comparing it with the available data from ground stations. Thus, it was indicated that the daily rainfall records from TRMM were almost coincident with the available records, and thus suitable to be used for the purpose of rainfall monitoring for each river basin independently.

2.2. MODIS-Terra Data

Thermal satellite images were used in this study to observe the water flow from rivers in the sea (plumes). It is mainly a process to monitor the time of water occurrence and its geographic distribution in the sea. The concept of plume identification based on measuring sea surface temperature (SST). Thus, freshwater is often cooler than saltwater, and this enables applying thermal differentiation between them by using thermal bands in MODIS images.

MODIS-Terra satellite images are useful in this regard, since they are retrieved two times a day, and can facilitate sequential monitoring of water flow. The selection of the images based on their coincidence time with the available records of rainfall peaks observed in the TRMM data.

In this study, day and night time Level 2 11μm MODIS-Terra images were retrieved from the *Goddard Space Flight Center* "DISC" website, which is also introduced by NASA. The spatial resolution of the used images is 250m, which is adequate for the purpose of this study. Images were downloaded for the period from January 2002 to February 2003 (~ one-year time interval). However, not all retrieved images were suitable for analysis, because of clouds masking, missing data in some instances, or due to other irregularities, such a stretching (Figure 2).

A. SHABAN   *ET   AL.*
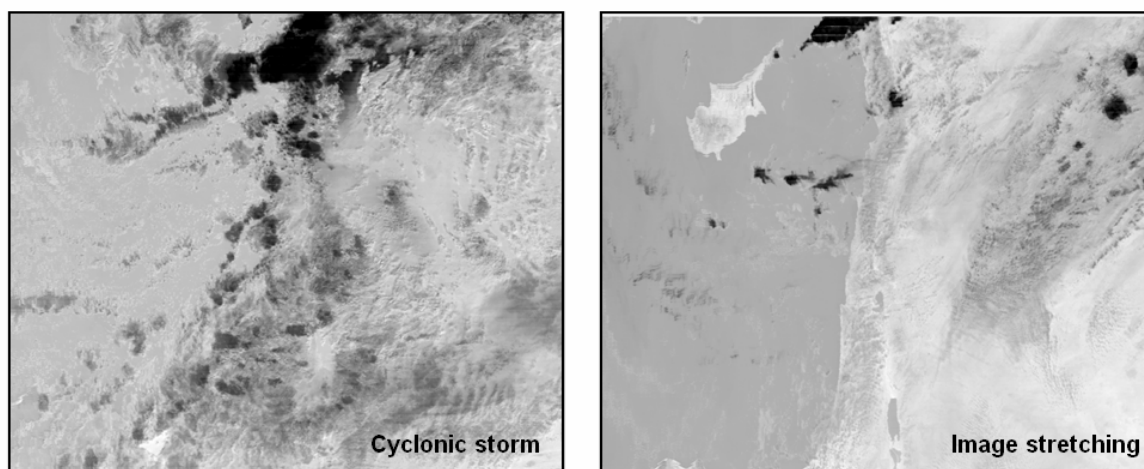
Figure 2. Two thermal MODIS images. The left one is not suitable for analysis because of extensive cloud cover, compared with the right one.

All selected images required geo-referencing procedures. Geo-referencing is needed to co-register the images; store them in a GIS database; and enable the geolocation of satellite observations in the sea and on land. This was performed using PCI's Geomatica GCPworks software, thus applying the UTM coordinate system and WGS84 datum. To attain clear observation, the advantage of digital enhancement was applied on the used images. The ENVI (Environment for Visualization Images) software was used for image processing.

The temperature difference between river water and seawater can be measured directly from MODIS image by selecting any point of interest in the sea. However, the resulting value from the image is primarily inaccurate and needed to be converted to the real temperature value.

A scaling/conversion algorithm is applied using the band math option, in order to map the "*real*" temperature in degrees Celsius. The scaling conversion equation is:

$$Scale\ type = "Y= Slope * X + Intercept";$$
$$Slope = 0.0099999998; Intercept = -300\ f;$$
$$Y\ (in\ Deg\ C) = 0.01\ times\ X\text{-}300$$

The difference in temperature between cooler freshwater plumes and the ambient temperature of seawater is called "*thermal anomaly*". In order to identify thermal anomalies on the images, a number of digital and optical advantages must be applied, such as density slices, enhancement, stretching, color scaling, etc. Figure 3 shows an example of thermal anomalies with temperature differences.
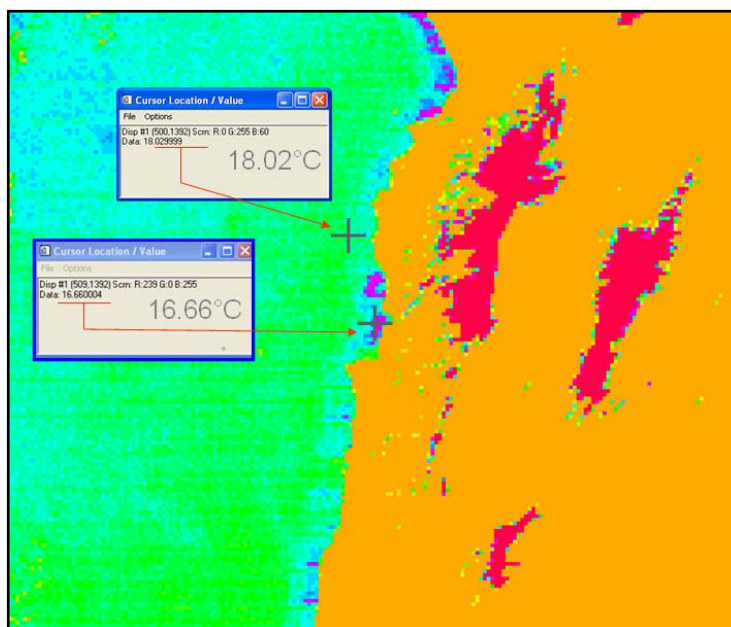
Figure 3. Density sliced MODIS images showing different temperature levels and cool freshwater plumes.

Copyright © 2009 SciRes.

The temperature difference along the investigated coast is often found to range between 2 and 4 Celsius, and varies slightly with the climatic conditions. The abrupt change in temperature indicates high-energy of water flow from rivers in the sea that allows no enough time for mixing seawater and freshwater.

Accordingly, the Lebanese coastal zone encompasses a number of groundwater discharges (submarine springs) [8]; however, these discharges were eliminated in this study in order to focus only on water plumes from occurred from rivers. This was done through the application of Geographical Information System (GIS) techniques. In this case, processed satellite images were overlain on topographic maps to show the exact geographic location of the outlets of river into the sea. Hence, only thermal plumes correspond with river outlets were considered.

2.3. Rainfall/Water Flow Responses

TRMM and MODIS data were prepared and the obtained results were tabulated for the selected period. This was a perquisite step for data correlations to assess the rainfall/water-flow relationship, the scope of this study. Consequently, a number of hydrologic relations were obtained as shown in Figure 4.

As a first step, the amount of rainfall as extracted from TRMM data was measured in millimeters (mm), and then it was multiplied by the area of the catchment (i.e., km^2) to convert it to million m^3 per day. The extent of water plumes into the sea was measured in km^2. Units were standardized for all calculations.

This was applied to all studied rivers for the selected period.

Five key elements were utilized for quantitative analysis (Figure 4; Tables 1 and 2). These are:

1) Rainfall peaks, which represent torrential rain events and intensity and their behavior (i.e. ascending or descending trends),

2) The coincidence between the plume area (*PA*) and recorded rivers discharge from gauging stations (*Qm*). It can be obtained by interpolating both parameters, and this enables recognizing rivers discharge from the areal extent of the plume as it appears in satellite image,

3) Lag time (τ) between precipitated water and the existence of water plumes into the sea, which is indicative to several terrain parameters including mainly, recharge, geology, slope and land cover/use,

4) The spatial extent of plumes into the sea (*PA*) after each rainfall peak, and this is related to water flow energy as well as the terrain parameters mentioned in point 3,

5) The ratio between the area of plumes with respect to the recorded discharge (*Rpd*).

3. Results

In coastal zone of Lebanon, rivers discharge varies according to the terrain characteristics of the corresponding basins, particularly the rainfall; geology and land cover use and water exploitation. For example, although the catchment area of El-Bared River is 202 km^2 and equals two times that of Zaharai River (140 km^2), yet the discharge from the Zaharai River (225 M m^3) is equals to 1.5 times that of El-Bared River (155 M m^3).
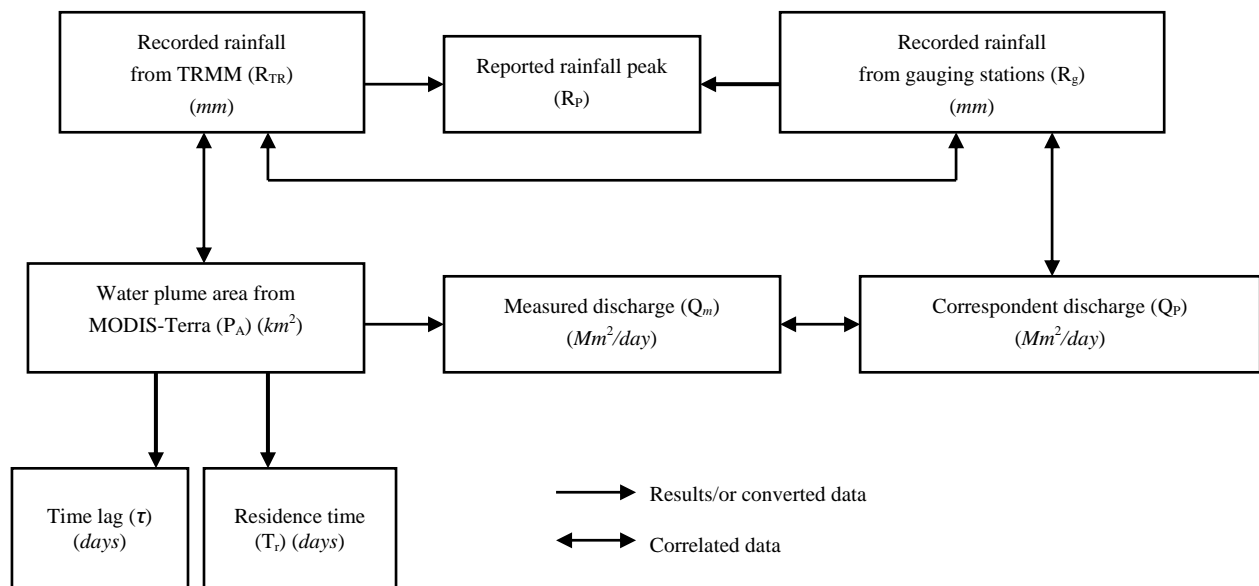
Figure 4. Schematic diagram showing the relationships of different hydrologic elements.

Therefore, monitoring the mechanism between water captured by a river basin and water discharged allows diagnosing the hydrologic behavior and even the anthropogenic activity for each basin. The availability of hydrologic and climatic records in combination with remotely sensed data gives a chance to obtain a monitoring approach. This can be easily done since the TRMM data provides daily information on rainfall, and also MODIS-Terra data provides daily images of the existing plumes in the sea. Hence, the use of TRMM and MODIS-Terra data, enables establishing a number of hydrologic relationships by the integration of different hydrologic elements (i.e., *rainfall peaks, PA, Qm, τ* and *Rpd*). The relationships might exist between two or more of these elements as illustrated in Figure 4.

As an example, Table 1 illustrates the calculation that carried out for the Abu Ali River (Figure 1). It shows that plumes appear in the Sea 3-4 days after a rainfall event takes place. These plumes were only visible for one day before disappear, as observed in 250m spatial resolution MODIS images. This timing of events varies in the issuing Lebanese costal rivers (Table 2), where the lag times ranges between 1 and 4 days, and residence times between 3 and 8 days.

3.1. Rainfall Gauges (R_g) and TRMM Data (R_{Tr})

Several worldwide studies have used TRMM data as a reliable source of rainfall information (examples are: [16,17]). In this study, rainfall records from available gauging stations were compared with TRMM data as an verifying approach for TRMM data (Table 2). Thus, both almost show similar results in a clear coincidence in the trend of rainfall amounts (i.e., ascending and descending), though the recorded amounts of rainfall from gauging station were found to be a little bit exceeded (example in Figure 5).

In average, the ratio of TRMM values for all rivers to the recorded data is 1:1.35 (Table 2). This often exists with peaks (main rainfall events). The lower values of rainfall appears in TRMM data is attributed to a distortion in the satellite images that may might occur during torrential events, thus creates error in data simulation. In general, the use of TRMM data is a capable tool to acquire rainfall information, notably in a time ground data is lacking.

Table 1. Example of datasets that are available for the Abou Ali River as recorded from field gauges, and TRMM and MODIS-Terra data. It shows plumes appear approximately 3-4 days after a rain event and are only visible for 1 day at 250m spatial resolution.

Abou Ali River-2002									
Date	**Rainfall TRMM**	**Rainfall gauges**	**Average rainfall**	**Ratio gauges /TRMM**	**Extent of plumes**	**River discharge**	**Ration discharge /Plume extent**	**Lag time**	**Residence time**
	R_{TR}	R_g	$R_g + R_{TR/2}$	R_g/R_{TR}	P_A	Q_m	Q_m/P_A	τ	T_r
	(mm)	*(mm)*	*(mm)*	*Ratio*	*(km²)*	*(Mm³/day)*	*Ratio*	*(days)*	*(days)*
Feb., 9	0.2	0	0.1	-	0.172	0.618	3.59		
Feb.10	1	1.6	1.3	1.60	0.169	0.625	3.69		
Feb.11	8	11.4	➡9.7	1.42	0.168	0.641	3.81		
Feb.12	0.5	1.43	0.96	2.86	0.166	0.623	3.75		
Feb.13	0	0	0	-	0.179	0.785	4.38		
Feb.14	0.9	0	0.45	-	0.488	0.853	1.74	↪4	*
Feb.15	0.4	0.7	0.65	1.75	1.217	1.034	0.89		*
Feb.16	0.3	0.7	0.5	2.33	1.531	1.132	0.74		*
Feb.17	0	0	0	-	1.552	1.214	0.78		*
Feb.18	0	0	0	-	1.435	1.201	0.84		
Feb.19	0.8	0	0.4	-	1.462	1.179	0.80		
Feb.20	0	0.4	0.2	-	1.368	1.094	0.79		
Feb.21	4	6.3	5.15	1.57	1.325	0.972	0.73		
Feb.22	0.4	0.9	0.65	2.25	1.226	0.946	0.77		
Feb.23	6.8	10.54	➡8.67	1.55	1.046	0.901	0.86		
Feb.24	0.7	2.1	1.4	3.00	1.033	0.894	0.78		
Feb.25	2.1	4.3	3.2	2.04	1.152	0.937	0.81	↪3	*
Feb.26	2.7	4.8	3.75	1.77	1.167	0.942	0.80		*
Feb.27	0.4	1.05	0.725	2.62	1.175	0.857	0.77		*
Feb.28	0.6	0.4	0.5	0.66	1.181	0.832	0.87		*
March 1	0.1	0.2	0.15	2.00	1.164	0.794	0.68		
March 2	0.1	0.3	0.2	3.00	1.169	0.758	0.65		

➡*Rainfall peak,* ↪*Lag time,* **Residence time*

Table 2. Major hydrologic components as obtained from TRMM, MODIS-Terra and field data for all 10 rivers investigated in this research.

Rivers Watershed	Rainfall TRMM R_{TR} (Mm³/year)	Rainfall gauges R_g (Mm³/year)	Ration rainfall/ TRMM R_g/R_{TR} Ratio	Extent of plume P_A Km²	River discharge (plumes) $Q»P_A$ (Mm³/year)	River discharge Q_m (Mm³/year)	Ration discharge/ plume extent Q_m/P_A Ratio	Lag time *Average* τ (days)	Residence time *Average* T_r (days)
Al-Bared	134	233	1.74	2.25	1.74	147	135	0.92	4
Abou-Ali	453	482	1.06	4.10	1.06	246	269	1.09	3
El-Jauz	111	120	1.08	1.75	1.08	101	85	0.84	4
Ibrahim	342	381	1.11	7.75	1.11	572	408	0.71	1
El-Kalb	226	348	1.54	3.55	1.54	258	191	0.74	2
Beirut	219	248	1.13	2.40	1.13	146	111	0.76	2
Damour	289	337	1.67	5.60	1.67	167	217	1.30	1
El-Awali	267	312	1.17	6.15	1.17	203	261	1.28	1
Siniq	58	101	1.74	1.55	1.74	61	55	0.90	3
Zahrani	103	137	1.33	1.95	1.33	254	225	0.88	3
Average	220.2	269.9	1.35	3.70	1.35	215.5	195.7	0.942	2.4
Total	2202	2699			2155	1957			

$Q » P_A$ *River discharge as indicated by the plumes dimensions*

Additionally, TRMM has been commonly used a data source, and utilized by many studies to support the ground recorded from gauging station [15,18]. The lack of sufficient gauging stations and the non-uniform geographic distribution is a major problem in data accuracy. Also, rainfall stations receive the amount of water that fall directly on the gauges, while TRMM estimates a comprehensive spatial cover. For this reason, in this study the average value was considered from both sources (Table 1).

3.2. Plumes Area (P_A) and Rivers Discharge (Q_m)

During dry seasons, water flow from rivers becomes low; consequently water plumes can not be well noticed due to their small-scale area. However, in normal climatic conditions, the flow the discharging from rivers become regular and this in turn gives enough time to the mixing between fresh and saltwater, hence water plumes are obviously seen. Therefore, the best observable plumes can be detected in regular conditions after rainfall slow-down. In this respect, some plumes along the Lebanese coast exceed an area of about 10km², like the case of Ibrahim River.

Normally, the areal extent of a plume on sea surface has a direct proportion with rivers discharge. Thus, the spatial extent of a plume, as well as the time it needs to exist on sea surface differs from one river to another
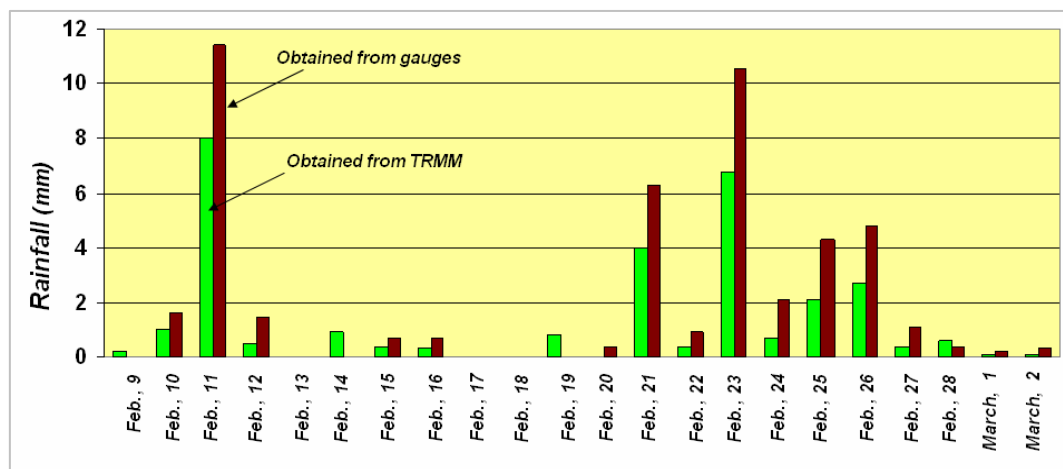

Figure 5. Example showing a comparison between ground rainfall data and TRMM-derived rainfall data for Abou Ali River. Both data follow the same rend (ascending & descending), but ground data (brown columns) show high values than TRMM Data (green columns).

depending on its flow regime. In this regard, interpolation approach was applied between plums area and rivers discharges. The resulting average ratio was found as 3:2. In other words, each one million m^3 of discharge is represented by approximately 1.5 km^2 of water plume on sea surface.

Figure 6 shows an example for this relationship, which was applied to Abou Ali River and for a selected period in the year 2002. The trend coincidence is obvious between the two measures, as well as the range in variance is often small and ranges between 0.1 and 0.4 as shown in the example (Figure 6). However, this variance is found to be larger in the rivers that located in the middle part of the region (from Ibrahim to El-Awali). This is attributed mainly to the higher altitudes of these river basins (>2500m), which results high precipitation rate and the dominant steep slopes.

3.3. Lag time (τ) and Residence Time (Tr)

As observed on TRMM data, after each rain event the time needed for a plume to appear on sea surface, i.e. lag time component (τ) could be estimated from MODIS image (example in Figure 7). The lag time (or *flushing time* as noted by Sheldon [19] is a function, in addition to rainfall intensity, of the catchment and river hydrologic characteristics. Nelson [20] stated that lag time depends on the amount of time over which the rain falls and the amount of infiltration and interception that takes place along the path to a stream. Thus, he concluded that:

  - If the amount of rain is high over a short time period, lag time is short.
  - If the amount of rain is high over a longer time period, lag time is longer.
  - Lack of infiltration and interception reduce lag time.

In the study area, the lag time is characterized by big variance between different issuing rivers as a reflection of the diversity in the basin and river hydrologic characteristics. It ranges between 1 to 4 days, with an average of 2.5, which is short due to the small area of the located basins in coastal Lebanon (<500 km^2).

Moreover, the located middle basins and their rivers show shorter lag time as a result of the steep slope (75-100 m/km). Of course, this was estimated to rainfall peaks occurred after a dry time. Whilst, if there are two close rainfall peaks, the lag time for the second one will be shorter and may reach few hours after the rain peak (example in Figure 7).

Accordingly, the residence time (*Tr*) is another hydrologic pillar that can be obtained from remote sensing. It represents the time that the plume remains in its maximum size on sea surface (example in Table1). However, some authors tackles this terminology for the average time the initially existing water parcels reside in the system before they are flushed out [21]. Residence time indicates the continuity of water flow, as well as the uniformity in drainage density within the catchment area [9].

For the Lebanese coastal rivers, the residence time of fresh water in the sea ranges between 1 to 4 days, and with an average of 2.4 days, as observed in the year 2002 (Table 2). The variation in mixing time is likely attributable to the influence of several factors, notably the physical contact between land and ocean [22]. In other words, the wideness of the continental shelf, depth of submarine canyons next to the river mouths and direction and energy of sea current, all influence the behavior of a plume. Accordingly, the Lebanese coastline is linear and measures approximately 225km long, with narrow continental shelf between 2 to 3 km, and a dominant current direction from south to north.
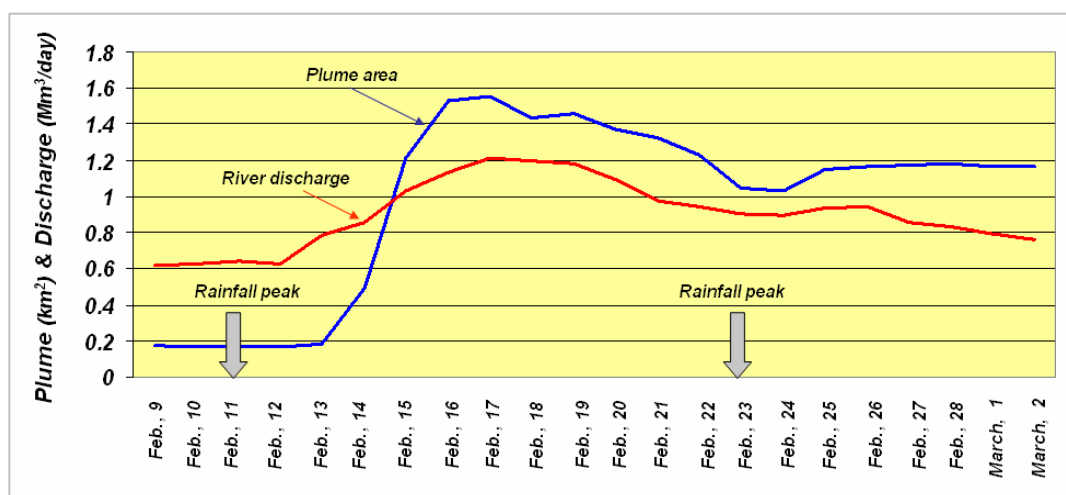
Figure 6. Comparison of plume area and water discharge for Abou Ali River. It shows the river's discharge is about 2:1, that is, 2 km^2 of water plume area.
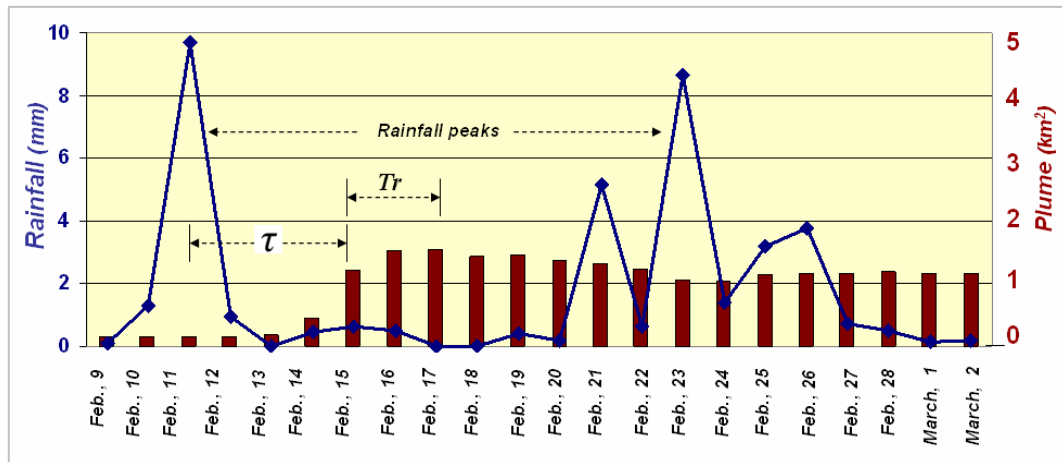
Figure 7. Example showing the lag and the residence time of plumes and rainfall peaks for Abou Ali River.

4. Conclusion

Recently, remote sensing techniques have been utilized in many scientific disciplines. In hydrological studies, sometime data availability controls the approaches to be used. In a broad sense, the topic of this study requires two major measures. These are: rainfall records and behavior; and the discharge from rivers to the sea.

Remotely sensed data is can provide information for the two measures; therefore, MODIS-Terra and TRMM data, with their short retrieve time (daily) permit establishing a monitoring approach between both. This approach, if more improved, can replace ground instrumental techniques. In addition, it is characterized by low cost and can be achieved in a short time.

The coastal zone of Lebanon is typical area for such application, because it encompasses a number of issuing rivers and a variety of climatic conditions, meanwhile gauging stations and hydrographs are lacking/or insufficient. Rainfall in this zone is characterized by high frequency of peaks, and high rate. Therefore, surface flow regime (run-off) and infiltration of water into rocks must be understood.

In the study area, the steep sloping terrain (75-100 m/km) as well as the short the rivers length (almost < 50km) create high flow energy of water towards the sea, which is often less than 5 hours. This is reflected with low value of lag time (average τ=2.4 days). The high flow energy of running water from the coastal rivers is tempered by the existing fracture systems and karstic conduits, as well as the high meandering ratio of river courses. The huge loss of freshwater from rivers in the existing hydrologic regime, suggests proposing urgent implements for surface water harvesting in the region, and this can be implemented to all rivers tributaries in the coastal zone of Lebanon.

Based on the applied method in this study, which proved the reliability of remote sensing data and its powerful in the assessment of rivers hydrology, it is prudent to apply this method to all rivers in Lebanon separately and in details considering all influencing factors in rivers discharge. It can be modified to be as a monitoring system that could provide information to a strategic water management system in their pursuits.

5. Acknowledgement

6. References

[1]   R. El-Qareh, "The submarine springs of Chekka: Exploitation of a confined aquifer discharging in the sea," Unpublished M. Sc. Thesis, American University of Beirut, Geology Department, pp. 80, 1967.

[2]   FAO, "Projet de développement hydro-agricole du Sud du Liban: Thermométrie aéroportée par Infra-Rouge," Programme des Nations Unies pour le Développement, HG, 110, pp. 15, 1973.

[3]   S. Gomis, "Evaluating the potential of locating submarine springs in the Gulf of Oman using Landsat Thematic Mapper data," Master's thesis, Boston University, pp. 47, 1996.

[4]   C. Travaglia, and O. Ammar, "Groundwater exploration by satellite remote sensing in the Syrain Arab Republic," Technical Report, FAO. TCP/SYR/6611, pp. 33, 1998.

[5]   K. Brink, R. Arnone, P. Coble, C. Flagg, B. Jones, J.

kindle, C. Lee, D. Phinney, M. Wood, C. Yentsch and D. Young, "Monsoons boost biological productivity in Arabian Sea," EOS. Vol. 79, NO. 13, pp. 233–253. 1998.

[6] W. Fielding and F. El-Baz, "Linear thermal anomaly offshore from Wadi Dayqah: A probable ground water seep along fracture zones," International Conference on the Geology of Oman, 12−16 January 2001, Sultan Qaboos University, Muscat, Oman, Abstract 1, pp. 33, 2001.

[7] C. Robinson, A. Buynevich, F. El-Baz and A. Shaban, "Integrative remote sensing techniques to detect coastal fresh-water seeps," Geological Society of America, Annual Meeting, Salt Lake City, Utah., pp. 16–19. October, 2005.

[8] A. Shaban, M. Khawlie, C. Abdallah, and G. Faour, "Geologic controls of submarine groundwater discharge: Application of remote sensing to north Lebanon," Environmental Geology, Vol. 47, No. 4, pp. 512–522, 2005.

[9] A. Shaban, M. Khawlie, C. Abdallah and M. Awad, Hydrological and watershed characteristics of the El-Kabir River, North Lebanon, Lakes and Reservoirs: Research and Management, Vol. 10, No. 2, pp. 93–101, 2005.

[10] B. Hakim, "Contribution à la détection des sources sous-marines et littorales de la côte libanaise par thermogravimétrie infrarouge (secteur Beyrouth-Enfé)," DESS, Faculté des sciences, Montpellier, pp. 30, 1974.

[11] B. Hakim, "Recherches hydrologiques et hydrochimiques sur quelques karsts méditerranéens: Liban, Syrie et Maroc," Publications de l'Université Libanaise, Section des études géographiques, tome II, pp. 701, 1985.

[12] NCRS, "TIR survey for freshwater sources in the marine environment," National Center for Remote Sensing, Final Report, LNCSR. NCRS, pp. 103, 1999.

[13] M. Khawlie, A. Shaban, and C. Abdallah. "Evaluation of potentials of submarine springs: An unconventional groundwater source for the coastal area-Lebanon," Expert Group Meeting on: Groundwater Rehabilitation for Water Resources Protection and Conservation. ESCWA, UNEP/ ROWA, BGR, MOWE, Beirut 14–17/11/2000.

[14] LRA-Litan River Authority, Unpublished Technical Report, pp. 29, 2001.

[15] A. Shaban and C. Robinson, "A systematic approach using MODIS and TRMM data to monitor rainfall peaks versus water flow from rivers," CNRS. Regional Workshop on: Monitoring of coastal zones and legislation for the implementation of a national observatory on environment and development, pp. 24–25, May 2006.

[16] C. Scott, C. Thomas and L. Scott, "A comparison of TRMM to other basin-scale estimates of rainfall during the 1999 Hurricane Floyd flood," Natural Hazards, Accepted online, 2007.

[17] Y. Ohsaki, A. Numata, T. Higashinwaatoko, Validation of rain/no-rain discrimination in the standard TRMM data products 1B21 and 1C21, IEEE 2, pp. 875–877, 2000.

[18] M. Nirala and A. Cracknell, "The determination of the three-dimensional distribution of rain from the Tropical Rainfall Measuring Mission (TRMM) Precipitation Radar," International Journal of Remote Sensing, Vol. 23, No. 20, pp. 4263–4304, 2002.

[19] J. Sheldon and M. Alber, "A comparison of residence time calculations using simple compartment models of the Altamaha River Estuary," Georgia, Estuaries. Vol. 2, No. 6, pp. 1304–1317, 2002.

[20] N. Nelson, River Flooding, Natural Disaster course, Tulane University, EENS 204, http://www.tulane.edu/~sanelson/geol204/riverflooding.htm, 2004.

[21] W. Chi-Fang, H. Ming-His, K. Albert and K. Residence, "Time of the Danshuei River Estuary," Taiwan, Coastal and Shelf Science, Vol. 60, No. 31, pp. 381−393, Chiu, L., Serafino, G. and Terg, W. (2001) Applications of Tropical Rainfall Measuring Mission (TRMM) data. IEEE 5, pp. 2118–2120, 204.

[22] W. Washington, "The community climate system model (CCSM) to simulate climate change on Earth," The National Center for Atmospheric Research (NCAR), ISC 2003 Conference, Heidelberg, 25th June, 2003.

Scientific
Research

Modelling the Financial Value of the Maroochy River to Property Values: An Application of Neural Networks

Andrew HIGGINS[1,*], Leonie PEARSON[2], Luis LAREDO[1]

[1]*CSIRO Sustainable Ecosystems* 306 *Carmody Road, St. Lucia Queensland,* 4067, *Australia*
[2]*CSIRO Sustainable Ecosystems PO Box* 56, *Highett, VIC,* 3190, *Australia*
E-mail: {*Andrew.higgins, Leonie.pearson, Luis.laredo*}@*csiro.au*
Received June 17, 2009; *revised July* 15, 2009; *accepted September* 6, 2009

Abstract

The Maroochy River, which is located on east coast of Australia, provides a variety of uses and values to the community. Changes in structure, function and management of the river will influence the value that the community derives from it. Therefore, critical to the river's continued management is the development of policy relevant tools based on the community's value of the river. This paper focuses on estimating the financial value the local residents derive from living close to the river through investigation of changes in residential property values due to attributes of the Maroochy River. It is a complex analysis since there are several confounding geographical and property variables. Given a large and complete dataset of 28,000 properties for the Maroochy region, Artificial Neural Networks (ANN) was applied to estimate the economic value of the properties. This ANN was then able to simulate scenarios for property values with respect to changes in environmental features. It showed the Maroochy River contributed AU$900,000,000 to the unimproved capital value of the whole region, a value that could not be estimated previously, and much higher than anticipated. Calculating potential annual payments to the Shire Council through land tax analysis from these property values, provides the council with means to justify expenditure to maintain a standard of water quality and ecosystem health.

Keywords: Natural Asset, Financial Value, Neural Network

1. Introduction

Estimating the economic value of natural assets, such as river systems, has become a topic of considerable interest by local governments in recent years. It provides a means for justifying different levels of expenditure for improving ecosystem function and water quality, so that the river can continue to provide desired value to its local community. It is a very complex task estimating a financial value of a river, particularly since there are so many different types of users (e.g. residents, industry, agriculture, energy, tourism). For each user, a river can generate multiple benefits, some of which are difficult to estimate in dollar values. Also, some users have a range of direct (e.g. fishing, food, aesthetic), and indirect values (e.g. flood control) from a river. These differences suggest a wide variety of economic and social science methods would be required to estimate a 'whole' value. In this paper we focus on a single beneficiary of the river,

namely local residents. Properties in the vicinity of the river can increase due to river access for boating and water sports and scenic value. Properties backing onto a river are expected to have the highest value adding from the river due to their direct access (e.g. canal properties, riverfront restaurants/hotels).

Estimating the value of a river to properties is complex, as there are many variables to consider. There are significant differences in housing stock in the vicinity of a river, such as property size, number of rooms, single unity dwelling versus unit complex, access to transport, etc. The market value of the property is influenced by all these attributes, whilst the land value (unimproved capital value) is influenced only by environmental attributes, e.g. proximity to the river, rather than the building itself. The value of the property derived from the river is not a linear function of distance to the river, and this function will vary at different parts of the river system (e.g. wider versus narrower estuaries). Some previous studies have

derived a relationship of property value versus distance to natural asset [1,2]. There are several confounding variables that influence the value of property that must be separated from the river itself. These include elevation, distance to townships and amenities, distance to the ocean, and higher versus lower socio-economic suburbs.

1.1. Methods for Estimating River Value

The literature contains several different methods for estimating economic value from a river. Choice experiments method was applied by [3] which is based on random utility theory to generate willingness to pay estimates for the different parameters that a river would offer. The popular approach of contingent valuation was applied by [4,5] to estimate what water users would pay to protect water quality. Contingent valuation method is commonly used to place a value on non-market goods, such as natural assets. Further examples include [4,6,7]. The contingent valuation method relies on responses to public surveys to estimate a consumer surplus in monetary terms for a nonmarket good. Surveys ask individuals to state their willingness to pay for the provision of a good. It could be applied to property values by asking residents their willingness to pay extra for a given proximity to a river. However, such an analysis could be strongly biased, residents' responses would be confounded by: market value of properties versus price willing to be paid; differences between housing stock across the landscape; and effects from other attractive features on the landscape.

Benefit transfer is an alternate method used heavily in policy development and testing, to estimate the value of a natural asset [8]. The method uses information available for a studied site (where data is available) to estimate the economic value at a site with insufficient data. A challenge for the benefit transfer method is that it relies on suitable analyses conducted elsewhere, to provide meaningful results for the site (e.g. river) of interest. In the case of several published analyses, [9] shows how the results can be collectively synthesised using a meta-analysis, in application of economic value of water quality.

The hedonic pricing method, introduced in the early 1970's [10] is the most common form of analysis adopted for investigation of housing price due to natural assets, including a river. Over the last 20 years, the literature exists on hedonic values of scenery and environmental amenities in urban settings. These include studies of the value of open space, watersheds, wetlands, views and national parks [2,11–15]. The economic value of environmental features to properties has also received extensive attention in the literature (e.g. [16–19]. Visibility of environmental amenities (e.g. ocean) as key drivers to property valuation, was incorporated by [14,20],

whilst [21,22] use a combination of views and distances to environmental amenities. Digital terrain models were applied by [23] to calculate measures of visual impact as a function of elevation and neighbouring landscape features. All of these hedonic pricing applications used small or sampled data sets ranging from 300 properties [16] up to 5100 properties [14].

In operation the hedonic pricing method has two stages in analysis (see [24,25]). The first stage identifies the value of a property in light of the environmental asset. The second stage infers how much people are willing to pay for an improvement in the environmental quality via estimating their consumer surplus. Hedonics is typically implemented through regression analysis or GIS coupled regression, these applications potentially have limitations in accommodating multiple confounding variables, particularly when the confounding effects are non-linear and across geographical space. Unlike the contingency valuation and benefit transfer method, the hedonic pricing method is more data intensive, requiring market data sets across housing stock, type of house, location and distance to different environmental features and amenities in a set time period (usually one year).

A large and complete data set is available for the Maroochy river case study, containing actual information about the properties and their land valuations for 2008. The hedonic method may have been applied if the data set was limited to a few hundred properties and market price data was available in a single period, however this was not the case. Though, given the availability of a large data set, an alternative approach was chosen that would better handle the complex and non-linear spatial interactions of landscape variables. For the analysis in this paper, we selected Artificial Neural Networks (ANN) [26,27]. It is a suitable and novel method to estimate the value of property as a function of proximity to a river and other landscape features. ANN was chosen since: 1) a lot of information is available in the case study of this paper about the property that can be used for a training set; 2) able to accommodate complex and nonlinear inter-relationships between the variables characterising property values, which is beyond capability of the hedonic method; 3) accommodate spatial variability and imprecise/incomplete information which is a feature of Maroochy River case study; 4) can be a self contained model able to explore several scenarios; and 5) learn to solve problems rather than just apply pre-programmed algorithms. A recent paper by [28] showed the ANN to be a better alternative to hedonic regression, when estimating house prices as a function of building features. ANN's have been frequently applied to landscape problems, particularly for determining characterising influential factors of landscape features. For example, they have been commonly applied to characterising drainage systems [29], cropping yield variability [30], and forest

structures [31]. ANN's have been applied to estimate housing and property valuations, though as a relation of the house features rather than land value as a function of landscape features, [32] applied ANN to housing value as a function of type, location, age and general building features. Their model was adopted to enhance market research for real estate, [33] also forecast housing value but as a function of a financial variables, including salaries, bank interest rate, household savings and mortgage equity withdrawal. In our paper, we forecast property value as a function of different types of variables again, namely geographical and natural features.

The paper is organised as follows. In Section 2, we introduce the Maroochy case study and how this paper is an integral part of describing the economic value of a river system. In Section 3, we highlight how the ANN was set up and applied, including assumptions made. Section 4 focuses on the application of the ANN to the Maroochy case study to estimate the value of the river to property values, and Section 5 contains the conclusions.

2. Maroochy River Case Study

The Maroochy Shire is located about 100km north of Brisbane, Australia, and is one of four shires that form the Sunshine Coast. Its population in 2006 was 152,000, and is expanding at a rapid rate of about 3.5 percent per year. A diagram of the shire is shown in Figure 1, which highlights the Maroochy River in relation to the townships, ocean and various land uses. These land uses include rural residential and urban footprint, agriculture (primarily sugarcane), and state forests (protected). The Maroochy River is divided into 8 different types of estuaries. Category 1 is the main river that flows into the ocean, whilst Category 2 are major streams that flow into the main river. Category 3 streams flow into category 2 and so on. Streams up to Category 3 are show in Figure 1. Minor estuaries do stretch about 60km into the Sunshine Coast hinterland, areas outside the scope of this study. The main economic driver for the Maroochy Shire is
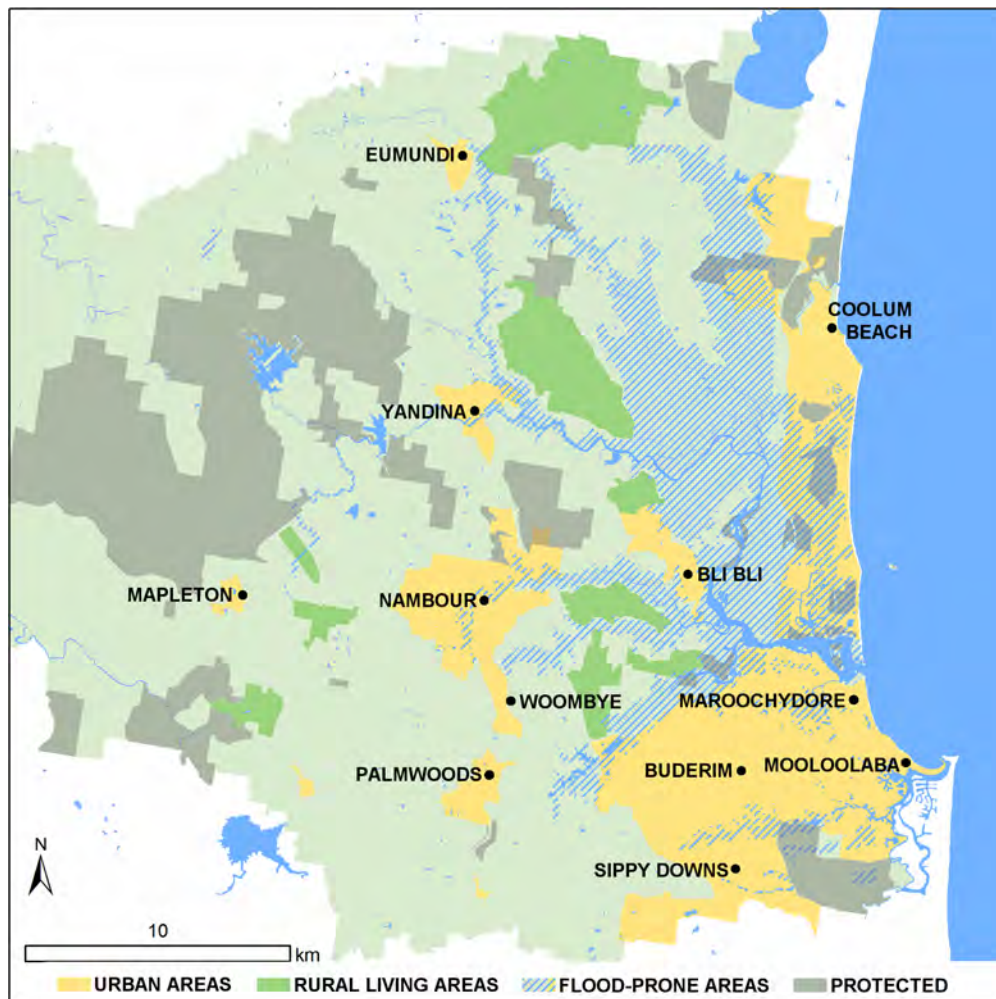

Figure 1. Diagram of Maroochy river catchment showing the location of the river, which is the blue river running inland north of Maroochydore, to the east of Bli Bli, then up to Yandina. The different colour codes represent the land uses.

tourism focused around nature-based activities, especially related to beach and river. It is a high socio-economic region, with average house sales of AU$626,000 (RPdata–www.rpdata.com.au). However, house prices are highly variable, with ocean or river front properties, selling for more than AU$1,500,000.

The aim of this study was to derive a value of the Maroochy River system to the local residents. A secondary issue was to identify how this value changed with different scenarios, e.g. poor water quality in the river resulting in the river not being valued by residents.

The Maroochy River is a dynamic natural asset and we have developed a conceptual model (Figure 2) to represent it. For example, further urban expansion may not lead to a static marginal increase in financial value of the Maroochy River to properties. This is because new dwellings would be built further from the river as the prime land has already been committed to urban development. More importantly, whilst the river contributes to property value, increased urban development and use of the River will decrease water quality and inturn decrease the value of the river (per capita) for its water users and properties close to the river. A decrease in water quality also means that there are greater costs in river restoration activities to improve water quality (Figure 2), and will also have

adverse effects on the property values. This figure also shows how the analysis of this paper fits into the bigger picture of assessing the value of the Maroochy River. By presenting a dynamic model of the Maroochy River, we highlight the types of complex interactions that must be understood quantitatively, before a "whole-of-system" economic model of the Maroochy River can be built.

This paper focuses on one component of Figure 2, the financial value of property attributed to the Maroochy River. One would expect property values to be by far the largest financial benefit from the Maroochy River, particularly due to the canal frontages, views and the overall high socio-economic status of the Sunshine Coast. Calculating the contribution that the Maroochy River makes to the financial value of the properties around it is difficult. Firstly, there are many other confounding landscape features that contribute to the property values, such as the ocean, mountains (producing views of the ocean) and the city centre. Secondly, availability of reliable data for the region can be a challenge, particularly at the individual property level. For the Maroochy Shire, suitable GIS data sets were available from the Council, and covered all 28,000 properties in the vicinity of the Maroochy River. Collectively, the data sets contained information on size of the property, location, zoning of the land (resi-
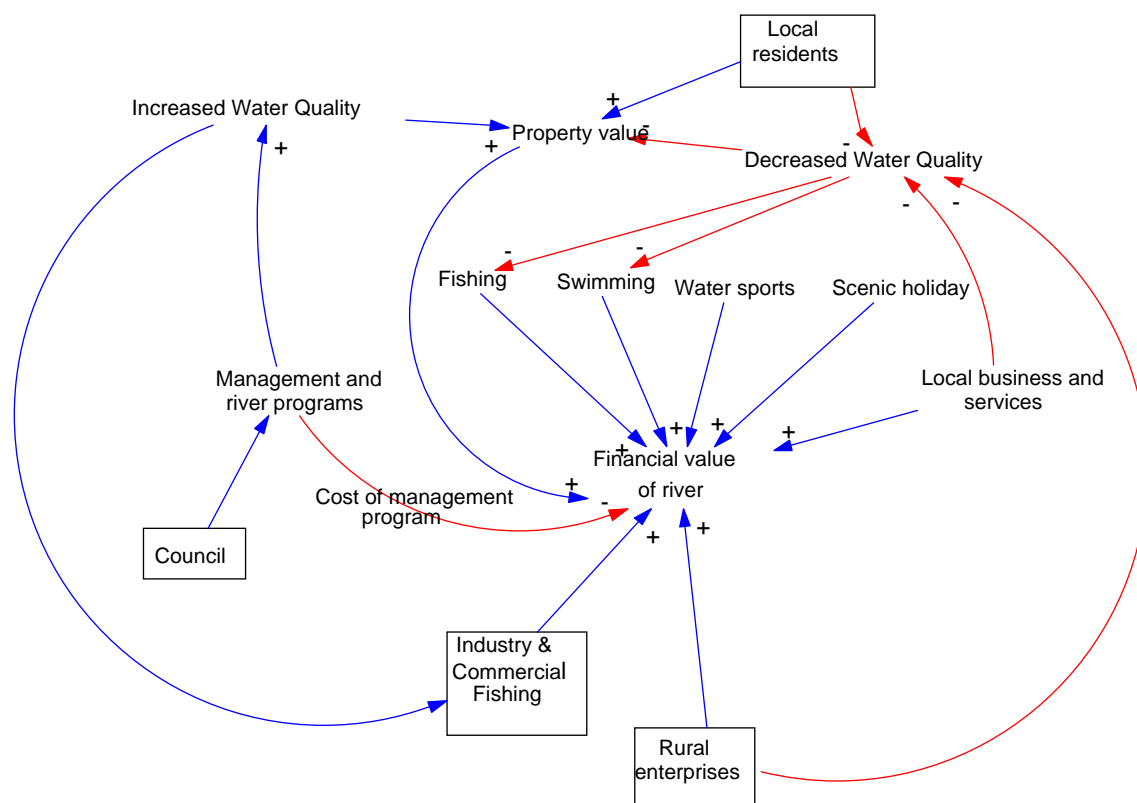

Figure 2. Dynamic relationship between water quality and financial value of the river, where the blue arrows (+) represent positive influences, and red arrows (-) represent negative influences.

ential, agriculture, commercial, units), land value (unimproved capital value), elevation. Other GIS layers provided information on property locations, and the location of the landscape features–ocean, rivers, towns, roads etc. Information on real estate sales prices of each property were obtained by RPdata (www.rpdata.com.au) and only contain information on properties that were sold in the last 5 years. This information only covered about 30 percent of properties.

We decided to base the analysis on unimproved capital value (UCV) rather than sales value of the properties, which was agreed upon by the Maroochy Shire Council. The main reason is that the value of the property, in relation to the natural assets (river, ocean) will be included in the land value (or UCV) rather than including confounding attributes such as the building itself. Additionally, there was inadequate sales data for the region over a set time period (ie. a thin housing market). UCV is the value of the land component of the property, as determined by the Queensland Valuer General, which is used by Maroochy Shire Council to calculate annual rates charged to the property owners. Since UCV is estimated through inspection, it doesn't always represent the sale value of the vacant land, and doesn't always capture the true value of environmental features to the resident. By using UCV we are able to ignore any confounding influences of building and landscaping (i.e. pools, etc.) that may be independent of location and proximity to the natural assets. A modelling approach needed to accommodate the 28,000 properties across the landscape, and the data set for these properties provided an excellent training set for the ANN developed for the analysis. For the case study, we focused on residential properties, and removed the commercial and agricultural properties from the original 28,000, leaving 26,500. The small number of commercial and agricultural properties (compared to residential) had highly variable UCV due to other variables (e.g. proximity to central business district) strongly affecting the UCV the council assesses these properties at. This made it very difficult to predict an economic value of these properties in relation to proximity, access or view of

natural assets, and thuswas omitted from the analysis. Whilst distance to the Maroochy River was the key driver of the analysis of this paper, a model needed to accommodate other confounding effects. One of the purposes of the project working group, which included representatives from the Maroochy Shire Council, was to decide on variables that have the greatest impact on property value where there are data available. We agreed that the key variables were: location, distance to the ocean, elevation above sea level, distance to the river and streams, and area of the property. One would expect each of these variables to have some correlation with UCV, and the next section explores the strength of correlation. Other variables are also expected to impact UCV (e.g. adjoining busy roads or schools, availability of public transport, sewerage networks under properties). However, these were either not available or difficult to derive in a reliable form during the data preparation.

3. Application of an Artificial Neural Network

Considerable data preparation was required to consolidate the GIS and UCV databases for the Maroochy shire and to generate the variables used in the ANN. This included merging and reprojecting available data to match, as well as adding property value data to the relevant areas, using a Geodatabase. ArcGIS was used to generate: location (X,Y co-ordinates of the property centroid), the distance to coast, distance to major stream and stance to the main river. We included the main river as well as major streams in the analysis since the majority of properties are a considerable distance (>2 km) to the main river but are close to a major stream that feeds into the river. In some instances, close proximity to a major stream can have negative implications on a property value due to flood prone risks. Figure 3 shows some of the stages of analysis, to derive distance to coast and distance to streams using GIS methods. These were combined for this study. Table 1 contains a sample of the 26,500 data points used in the ANN after the data preparation phase.

An ANN is an information processing model inspired by the way the interconnected structure of the brain proc-

Table 1. Sample of data used for the ANN.

Property ID	UCV 2008 ($)	Distance to Coast (m)	Area (m2)	X co-ord	Y co-ord	Zoning	Distance to nearest stream	Distance to main river	Elevation (m)
2103	300000	1000	780	509758.8	7050330	Single Unit Dwelling	1600	1600	9.5
2104	280000	1000	631	509802.3	7050368	Single Unit Dwelling	1550	1550	8.7
2167	1700000	1500	11363	509371.8	7050072	Building Units	1800	1900	4.7
5286	275000	6500	2143	503958.3	7055305	Single Unit Dwelling	550	550	23
5287	215000	6500	1756	504031.4	7055404	Single Unit Dwelling	500	500	14.7
5288	207500	6500	1540	504058.7	7055412	Single Unit Dwelling	450	450	11.3
5291	600000	6000	3526	504305.3	7055473	Vacant Urban Land	200	200	18

esses information. ANN's are simplified mathematical models of biological neural networks. They consist of an interconnected group of artificial neurons and processes information using a connectionist approach to computation. In most cases an ANN is an adaptive system that changes its structure based on external or internal information that flows through the network during the learning phase. In more practical terms ANN's are non-linear statistical data modelling tools. They can be used to model complex relationships between inputs and outputs or to find patterns in data. A widely used ANN structure is the multi-layer perceptron, which we have employed in this paper. It contains one input layer, two hidden layers and one output layer. Each layer employs several neurons and each neuron in the layer is connected to neurons in the adjacent layer through various weights. An illustration for the Maroochy case study is contained in Figure 4. Not all of the 30 neurons of hidden layer 1 and 15 neurons of hidden layer 2 are shown due to space limitations. The ANN was coded in NeuroSolutions 5. Twenty percent of the 26,500 properties in the dataset were used as cross validation, whilst the remaining 80 percent were used for the training set. The standard learning algorithm, back propagation, was used as the learning algorithm. Other parameters used in the ANN were: maximum epochs=12,000 where the mean square error of the cross validation set was minimal at this point; momentum=0.9; tolerance=0.0001; Tanh transfer function with beta=1.0; learning rate=0.1. We experimented with various combinations of number of neurons (5-100) and hidden layers (1-3) before arriving at the best combination for the analysis in terms of mean square error (MSE) for the cross validation data set. Whilst removing any of the input variables increased the MSE of the cross validation set, the contribution to the model did vary. When an ANN was fitted to each input variable to estimate UCV, the MSE varied from 0.00039 to 0.00045. The small difference between MSE of individual variables was likely due to large diversity of properties in the Maroochy shire, and the variables that influence their individual UCV. For example, for properties close to the ocean, 'distance to coast' was the most influential variable. UCV of large properties were influenced by the 'area of property' variable. This feature was also common to the 'distance to river', 'location', and 'elevation' variables. Zoning was a categorical variable, and was needed to separate out units from single unit dwellings, from large acre blocks, since UCV was calculated differently depending on the zoning. These reasons, along with the small MSE for each variable, were justification to include all variables selected by the Maroochy Shire Council. When all variables were included in the model, the MSE was 0.00032.

Correlation between actual UCV and those estimated using the ANN model was 0.62, and a scatter plot of the cross-validation data set is shown in Figure 5. A linear trend line is also shown as well as a one to one relationship (dotted line). The main deficiency of the ANN was the underestimation for high UCV, with an average error
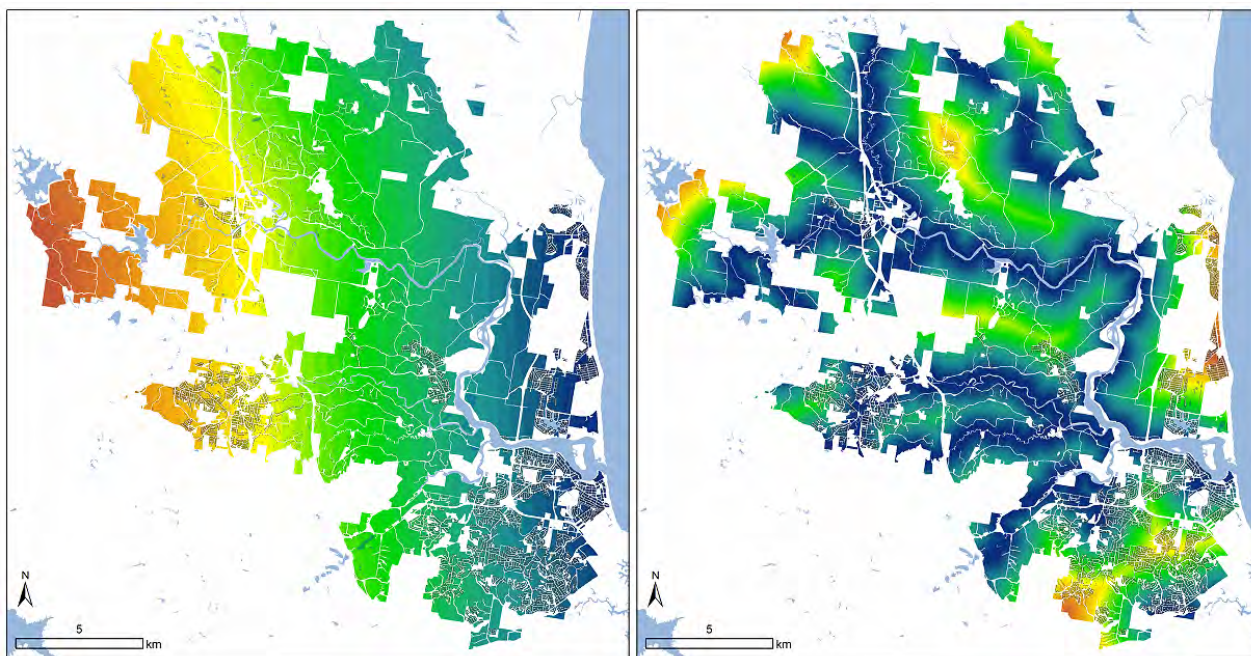
Figure 3. Data preparation-modelling of distances from ocean (left) and major stream (right), where blue represents closer distances and yellow/orange represents further distances.
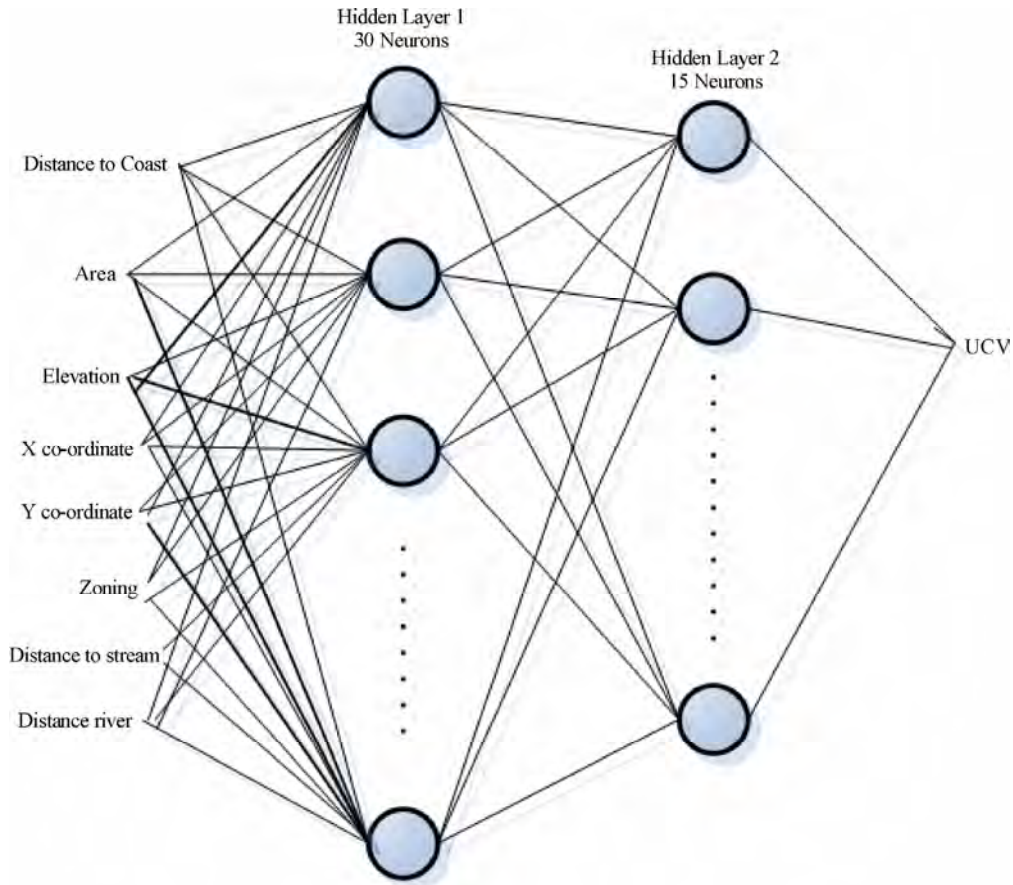
Figure 4. ANN architecture for Maroochy case study.
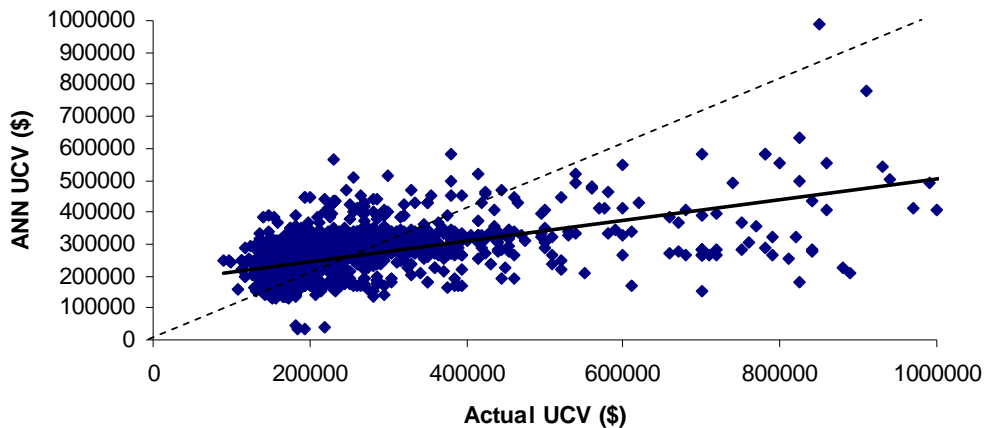
Figure 5. Relationship between actual UCV and those produced by the ANN for the cross-validation data.

of 39%. For the mainstream UCV values of AU\$ 150,000 to AU\$300,000 (with a median value of AU\$ 197,000), underestimation was not a major problem, and the average error of estimation was 18%. Congestion of points between this range in Figure 5, makes it difficult to visually see the number points close to the trend line. A correlation of 0.62 and average error of 18%, would

unlikely be high enough to use for the pur-pose of forecasting UCV's for individual properties, particularly outside the current dataset. There are several other variables that the Valuer General accounts for when judging a property (e.g. closeness to main roads, intersections and public transport, major sewerage pipes under the property) which would have improved the correlation,

though we were not able to accommodate in our current model. However, it was not important to include these other variables, since they were unlikely to have confounding impacts on the 'distance to river and stream' variables. The purpose the current model was to estimate the influence of the major environmental feature, the Maroochy River, on overall property values. Our priority was to capture that relationship as best as possible for the Maroochy dataset, whilst accommodating variables that would confound it (e.g. distance to ocean).

4. Application to Maroochy River Value and Scenarios

To estimate the value of the Maroochy River to property values, we needed to compare two scenarios: the current landscape as is, which we refer to as the base case; and the landscape with no river. The difference in property value between the two scenarios provides us with the estimated unimproved capital values with the river removed. To simulate the scenario with no river we allocated each property a 2.5km distance (minimum) to the main Maroochy River, and estimated the UCV using the ANN. The Maroochy Shire Council felt a 2.5km value is far enough from the river so that it does not influence UCV, which for the scenario would be analogous to not having a river. Since the ANN underestimated the actual UCV when the values were large, we needed to adjust the UCV's produced by the ANN to produce a true representation of the value of the Maroochy River. We did this using the following formula:

$$UCV_i^j = UCV_i^{ACT} * \frac{UCV_i^{ANN,j}}{UCV_i^{ANN,0}}$$

where:

UCV_i^j = estimated UCV for property i in scenario j using the ANN after correcting for underestimation bias

UCV_i^{ACT} = actual UCV for property i as per the raw data from the Maroochy council (base case), $UCV_i^0 = UCV_i^{ACT}$

$UCV_i^{ANN,j}$ = raw UCV output from the ANN for property i in scenario j

$UCV_i^{ANN,0}$ = raw UCV output from the ANN for property i in the base case scenario.

Let the scenarios be defined as follows:

Base case:- $j = 0$

Main river removed:- $j = 1$

Main river and main streams removed:- $j = 2$. In this scenario each property is allocated a minimum distance of 2.5km to the nearest main stream.

The total unimproved capital value for all residential

properties in the base case (with the river $j = 0$) is AU\$6,778,916,814, $= \sum_i UCV_i^0$, which is summation of modelled UCV over all 26 500 residential properties in the Maroochy area. The first analysis was to remove the main river (Figure 6). By doing this, the total non-improved capital value for all residential properties reduced to AU\$5,880,347,570$= \sum_i UCV_i^1$. This means the main section of the river is worth approximately AU\$900,000,000 (AU\$6,778,916,814 - AU\$5,880,347,570) to the residential property stock in the Maroochy region. There was some variability around this value depending on the ANN weights obtained during training, as each time the ANN is trained, a slightly different set of weights are obtained. Such variability led to an error bar of AU\$900,000,000 plus or minus 22 percent. Figure 6 shows the value of the main river (scenario $j = 1$) the across properties on a geographical basis, where the insert is the township of Maroochy. The colour codes represent the percentage of UCV remaining if the river was removed = $UCV_i^1 / UCV_i^0 * 100$. Areas in red and pink highlight properties where the main river is of greatest value, since they represent the greatest decrease in UCV with the river removed scenario (scenario $j = 1$). These are generally properties closest to the river. Many of the properties in red are waterfront (canal) residents who have direct access for boating. In practice these properties sell for up to four times the price compared to properties without a canal frontage, so the ANN has predicted these instances very well. Some larger properties increased in value with scenario 1, and are due to removing the flood prone risks.

The second scenario ($j = 2$) simulated the removal of the main Maroochy River and the main streams that feed into the main river. By doing this, the total non-improved capital value for all residential properties reduced to AU\$5,828,577,742 $= \sum_i UCV_i^2$. This means the major streams (minus the main river) are worth about AU\$52,000,000 (AU\$5,880,347,570-AU\$5,828,577,742) to residential properties. Actually, the main streams were found to have a negative impact on some properties (i.e. increased UCV from removing the streams, represented by dark green properties in Figure 7), because the streams created flood prone problems. Figure 7 colour codes represent the percentage of UCV remaining if the river and main streams were removed = $UCV_i^2 / UCV_i^0 * 100$. This an accurate representation of practice for most properties highlighted in dark green in Figure 7, which tend to be the larger low lying peri-urban areas. The scenarios highlight the capability of the ANN to accommodate the confounding relationships between

variables such as elevation and distance to the river and ocean, as it can capture the negative implications of low lying land near the river.

The above capitalised values for each scenario can also be used to estimate rates income to Maroochy Shire Council, resulting from the river. Council uses a differential rating system based on UCV value of residential properties. We have simplified the analysis to provide the breadth of rate income council could derive from the Maroochy River based on the total changes in UCV expected by the ANN. To this end we assumed that all properties

were in a range between AU$160,000 and AU$1 million and we have estimated the spread of council derived rates, due to the Maroochy River in Table 2. By estimating the annual rates to council resulting from the presence of the Maroochy River (Table 2), the Maroochy Shire Council will justify expenditure for protecting the ecosystem function of the river. This management program expenditure is highlighted in Figure 2 as part of the overall system of defining financial value of a river.

There are a broader range of planning and policy scenarios that the ANN for the Maroochy River could be
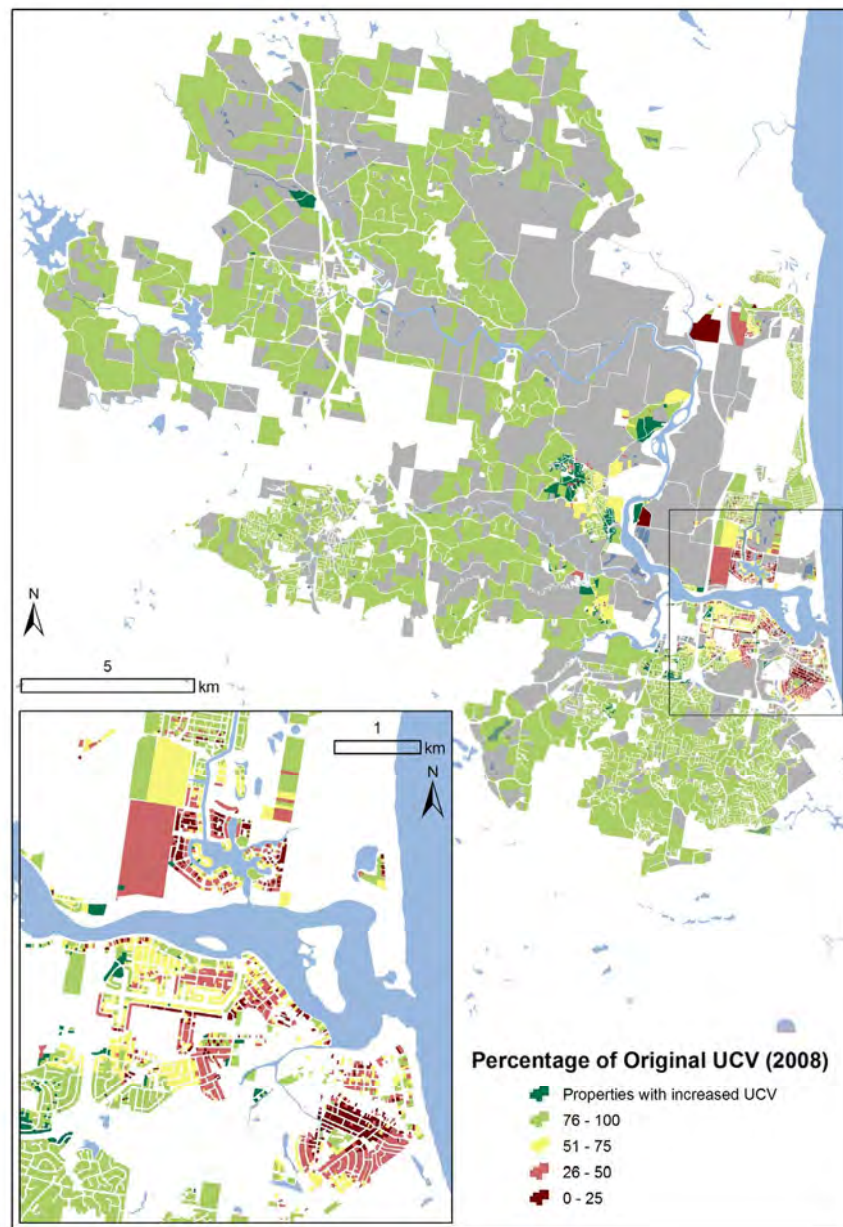
Figure 6. Spatial analysis of the impact of the Maroochy River on residential unimproved land values in Maroochy, based on removal of the main river.
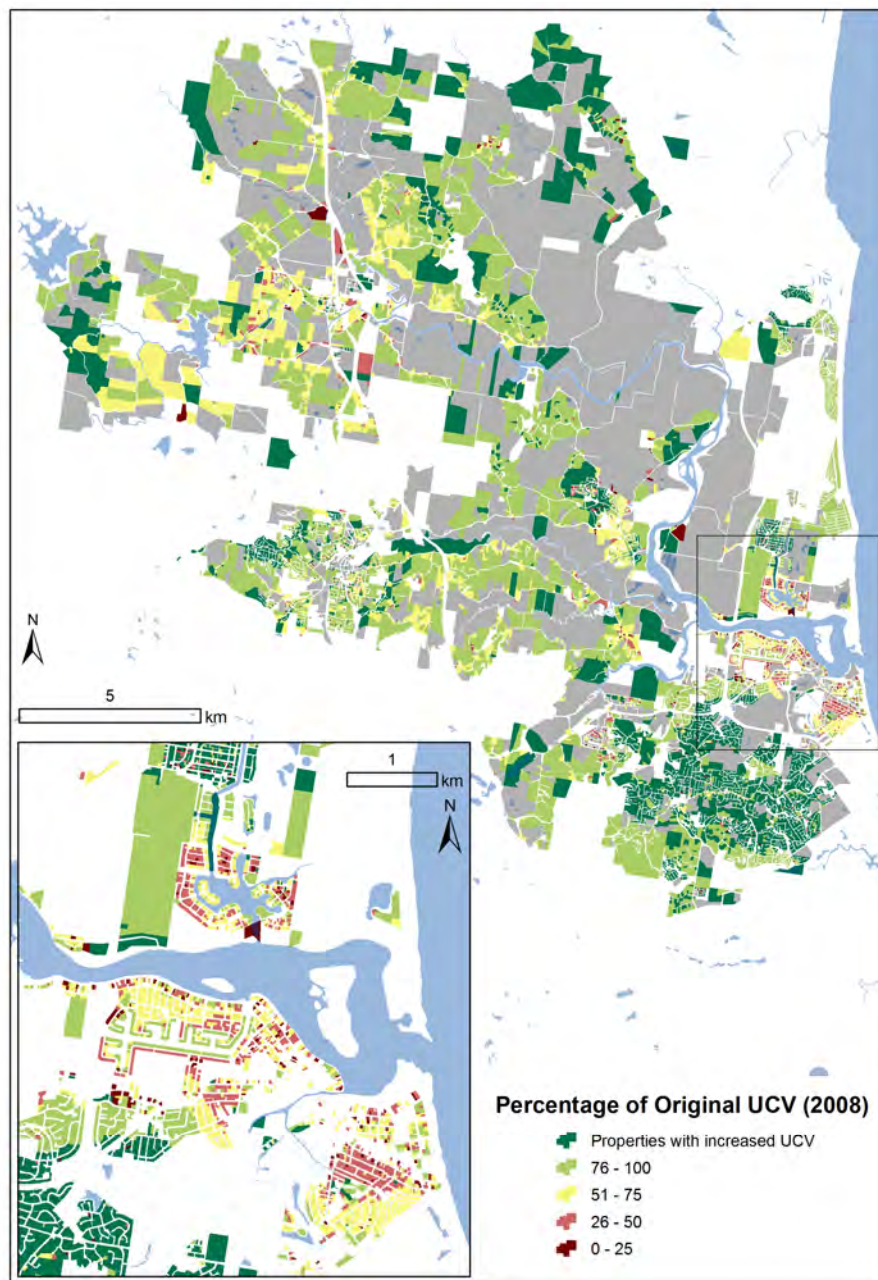
Figure 7. Spatial analysis of the impact of the Maroochy River on residential unimproved land values in Maroochy, based on removal of major stream and main river channel.

applied to in the future. This includes assessing the value of new residential property estates in a regional development plan for urban expansion, which would provide the Council with projections of future rates income. By applying the ANN to sales values as well as UCV, one can estimate the financial value of a property in terms of a relationship between building features and location. Such a capability would provide property developers with a means of tailoring housing stock designs in different locations (accommodating proximity to environ-

mental assets) with market trends.

5. Conclusions

In this paper, we have addressed a novel application of assessing the financial value of a river to residential properties. It is also a novel application of ANN, which was shown to be a suitable method for estimating property value as a function of various landscape features, in the presence of a complete data set at property level.

Table 2. Estimate of the possible range of Council residential rates derived from Maroochy River.

	Rates used	Considering only main river	Considering main streams	Annual rates to council
Low property value ($160,000)	0.44%	$3.96 million	$228 800	$4.2 million
High property value ($1,000,000)	0.29%	$2.96 million	$150 800	$2.8 million

Whilst the ANN consistently underestimated large value of UCV, it was able to be corrected when applied to scenarios of economic value of the river to residents. The modelling approach was strongly welcomed by researchers and policy analysts, as it provided a credible value of Maroochy River for the first time without extensive primary data collection. By having a financial value of the river, the local River managers can go to the next step in justifying management expenditure in protecting the value of the river.

The existing analysis does have some challenges though. There is some room for improvement in accuracy of the model (correlation = 0.62), which can be done through introducing more variables such as proximity to amenities, busy roads, schools, and other features that impact land value. The use of UCV as an indicator of land value can also be questioned. It is the best indicator from the perspective of estimating financial income to the council through land rates, and is also suitable when a complete data set is needed. However, it is often not a true representative value of the sale price of the vacant land, as the sale price is usually higher than the UCV. Also, UCV's of properties are often estimated using expert 'valuer' opinions. There is limited data available on sales of vacant land, as more properties are sold with a house, though the limited sales information could be used to calibrate UCV's if there is sufficient representation. These opportunities will be investigated as part of future research.

The analysis of this paper is one step towards estimating the full economic value of the Maroochy River, and other research is being conducted to estimate contributions from tourism, water sports, industry and agriculture [34]. The Maroochy Shire council, like many government bodies, wish to better understand the relationship between environmental and economic value and hence ensure more effective management of its environmental assets into the future. A next major step of the research will be turn the framework of Figure 2 into dynamic systems model linking the modelling work of this paper with models representing other components of Figure 2.

6. Acknowledgements

7. References

[1] C. Lee and P. Linneman, "Dynamics of the greenbelt amenity effect on the land market-The case of Seoul's greenbelt," Real Estate Economics, Vol. 26, pp. 107–129, 1998.

[2] L. J. Pearson, C. Tisdell and A. T. Lisle, "The impact of Noosa national park on surrounding property values: An application of the hedonic price method," Economic Analysis and Policy, Vol. 32, No. 2, pp. 155–171, 2002.

[3] N. Hanley, R. E. Wright and B. Alvarez-Farizo, "Estimating the economic value of improvements in river ecology using choice experiments: An application to the water framework directive," Journal of Environmental Management, Vol. 78, pp. 183–193, 2006.

[4] H. Chen, N. Chang and D. Shaw, "Valuation of in-stream water quality improvement via fuzzy contingent valuation method," Stochastic Environmental Research Risk Assessment, Vol. 19, pp. 158–171, 2005.

[5] R. A. Kramer and J. I. Eisen-Hecht, "Estimating the economic value of water quality protection in the Catawba River basin," Water Resources Research, Vol. 30, No. 9, pp. 1182, 2002.

[6] R. C. Mitchell and R. T. Carson, "Using surveys to value public goods: The contingent valuation method," Resources of the Future, Washington, D.C, 1989.

[7] M. K. Alam and D. Marinova, "Measuring the total value of a river cleanup," Water Science and Technology, Vol. 48, pp. 149–156, 2003.

[8] R. S. Rosenberger and J. B. Loomis, "Benefit transfer of outdoor recreation use values. A technical Document Supporting the Forest Service Strategic Plan," Gen. Tech. Rep. RMRS-GTR-72. Fort Collins, CO: U.S. Department of Agriculture, Forest Service, Rocky Mountain Research Station, pp. 59, 2001.

[9] G. Van Houtven, J. Powers and S. K. Pattanayak, "Valuing water quality improvements in the United States using meta-analysis: Is the glass half full or half empty for national policy analysis?" Resource and Energy Economics, Vol. 29, pp. 206–228, 2007.

[10] S. Rosen, "Hedonic prices and implicit markets: Product differentiation in perfect competition," Journal of Political Economy, Vol. 82, No. 1, pp. 34–55, 1974.

[11] S. D. Shultz, "The use of census data for hedonic price estimates of open-space amenities and land use," Journal of Real Estate Finance and Economics, Vol. 22, No. 2/3, pp. 239–252, 2001.

[12] G. Acharya and B. L. Lewis, "Valuing open space and landuse patterns in urban watersheds," Journal of Real Estate Finance and Economics, Vol. 22, pp. 221–237, 2001.

[13] B. L. Mahan, S. Polasky and R. M. Adams, "Valuing urban wetlands: A property price approach," Journal of Land Economics, Vol. 76, pp. 100–113, 2000.

[14] E. D. Benson, J. L. Hansen, J. Arthur, L. Schwartz, G. T. Smersh, "Pricing residential amenities: The value of a view," Journal of Real Estate Finance and Economics, Vol. 16, pp. 55–73, 1998.

[15] B. Colby and S. Wishart, "Riparian areas generate property value premium for landowners," Working paper, University of Arizona College of Agriculture and Life Sciences, Department of Agricultural and Resource Economics, 2002.

[16] K. Boyle and L. Taylor, "Does the measurement of property and structural characteristics affect estimated implicit prices for environmental amenities in a hedonic model?" Journal of Real Estate Finance and Economics, Vol. 22, No. 2/3, pp. 303–318, 2001.

[17] L. Tyrvainen, "The amenity value of the urban forest: an application of the hedonic pricing method," Landscape and Urban Planning, Vol. 37, pp. 211–222, 1997.

[18] W. A. Donnelly, "Hedonic price analysis of the effect of a floodplain on property values," Journal of the American Water Resources Association, Vol. 25, No. 3, pp. 581–586, 2007.

[19] S. Sengupta and D. E. Osgood, "The value of remoteness: A hedonic estimation of ranchette prices," Ecological Economics, Vol. 44, pp. 91–103, 2003.

[20] B. Fraser and G. Spencer, "The value of an ocean view: An example of hedonic property amenity valuation," Australian Geographical Studies, Vol. 36, No. 1, pp. 94–98, 1998.

[21] J. Luttik, "The value of trees, water and open space as reflected by house prices in the Netherlands," Landscape and Urban Planning, Vol. 48, pp. 161–167, 2000.

[22] C. Bastian, D. McLeod, M. Germino, W. Reiners and B. Blasko, "Environmental amenities and agricultural land values: A hedonic model using geographical information systems data," Ecological Economics, Vol. 40, pp. 337–349, 2002.

[23] I. R. Lake, A. Lovett, I. J. Bateman, I. H. Langford, "Modelling environmental influences on property prices in an urban environment," Computers, Environment and Urban Systems, Vol. 22, pp. 121–136, 1998.

[24] A. Freeman and I. I. I. Myrick, "The measurement of environmental and resource values," Theory and Methods, Resources for the Future, 1997.

[25] D. W. Pearce and A. Markandya, "Environmental policy benefits: Monetary valuation," Organisation for Economic Co-operation and Development, Paris, 1989.

[26] J. A. Anderson, "An Introduction to Neural Networks". M. I. T. Press, 1995.

[27] T. Khanna, "Foundations of Neural Networks," Addison-Wesley, 1990.

[28] H. Selim, "Determinants of house prices in Turkey: Hedonic regression versus artificial neural network," Expert Systems with Applications, In press, 2008.

[29] R. O. Strobl and F. Forte, "Artificial neural network exploration of the influential factors in drainage network derivation," Hydrological Processes, Vol. 21, pp. 2965–2978, 2007.

[30] Y. Miao, D. J. Mulla, and P. C. Robert, "Identifying important factors influencing corn yield and grain quality variability using artificial neural networks," Precision Agriculture, Vol. 7, pp. 117–135, 2006.

[31] J. C. Ingram, T. P. Dawson, R. J. Whittaker, "Mapping tropical forest structure in southeastern Madagascar using remote sensing and artificial neural networks," Remote Sensing of Environment, Vol. 94, pp. 491–507, 2004.

[32] N. Garcia, M. Gamez and E. Alfaro, "ANN+GIS: An automated system for property valuation," Neurocomputing, Vol. 71, pp. 733–742, 2008.

[33] P. S. Jarvis, I. D. Wilson and S. E. Kemp, "The application of a new attribute selection technique to the forecasting of housing value using dependence modelling," Neural Computing and Applications, Vol. 15, pp. 136–153, 2006.

[34] L. J. Pearson, A. J. Higgins, L. Laredo and S. Whitten, "Maroochy River Value Project," Final Report submitted to the Sunshine Coast Regional Council, 2008.

Optimal Extraction of Groundwater in Gaza Coastal Aquifer

Khalid QAHMAN[1], Abdelkader LARABI[2], Driss OUAZAR[3], Ahmed NAJI[4], Alexander H.-D. CHENG[5]

[1]*Environment Quality Authority, Al-Naser Street, Gaza-Palestine*
[2] *Department of Mineral Engineering, Ecole Mohammadia d'Ingénieurs, Université Mohammed V-Agdal, Agdal, Morocco*
[3] *Department of Civil Engineering, Ecole Mohammadia d'Ingénieurs, Université Mohammed V-Agdal, Agdal, Morocco*
[4] *Faculty of Science, Université Abdelmalek Essaadi, Tangier, Morocco*
[5] *Department of Civil Engineering, University of Mississippi, University, USA*
*E-mail: kqahman@gmail.com; {larabi, ouazar}@emi.ac.ma;
naji@dns1.fstt.ac.ma; acheng@olemiss.edu*
*Received June*17, 2009; *revised July* 13, 2009; *accepted September* 10, 2009

Abstract

Two multi-objective management models are applied on a local area selected from the regional Gaza coastal aquifer. The objectives and constraints of these management scenarios include maximizing the total volume of water pumped, minimizing the salt concentration of the pumped water, and controlling the drawdown limits. The physical model is based on the CODESA-3D density-dependent advective-dispersive solute transport model. Genetic algorithm is used as the optimization tool. The models are tested on a part of the aquifer ($2000\,\text{m} \times 2000\,\text{m}$) with 9 existing pumping wells located at various depths. The results of the optimization show that the optimization/simulation approach can give better decision if there is enough information to feed to the model. It confirms that the use of the concept of safe yield alone is not enough for sustainable development of the coastal aquifer. It shows that the optimum pumping rate is in the range of 26%–34% of the total natural replenishment. The application shows that the proposed technique is a powerful tool for solving this type of management problems.

Keywords: Seawater Intrusion, Genetic Algorithm, Pumping Optimization, Density-dependent Miscible Transport

1. Introduction

Water is the most precious and valuable natural resource in the Middle East in general and in Palestine (Gaza strip) in particular. It is vital for socio-economic growth and sustainability of the environment. The development of groundwater resources in coastal areas is a sensitive issue, and careful management is required if water quality degradation, due to the encroachment of seawater, is to be avoided. In many cases, difficulties arise when aquifers are pumped at rates exceeding their natural capacity to transmit water, thus inducing seawater to be drawn into the system. Problems can also occur when excessive pumping at certain individual wells lowers the potentiometric surface locally and causes upconing of the interface between fresh water and saline water [1]. To combat these situations, saltwater intrusion management models need to be implemented to design optimal and sustainable groundwater abstraction strategies.

Optimization solutions in saltwater intrusion that consider the existence of transition zone between the freshwater and seawater are relatively few. Das and Datta [2,3] considered the multi-objective management in coastal aquifers that maximized pumping in the freshwater zone, and minimized it in the saline zone, with the pumped salt concentration as a constraint or the third objective. The nonlinear finite difference solution of the density-dependent miscible flow and transport equations was embedded in the management model as constraints. The MINOS optimization solver was used to solve the resulting large-scale problem. Gordon *et al.* [4] developed a model for the optimal management of a regional (two dimensional) aquifer under salinization. The sources of salinization were from irrigation water, saline waters from faults at the bottom of aquifer, and inflow from adjacent saline water bodies. The objectives were to maximize the volume of water pumped and to minimize the amount of salt extracted. The model was based on a

combination of simulation and optimization. The simulation model uses finite element formulation for the flow and upwind Petrov-Galerkin formulation for the transport. The gradients of the state variables (heads and concentrations) with respect to the decision variables (pumping rates) were used in a Bundle-Trust non-smooth optimization procedure to improve the solution. Qahman *et al.* [5] investigated four examples for the optimal and sustainable extraction of groundwater from a coastal aquifer under the threat of seawater intrusion. The physical model is based on the density-dependent advective-dispersive solute transport model. Genetic algorithm (GA) [6] is used as the optimization tool. The models are tested on a hypothetical confined aquifer with 4 pumping wells located at various depths. These solutions establish the feasibility of simulating various management scenarios under complex three-dimensional flow and transport processes in coastal aquifers for the optimal and sustainable use of groundwater.

In this study, two multi-objective management models of saltwater intrusion was applied on a local area selected from the Gaza coastal regional aquifer and solved using the same approach presented by Qahman *et al.* [5]. These management schemes for the prevention of saltwater intrusion as proposed here are new for the Gaza aquifer and can be applied to other areas where there is a potential risk of saltwater intrusion. Therefore, the saltwater intrusion management problem presented in this work will give more insight in the planning and future management of the study area.

2. Genetic Algorithm

The GA is used in many engineering fields to seek optimal solutions to complex problems. A number of researchers have demonstrated that the GA can yield significant better results [7,8]. The GA is an optimization technique based on the process of biological evolution. After its introduction by Holland [9], it has gained popularity in many fields. For water resources, the GA has been applied to problems such as pipe network optimization [10], groundwater parameter determination [11], and groundwater cleanup [12,13]. A review of the GA technique in water resources applications is given by Ouazar and Cheng [14].

Goldberg [6] stated that genetic algorithms are different from other optimization and search procedures in the following aspects:

1. GA works with a coding of the parameters set, not the parameters themselves.

2. GA searches from a population of points, not a single point.

3. GA uses payoff (objective function) information, not derivatives or other auxiliary knowledge.

4. GA uses probabilistic transition rules, not deterministic rules.

In this work, a FORTRAN version of a genetic algorithm driver is adopted. The program initializes a random sample of individuals to be optimized. The selection scheme is a tournament competition with a shuffling technique for choosing pairs for mating. The genetic operators used include jump mutation, creep mutation, and the option of single-point or uniform crossover. Niching (sharing) and an option for the number of children per pair of parents have been added.

Linkage of simulation model to optimization model. An important part of this methodology is the linkage between the optimization model and the 3D variable density seawater intrusion model. Basically, an iterative procedure is followed in which GA tests new decision variables (pumping rates) for feasibility and optimality. The objective function and constraints are functions of the state variables (heads and concentrations). These values are obtained from the CODESA-3D model. The model simulates the water movement in the aquifer, taking into account different forcing inputs such as pumping rates, and computes the heads and concentrations. The objective function calculated using the heads and concentrations are then optimized in the GA procedure.

3. Study Aquifer

The real world problem is addressed in a particular study area, selected from the coastal aquifer of the Gaza Strip. The area is intruded by saltwater with the current interface (transition zone) position located near the existing pumping wells. The selected area is located in the northeast of Wadi Gaza and is parallel to the coastline, as shown in Figure 1.

This part of the aquifer is considered unconfined, homogeneous and isotropic with respect to freshwater hydraulic conductivities, molecular diffusion, and longitudinal and transverse dispersivities. The aquifer system is subjected to seawater intrusion along the sea face boundary and a uniformly distributed lateral flow along the inland face. It is a problem of steady state saturated flow and transport in three dimension domain. The geometry and boundary conditions are shown schematically in Figure 2a. The dimensions of the aquifer are 2000 m in length, 2000 m in width parallel to sea face, and about 100 m in average thickness. The domain is discretized using three dimensional grid ($\Delta x = \Delta y = 200\,\text{m}$, and $\Delta z = 10\,\text{m}$). The simulation code divides each rectangular cell into
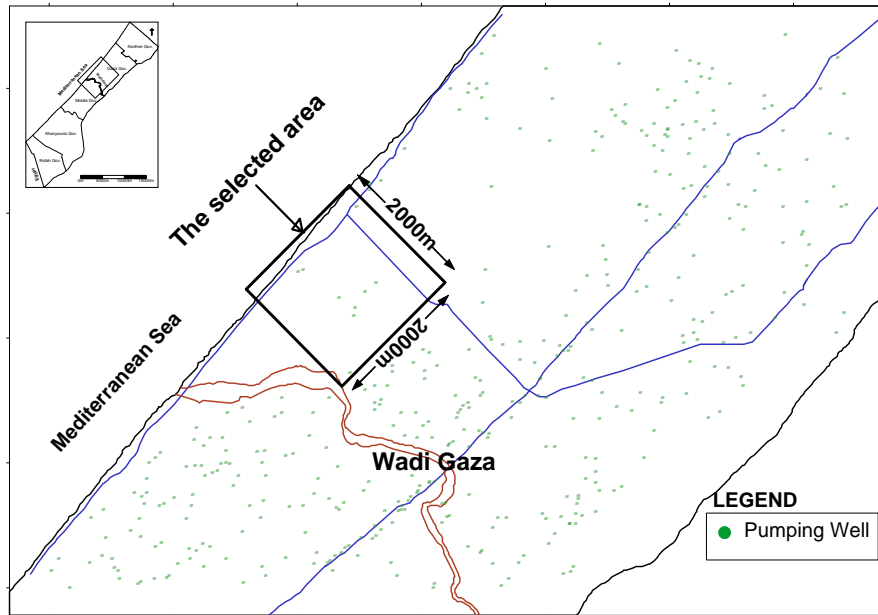
Figure 1. Location of the selected area for optimization.

two triangles to have tetrahedral elements. The flow boundary conditions consist of impermeable border along the bottom of the computational domain and recharge boundary along the top of the aquifer. The bottom side wall is also impervious for diffusive solute fluxes. Hydrostatic pressure is assumed along the vertical boundary of the sea side. The aquifer is charged with freshwater at constant flux from the inland side. At the inland side the concentration is zero (freshwater condition), while at the coastal side the relative concentration of seawater is imposed for a height of 80 m from the aquifer bottom. Initial conditions of heads and solute concentrations throughout the domain are taken from the results of the regional 3-D seawater intrusion model done in previous work [1]. Existing pumping locations (in plan view) are identified with number 1 through 9, as shown in Figure 2b. The screened portions of the well are at different vertical levels as shown.

The simulation parameters for the problem are given in Table 1. Table 2 shows the annual abstraction from the existing wells.

4. The Formulation of Optimization Problems

In groundwater management, the concept of the so called safe yield has been used for several decades by hydrogeologists all over the world to establish the limits of pumpage from a groundwater basin. Traditionally, it has been defined as the attainment and maintenance of a long-term balance between the amount of groundwater withdrawn annually and the annual amount of recharge [15]. Thus, it limits the pumpage to the amount that is replenished naturally through precipitation and surface-water seepage. Because the concept of safe yield ignores the discharge from the aquifer by evapotranspiration

Table 1. Simulation parameter of the aquifer.

Parameters	Value	Units
D_0 (molecular diffusion coefficient)	7.7×10^{-6}	m^2/s
g (gravitational constant)	9.81	m/s^2
K_{sx} (saturated hydraulic conductivity in the x direction)	2.315×10^{-4}	m/s
K_{sy} (saturated hydraulic conductivity in the y direction)	2.315×10^{-4}	m/s
K_{sz} (saturated hydraulic conductivity in the z direction)	2.315×10^{-6}	m/s
α_L (longitudinal dispersivity)	10	m
α_T (transversal dispersivity)	1	m
q_n (lateral freshwater flux)	0.0	m^3/s
ϕ (effective porosity)	0.26	
Spatial infiltration (recharge)	1.0×10^{-8}	m/s

Table 2. Annual abstraction from the existing wells.

ID	Well name	Max withdrawal (m³/y)	Mean withdrawal (m³/y)	Min withdrawal (m³/y)	Remark
Well 1	F/151	27680	17419	10090	From measurements
Well 2	G/50	37210	6142	430	Estimated from G/43
Well 3	G/24A	37210	6142	430	Estimated from G/43
Well 4	G/43	37210	6142	430	From measurements
Well 5	G/24b	10728	4879	1219	Estimated from G/42
Well 6	G/42	10728	4879	1219	From measurements
Well 7	G/24c	37210	6142	430	Estimated from G/43
Well 8	G/505	37210	6142	430	Estimated from G/43
Well 9	R/236	53004	35265	16243	From measurements
Total		288190 (790 m³/d)			From measurements

or into streams, seeps, and springs, groundwater management policies based upon it ended up with some unintended consequences, such as drying up of streams, springs and wetlands with loss of ecosystems, contamination of groundwater by polluted streams. When withdrawals exceeded the recharge on a continual basis, eventual depletion of the aquifers can lead to seawater intrusion. This has happened in a number of places in the world, including the Gaza Strip. Thus, aquifer development based upon the concept of safe yield is not safe and sustainable, as pointed out by Sophocleous [15,16] and Bredehoeft [17].
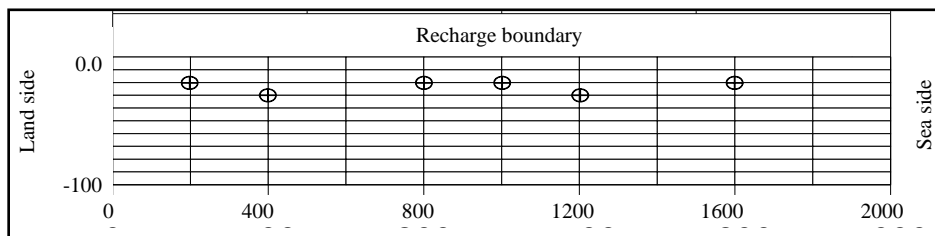

Figure 2a. Schematic elevation description of the aquifer with the projected well screens locations at the proper layer.
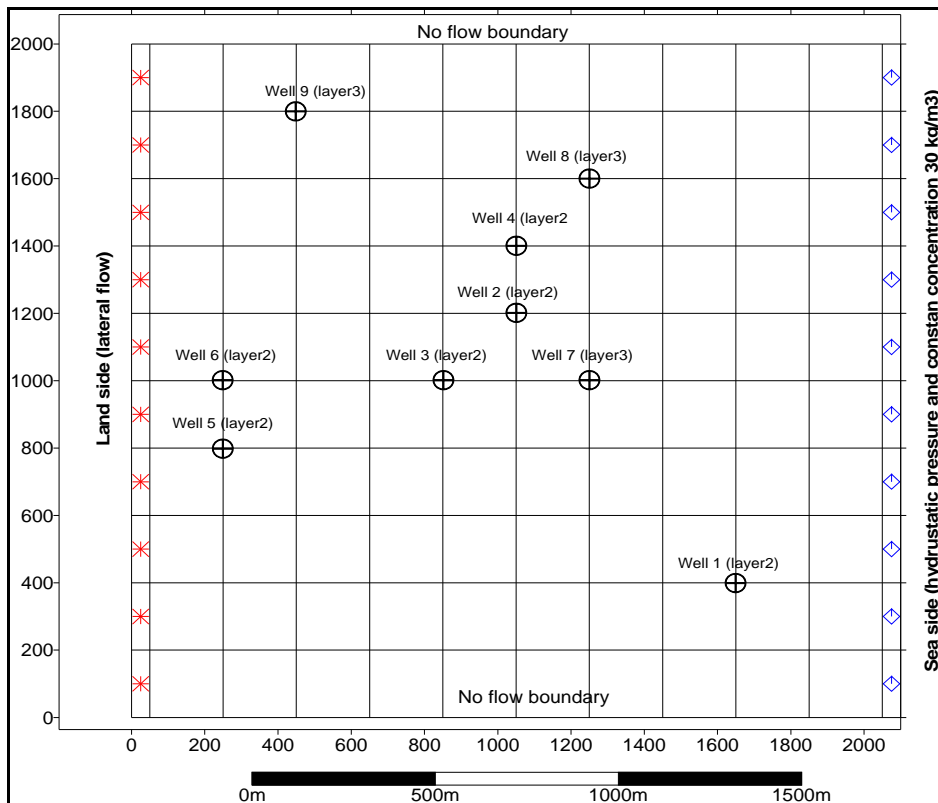

Figure 2b. Schematic Plan-view description of the aquifer with the pumping well locations.

As first elucidated by Theis [18] and eloquently reiterated by Bredehoeft *et al*. [19], Bredehoeft [17,19], Sophocleous [15,16] and Alley *et al*. [20], the source of water for pumpage is supplied by 1) increased or induced recharge, 2) decreased discharge or capture, and 3) removal of water from groundwater storage or some combinations of these three. For a sustainable groundwater development, the rate of removal of water from storage should be zero and the pumpage must be balanced by the induced recharge and/or decreased discharge [17]. Thus, it becomes mandatory to evaluate the amount of water available from changes in groundwater recharge, discharge, and storage for different levels of groundwater development. Furthermore, there is always a trade-off between the size of groundwater development and the changes that will occur in the surface and subsurface environment (i.e. changes in base-flow conditions, declines in groundwater reserves and water levels, salinity concentrations etc.). Hydrogeologists should be able to evaluate these changes and present them in a form that can be easily understood by the public and decision makers [21].

In this section we examine two management scenarios with different objectives and constraints, and find the optimal solutions for them. This study was conceived on the basis of a desire to establish a management policy for the sustainable development and management of part of the Gaza Strip aquifer system. To that end, it was envisaged to achieve the following objectives:

- Evaluation of a development strategy that will protect this part of the Gaza aquifer in terms of quantity and quality for continued use by future generations,
- To determine the safe and sustainable yields and the limits of utilization for this part of aquifer system by establishing trade-off curves between alternatives from which decision makers may select optimum development strategy.

To achieve these objectives the multi-objective management models (model 1 and model 2) of the aquifer system will be applied to this case of the Gaza aquifer. The full description of these models is presented in the previous work [5] and only the final mathematical representations are given as follows:
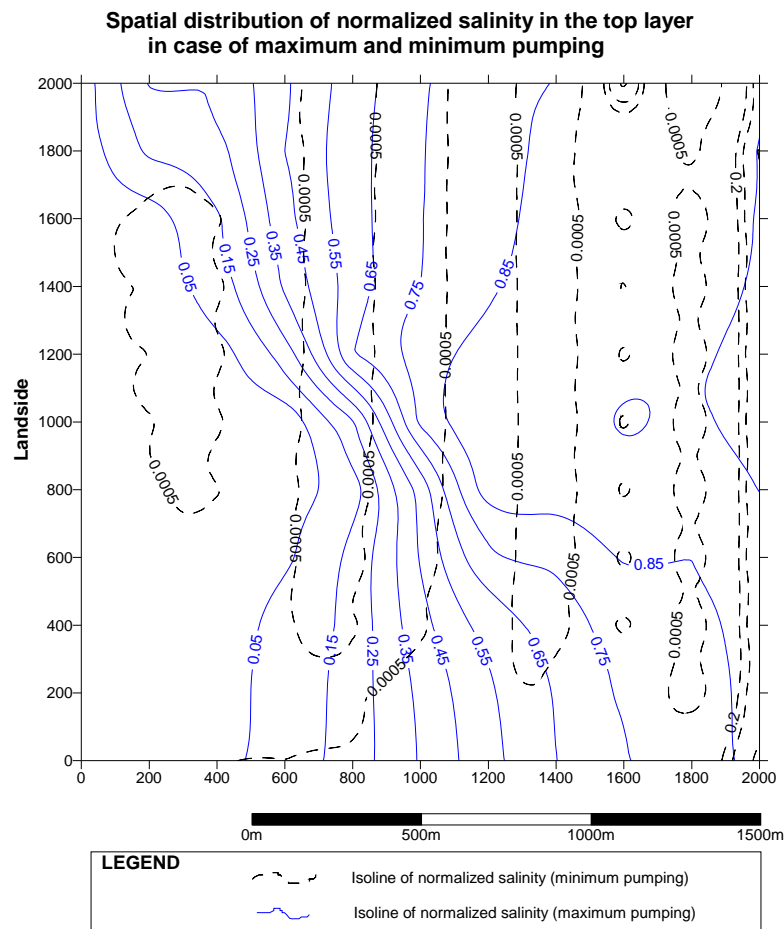
Spatial distribution of normalized salinity in the top layer in case of maximum and minimum pumping

Figure 3. Simulated normalized concentration in layer 1 in case of minimum and maximum pumping.

$$\text{Max}_{Q_i} Z = P_1 \sum_{i=1}^{n} Q_i - P_2 \sum_{i=1}^{n} Q_i c_i \qquad \text{(model 1)}$$

$$\text{Max}_{Q_i} Z = P_1 \sum_{i=1}^{n} Q_i - P_2 \sum_{i=1}^{n} Q_i c_i - r \sum_{i=1}^{n} N_i \left(\frac{h_i}{h_{min}} - 1 \right)^2$$
$$\text{(model 2)}$$

For both models, the discharge of each pumping well should stay within the specified limits; the aquifer safe yield (*S*) divided by the number of pumping wells ($Q_{max} = S/n$) for the upper limit and no pumping (Q_{min}=zero) for the lower limit. This constraint is automatically satisfied by definition of population space in GA.

4.1. GA Parameters Determination

In order to specify the limits of the management models constraints (salinity), the upper and lower limits have to be determined before using the optimization process. The lower limit of the maximum salinity level (C_{max}) is a solution with no water withdrawal; while the upper limit is a solution with maximum water withdrawal which is assumed to be equal the safe yield of the aquifer divided by the number of pumping wells as described previously. The results of simulation using the above mentioned conditions for steady state using the CODESA-3D (COupled variable DEnsity and SAturation 3-Dimensional model) [22,23], without optimization are shown in Figure 3. It shows the spatial distribution of normalized concentrations in layer 1 in case of no pumping and also in case of maximum

pumping (total recharge/number of pumping wells) for each well, which is 0.004 m³/sec for each well and for a total of 0.036 m³/sec (3,110 m³/day=1,135,296 m³/yr). This amount of maximum pumping is about 4 times the current pumping in its maximum case (790 m³/day = 288,190m³/yr) as presented in Table 2.

In the GA optimization, there are 9 decision variables, representing the 9 pumping rates. The GA is applied using the following parameters: population size=5; maximum generations parameter is determined according to the optimization results, when the fitness value is not changed by increasing the number of generations; and the values of crossover and mutation probabilities are 0.02 and 0.5, respectively. Table 3 summarized the GA parameters used in the management models.

Table 3. Summary of the parameters used in solving the management models.

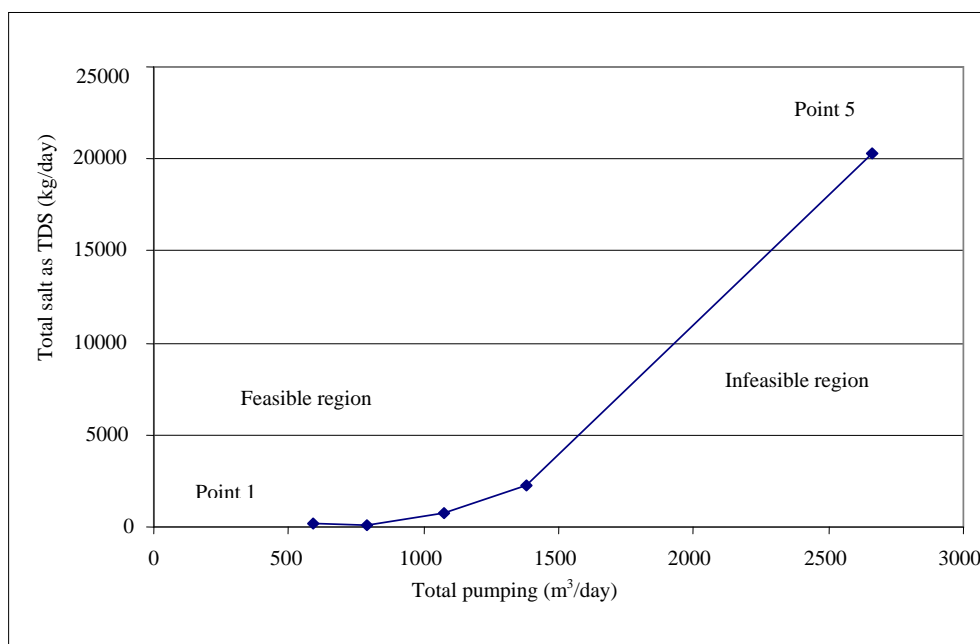| Parameter	Value
Number of decision variables (pumping wells)	9
P_1	1
P_2	1; 5; 10; 20, 50
R	0.01; 0.05; 0.1
Population size	5
Crossover probability	0.5
Mutation probability	0.02
Q_{min} (m³/s)	0.0
Q_{max} (m³/s) for each well	0.004
h_{min} (m)	1 m above mean see level (AMSL)

Figure 4. Two-objective trade-off curve (Model 1).

5. Results of Application of Management Model 1

The trade-off between the two objectives of maximizing pumping and minimizing extracted salts was investigated by combining them into a single objective, and then changing the relative weights parametrically to generate the trade-off curve shown in Figure 4. The results of op-

timal strategies and maximum concentration at the pumping wells are presented in Table 4.

As seen in Figure 4 and Table 4, the increase of pumped water amounts also increases the salt mass pumped from the aquifer because of the need to pump water from wells with higher salinity. One way of interpreting the results in Figure 4 is as follow. Between points 4 and 5 the pumping increases by 1279 m^3/d,

Table 4. Results of optimal pumping rates and chloride concentration (Model 1).

Point No.	Objective weight (P2)	Total pumping (m^3/sec)	Average con. (normalized)	Total pumping (m^3/day)	Total salt mass extracted (kg/day)	Average Chloride Con. (mg/l)
1	50	0.00683	0.00025	590	4.4	5.0
2	20	0.00913	0.00531	789	126	106
3	10	0.01247	0.02455	1077	794	491
4	5	0.01597	0.05363	1380	2220	1073
5	1	0.03077	0.25429	2659	20282	5086

Table 5. Results for three optimal solutions of Model 1.

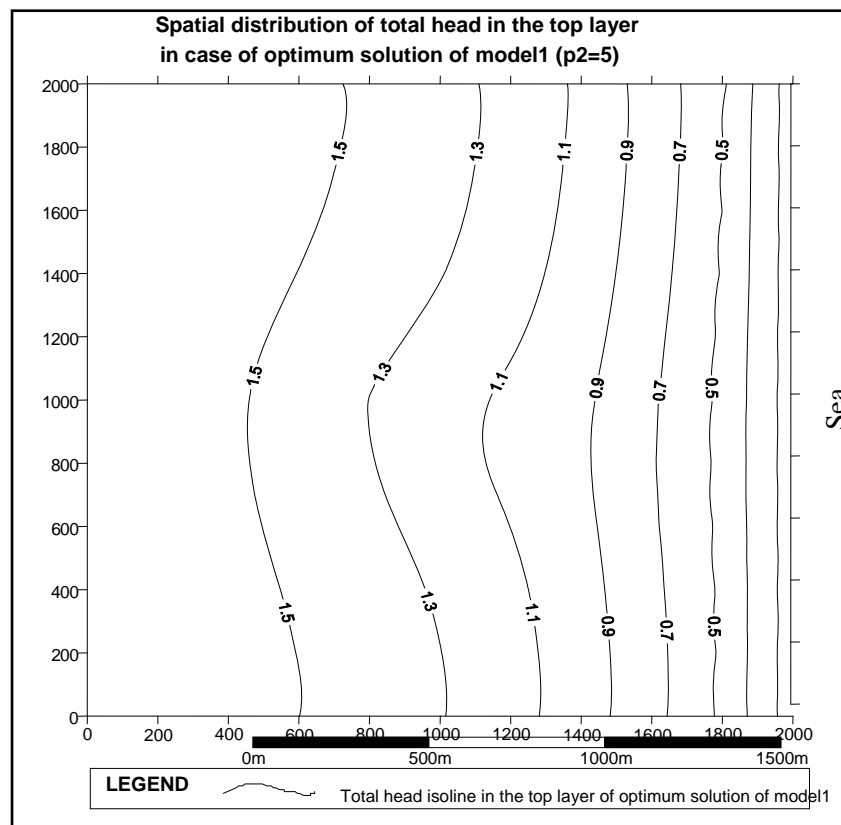| Well number	Optimal pumping rates (m^3/d)			Chloride concentration (mg/l)		
	point 3	point 4	point 5	point 3	point 4	point 5
Well 1	177	63	114	103	40	942
Well 2	340	313	329	272	207	1670
Well 3	201	335	297	976	1599	4440
Well 4	163	327	346	752	1470	3462
Well 5	2.7	22	307	2901	4092	9803
Well 6	8.1	14	332	3153	4485	9649
Well 7	8.1	44	335	81	183	1425
Well 8	174	240	259	328	565	1923
Well 9	2.7	24	340	2896	4258	9285
Total	1077	1380	2659	491	1073	5086

Figure 5a. Hydraulic head distribution (meters AMSL) for point 4 of the trade-off curve.

Spatial distribution of normalized salinity in the top layer in case of optimum solution (model1; p2=5)
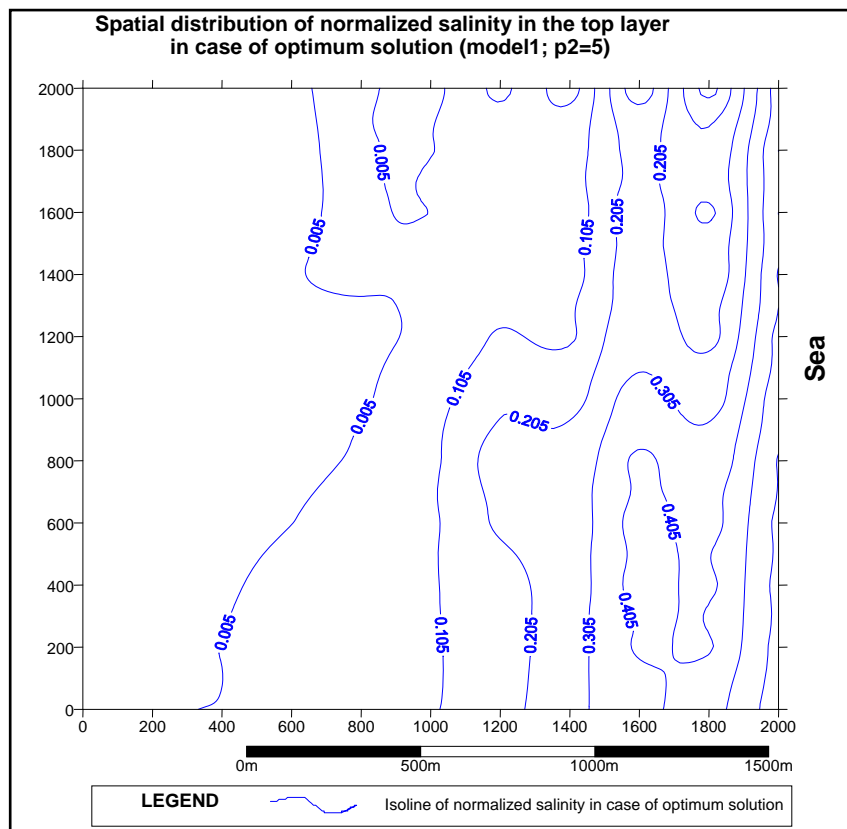

Figure 5b. Concentration distribution (normalized) for point 4 of the trade-off curve.

while the total amount of salt increases by 180,062 kg/d. This corresponds to an average additional salinity of the added water of 4,013 mg/l, which corresponds to the slope of the trade-off curve between point 4 and 5.

At point 5 the weight of salt mass objective (P2=1), which depends on concentration, is small, so the total pumping is at its maximum value and pumping rates are high even at wells with high salinity. Thus the increase of the pumping from 1379.6 m^3/d (point 4) to 2658.7 m^3/d (point 5) (a rise of 93%) results in an increase of salt mass extracted by a factor of 9. For other points the changes are less drastic.

The most interesting points are probably around the middle of the curve, where the trade-off between the two objectives is significant. One of these points (point 3) is presented in Table 5. The optimal strategy for this case is to pump more at wells of low salinity, almost not to pump at wells of very high salinity and sensitive ones like well 6 and well 9, and gradually decrease pumping rates with an increase in salinity of the water pumped. The total abstracted amount is 1077 m^3/d with average chloride concentration of 491 mg/l.

Figure 5a presents the hydraulic head distribution in layer 1 for the optimum solution of the trade-off curve at point 4 (Figure 4). It is clear from this figure that the increased pumping draws the head down near wells 2, 3, 4, 7, and 8, which are very close to each others.

Figure 5b presents the distribution of normalized concentration in layer 1 for the optimum solution of point 4 of the trade-off curve. Again, the figure shows that the salinity concentration is the highest near wells 5, 6, and 9 because they are very close to the coastline. Also the salinity contours are relatively high near wells 2, 3, 4, 7 and 8 because they are very close to each others and together draw a large amount of water.

6. Results of Application of Management Model 2

This model is introduced with more constraint on the hydraulic head in order to prevent unfavorable drop in water level due to groundwater abstraction. The results of solution of model 2 with the constraint of minimum head (h_{min}) of 1m AMSL are presented in Table 6 and Figure 6.

One way of interpreting the result in Table 6 and Figure 6 is as follows. Between points 2 and 4 the pumping increases by 323.7 m^3/d, while the total amount of salt increases by 1559 kg/d. This corresponds to an average additional salinity of the added water of 655 mg/l, which is the slope of the trade-off curve between point 2 and 4.

Table 6. Results for optimal solutions (Model 2).

Point	Penalty (*r*)	Total pumping (m³/sec)	Average con. (normalized)	Total pumping (m³/day)	Total salt mass extracted (kg/day)	Average Chloride Con. (mg/l)
1	0.1	0.00923	0.00649	797	155	130
2	0.05	0.01222	0.02087	1056	661	417
3	0.01	0.01471	0.04152	1271	1583	830
4	0.0 (model 1)	0.01597	0.05363	1380	2220	1073
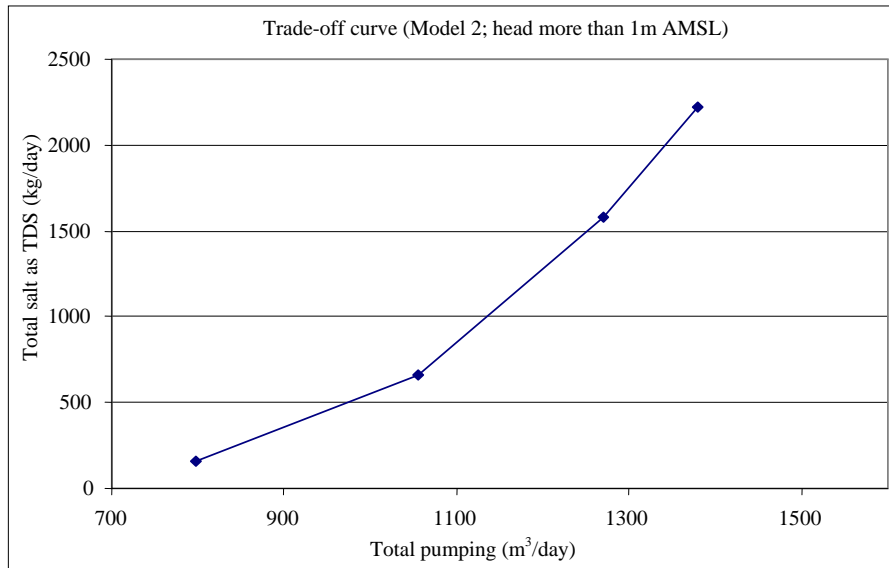
Figure 6. Two-objective trade-off curve (Model 2).
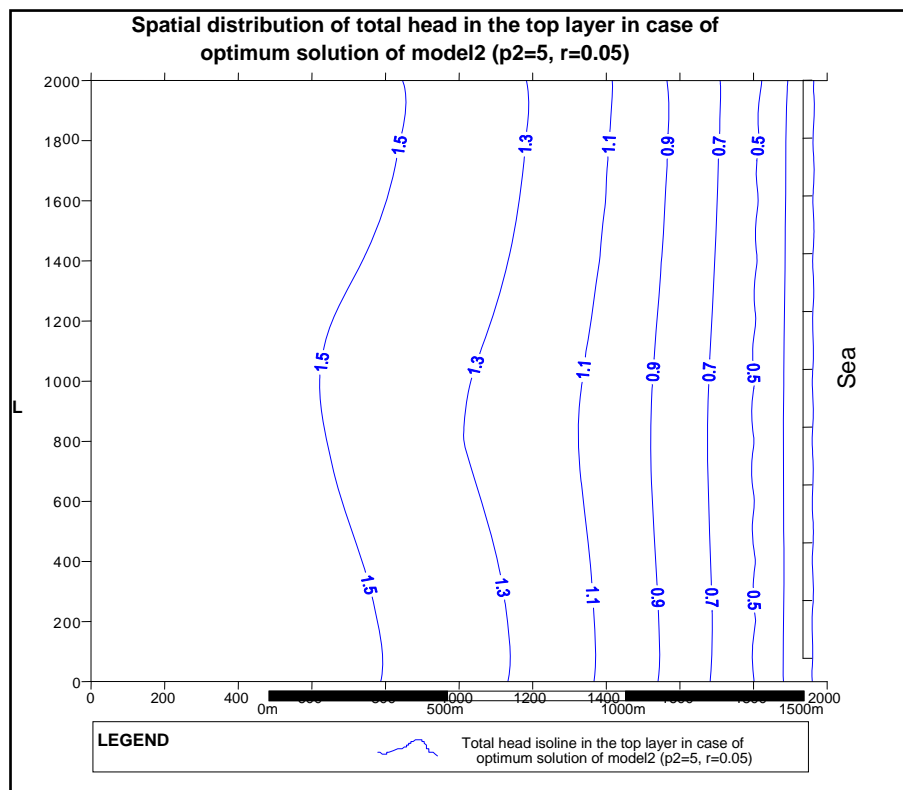
Figure 7a. Hydraulic head distribution (m AMSL) for optimum solution of model 2.

Figure 7b. Concentration distribution (normalized) for optimum solution of model 2.

Figure 7a presents the hydraulic head distribution in layer 1 for the optimum solution of model 2 with minimum head 1 m AMSL and penalty (*r*) of 0.05. It is clear from this figure that there is an outflow from the aquifer to the coastline boundary. Also, the major flow direction is towards the sea similar the case of no pumping.
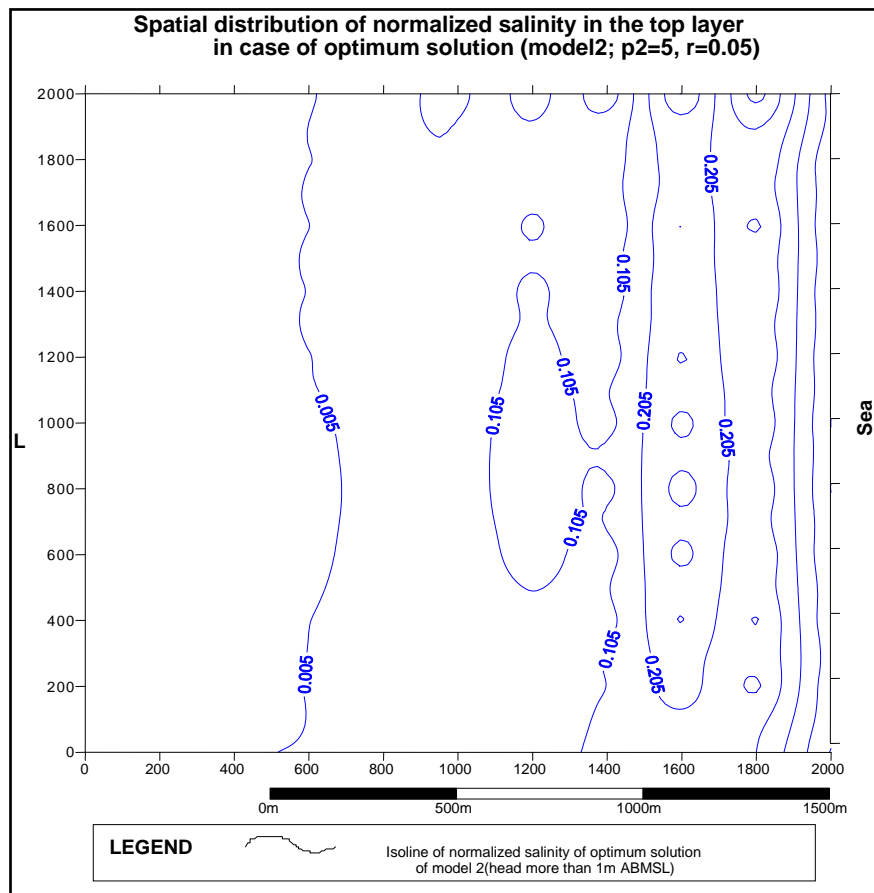
Figure 7b presents the distribution of normalized concentration in layer 1 for the optimum solution of model 2 with minimum head 1 m AMSL and penalty (*r*) of 0.05.

7. Summary and Conclusions

This study presented the numerical solution of maximum pumping rate of wells located in seawater invaded coastal aquifer in the Gaza Strip. Two multi-objective management models with different objective functions are formulated and solved for sustainable exploitation of groundwater from coastal aquifer. The simulation optimization approach links the 3D simulation model with the GA optimization model.

The application to the Gaza aquifer shows that the optimization/simulation approach can assist the managers to make better decisions and to improve the planning and management policies. It confirms that the use of the concept of safe yield alone is not enough for sustainable development of the coastal aquifer. The results on this part of Gaza aquifer show that the optimum pumping rate according to model 2 is in the range of 26%–34% of the total natural replenishment.

A relatively small size problem involving a 3D aquifer with 9 pumping wells at various depths is solved. The size of the problem is only limited by the computing resources of a Pentium 4 microcomputer. If a higher computing capability is used, optimization in a regional groundwater basin with miscible salt transport might be feasible. The present management objectives are based on the sustainability of long term operation; hence only steady state conditions are examined. For short term goals, transient objectives and transient simulations are needed. In the present models, we assumed the certainty of aquifer data. In a real-world situation, aquifer data can contain a large degree of uncertainty. This factor is not yet considered in the present study. These and other improvements will be considered in future studies.

8. Acknowledgements

6. References

[1] K. Qahman and A. Larabi. "Evaluation and numerical modeling of seawater intrusion in the Gaza aquifer (Palestine)," Hydrogeology Journal (in press), 2005a.

[2] A. Das, and B. Datta, "Development of multi-objective management models for coastal aquifers," J. Water Resour. Plann. Manage., Vol. 125, pp. 76–87, 1999a.

[3] A. Das and B. Datta, "Development models for sustainable use of coastal aquifers," J. Irrig. Drain. Eng., Vol. 125, pp. 112–121, 1999b.

[4] E. Gordon, U. Shamir, and J. Bensabat, "Optimal extraction of water from regional aquifer under salinization," J. Water Resour. Plann. Manage. Vol. 127, pp. 71–77, 2001.

[5] K. Qahman, A. Larabi, D. Ouazar, A. Naji, and A. H.-D. Cheng, "Optimal and sustainable extraction of groundwater in coastal aquifers," Stochastic Environmental Research and Risk Assessment Journal, Vol. 19, No. 2, pp. 99–110, 2005b.

[6] D. E. Goldberg, "Genetic algorithms in search, optimization and machine learning," Addison-Wesley-Longman, Reading, Mass, 1989.

[7] C. Huang and A. S. Mayer, "Pump-and-treat optimization using well locations and pumping rates as decision variables," Water Resour Res, Vol. 33, pp. 1001–1012, 1997.

[8] D. C. McKinney and M. Lin, "Genetic algorithms solution of groundwater management models," J. Water Resour. Res., Vol. 30, pp. 1897–1906, 1994.

[9] J. Holland, "Adaptation in natural and artificial systems," University of Michigan Press, Ann Arbor, 1975.

[10] D. Halhal, G. A. Walters, D. Ouazar and D. A. Savic, "Water network rehabilitation with structured messy genetic algorithm," J. Water Resours. Plann. Manage, Vol. 123, pp. 137–146, 1997.

[11] H. K. El, D. Ouazar, G. A. Walters and A.H.-D. Cheng, "Groundwater optimization and parameter estimation by genetic algorithm and dual reciprocity boundary element method," Eng. Anal. Boundary Elem., Vol. 124, pp. 129–139, 1998.

[12] A. H. Aly and P. C. Peralta, "Comparison of a genetic algorithm and mathematical programming to the design of groundwater cleanup systems," Water Resour. Res., Vol. 35, pp. 2415–2425, 1999a.

[13] A. H. Aly and P. C. Peralta, "Optimal design of aquifer cleanup systems under uncertainty using a neural network and a genetic algorithm," Water Resour. Res., Vol. 35, pp. 2523–2532, 1999b.

[14] D. Ouazar and A.H-D. Cheng, "Application of genetic algorithms in water resources," In: Katsifarakis KL (ed) Groundwater Pollution Control, WIT Press, Boston, pp. 293–316, 1999.

[15] M. Sophocleous, "Managing water resources systems: Why safe yield is not sustainable," Ground Water, New York, NY, Vol. 35, No. 4, 1997.

[16] M. Sophocleous, "From safe yield to sustainable development of water resources: The Kansas experience," Journal of Hydrology, Vol. 235, pp. 27–43, 2000.

[17] J. D. Bredehoeft, "The water budget myth revisited: Why hydrogeologist's model," Ground Water, Vol. 40, No. 4, pp. 340–345, 2002.

[18] C. V. Theis,. "The source of water derived from wells: Essential factors controlling the response of an aquifer to development," Civil Eng., Vol. 10: pp. 277–280, 1940.

[19] J. D. Bredehoeft, S. S. Papadopulos and H. H. Jr. Cooper, "The water budget myth," In: Scientific Basis of Water Resource Management, National Academy Press, Studies in Geophysics, pp. 51–57, 1982.

[20] W. M. Alley, T. E. Reilly and O. L. Frank "Sustainability of groundwater resources," US Geological Survey Circular 1186, 1999.

[21] J. Sakiyan and H. Yazicigil, "Sustainable development and management of an aquifer system in western Turkey," Hydrogeology Journal, Vol. 12, pp. 66–80, 2004.

[22] G. Gambolati, M. Putti , and C. Paniconi, "Three-dimensional model of coupled density-dependent flow and miscible transport in groundwater," Chap. 10 in Seawater Intrusion in Coastal Aquifers: Concepts, Methods, and Practices, (eds.) Bear *et al.*, Kluwer, Dordrecht, The Netherlands, pp. 315-362, 1999.

[23] G. Lecca, "Implementation and testing of the CODESA-3D model for density-dependent flow and transport problems in porous media," CRS4-TECH-REP-00/40, Cagliari, Italy, 2000.

Scientific Research

Adsorption Capacity for Phosphorus Comparison among Activated Alumina, Silica Sand and Anthracite Coal

Junling WANG[1,2,*], Yajun ZHANG[2], Cuimin FENG[2], Junqi LI[2], Guibai LI[1]

[1]*School of Municipal and Environmental Engineering, Harbin Institute of Technology, Harbin, China*
[2]*School of Environment and Energy Engineering, BUCEA, Beijing, China*
E-mail: wangjunling@bucea.edu.cn

Abstract

Experimental researches on adsorptive capacity of activated alumina, silica sand and anthracite coal for phosphorus were conducted. Results showed that performances of three filter media were all in line with Langmuir isotherm, and activated alumina adsorptive performance was much better than silica sand and anthracite coal for phosphorus removal. The adsorptive capacity of activated alumina, silica sand and anthracite coal for phosphorus was 3333μg/g, 49μg/g and 100μg/g respectively. Activated alumina displayed adsorptive function well for phosphorus, because its inner porosity, specific surface area and surface isoelectric pH value were all higher than those of other two filter media. While activated alumina was used as filter material in water treatment process, phosphorus would be removed strongly because of adsorptive characteristic of activated alumina.

1. Introduction

Generally the proportion of organic carbon, nitrogen and phosphorus is 100:10:1 for microorganism growing in pipe water, therefore, removal of phosphorus as a kind of nutrient in drinking water may be a method to restrain the regrowth of microorganism. Lehtola [1,2] reported that phosphorus could replace the organic matter as the limitation factor for microbial regrowth in drinking water with high organic matter concentration. In China, a great many surface water sources have been contaminated severely by organic matter, thus the phosphorus will be the limitation factor in drinking water and raw water there.

Many researchers have studied the removal technology for phosphorus in drinking water. Membrane treatment technology [3] and ozonation process [4] were two techniques that have been tested to remove phosphorus in drinking water, but removal rate did not get promoted. In addition, researchers [5,6] experimented and concluded that traditional water treatment process in water plant couldn't achieve efficient performance for phosphorus removal. It is unknown whether traditional filter media hold strong adsorptive capacity for phosphorus or

not. New technique and application of new filter media to improve the removal of phosphorus were creative and beneficial explored for keeping drinking water biological stability. Activated alumina was one unique media with high adsorptive capacity for many pollutants, but the character for phosphorus removal in drinking water has not been disclosed, so it is worth testing and confirming the efficiency to remove or adsorb phosphorus, at the same time, adsorptive capacity of traditional filter media silica sand and anthracite coal are tested to compare, moreover, application feasibility of activated alumina should be considered.

2. Experimental Materials and Methods

2.1. Experimental Materials

Three filter media including activated alumina, silica sand and anthracite coal were utilized in experiments. Silica sand and anthracite coal were mostly used in filtration process of water works. All materials purchased in local market showed the characteristics in Table 1.

The appliance used in experimentation included beaker flask, constant temperature oscillator, 0.45 μm

Table 1. Physical characteristics of filter media.

Item	Activated alumina	Silica sand	Anthracite coal
Granular size(mm)	1.2	0.5~1.25	1~1.8
density(g/cm^3)	1.04	2.64	1.6
porosity (%)	44.9	43.1	52.7

microporous membranes, and main chemical was KH_2PO_4.

2.2. Experimental Methods

Step one, KH_2PO_4 was dissolved into ultrapure water to form samples with various phosphorus concentration in five beaker flasks, and each volume was 1000mL. Phosphorus concentration of prepared water in beaker flasks were 500μg/L, 2000μg/L, 5000μg/L, 8000μg/L, 10000μg/L respectively. Step two, 5g activated alumina filter media was added to every beaker flask and put into constant temperature oscillator. After operating for 24h at 40 degree Celsius, samples in all beaker flasks were filtered through 0.45μm membrane, the phosphorus concentration in supernatant was examined and adsorptive capacity value was obtained.

Experimental procedure with silica sand and anthracite coal were as same as activated alumina, but phosphorus concentration varied. It was conjectured that adsorptive capacities of silica sand and anthracite coal were all lower than activated alumina, so experimental initial concentration was set at low level. Six water samples with phosphorus concentration 100μg/L, 200μg/L, 300μg/L, 500μg/L, 800μg/L, and 1000μg/L were prepared for silica sand experiment, and 50μg/L, 100μg/L, 200μg/L, 300μg/L, 500μg/L, and 1000μg/L for anthracite coal. Silica sand and anthracite coal were added by 5g respectively.

3. Results

3.1 Experiment on Phosphorus Adsorption by Activated Alumina

The formula is:

$$q_e = \frac{x}{m} = \frac{V(C_i - C_e)}{m} \qquad (1)$$

where x=quality of adsorbed adsorbate, μg
m=quality of adsorbent, g
V=volume of water sample, L
C_i=the initial concentration of adsorbate, μg/L
C_e=equilibrium concentration of adsorbate, μg/L
q_e=adsorptive capacity, μg/g
Experimental result was presented in Table 2 and plotted in Figure 1.

In view of the variation of the isotherm, it seems to obey the Langmuir isotherm. The adsorption equations are:

$$q_e = \frac{x}{m} = \frac{V(C_i - C_e)}{m} = b(q_e)^0 \frac{C_e}{1 + bC_e} \qquad (2)$$

$$\frac{C_e}{q_e} = \frac{1}{(q_e)^0} C_e + \frac{1}{b(q_e)^0} \qquad (3)$$

where b=constant value
$(q_e)^0$=adsorptive capacity extreme value, μg/g
Taking the C_e as x-axis and C_e/q_e as y-axis, Langmuir formula was plotted in Figure 2. Then

Table 2. Adsorption experimental result for phosphorus by activated alumina.

Initial Concentration C_i(μg/L)	Equilibrium Concentration C_e(μg/L)	Adsorptive Capacity q_e(μg/g)	C_e/q_e
500	56.32	88.74	0.63
2000	236.54	352.69	0.67
5000	723.83	855.23	0.85
8000	1452.49	1309.50	1.11
10000	2038.34	1592.33	1.28
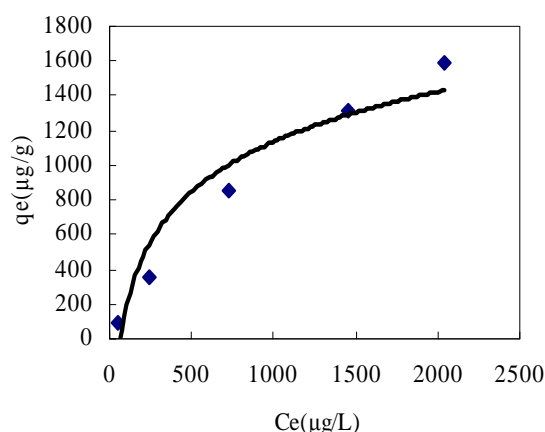
Figure 1. Phosphorus adsorption isotherm of activated alumina.
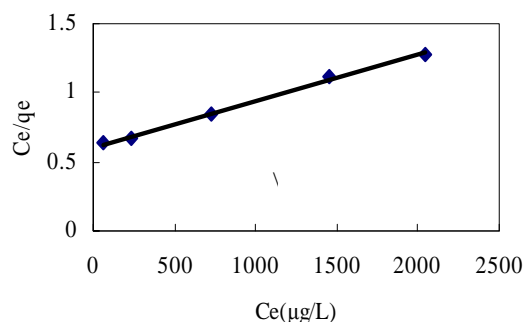
Figure 2. Simulated line of activated alumina adsorption.

the adsorptive capacity extreme value and constant *b* value can be obtained from the line intercept and line slope.

In Figure 2, the coefficient of determination was 0.9979, and the adsorption isotherm was the type of Langmuir. Based on the isotherm, the process of adsorption for phosphorus was predominant by single molecule adsorption. Then result was obtained as followed:

$$\frac{1}{(q_e)^0} = 0.0003, \quad \frac{1}{b(q_e)^0} = 0.6059, \quad b = 0.0005, \quad (q_e)^0 = 3333 \mu g/g$$

$$q_e = \frac{x}{m} = \frac{V(C_i - C_e)}{m} = b \; (q_e)^0 \frac{C_e}{1 + bC_e} = 1.67 \frac{C_e}{1 + 0.0005C_e} \tag{4}$$

Finally, the adsorptive capacity of activated alumina was 3333μg/g.

3.2. Experiment on Silica Sand

The result was shown in Table 3.

The result was obtained as followed:

$$\frac{1}{(q_e)^0} = 0.0205, \quad \frac{1}{b(q_e)^0} = 18.149, \quad b = 0.0011, \quad (qe)^0 = 48.78 \mu g/g$$

$$q_e = \frac{x}{m} = \frac{V(c_i - c_e)}{m} = b \; (q_e)^0 \frac{C_e}{1 + bC_e} = 0.054 \frac{C_e}{1 + 0.0011C_e}. \tag{5}$$

The adsorptive capacity of silica sand for phosphorus was 49μg/g.

The result showed that silica sand could adsorb phosphorus weakly, but its adsorptive capacity was far less than activated alumina.

3.3. Experiment on Anthracite Coal

The adsorption experimental result was shown in Table 4.

Then result was obtained as followed:

$$q_e = \frac{x}{m} = \frac{V(c_i - c_e)}{m} = b \; (q_e)^0 \frac{C_e}{1 + bC_e} = 3.48 \frac{C_e}{1 + 0.0348C_e} \tag{6}$$

Adsorptive capacity was 100μg/g.

More times of experiment for each filter media were conducted, results were similar to previous data respectively.

4. Discussion

4.1. Adsorption Mechanism of Activate Alumina

Experimental result demonstrated that activated alumina adsorption was consistent with the langmuir isotherm. Feng [7] reported that one type of activated alumina has large adsorptive capacity of 3950μg/g for soluble ortho-phosphorus and it was in agreement with result of this paper. Ning [8] reported that activated alumina adsorptive capacity was higher than activated carbon, and it was 3-9 times as high as activated carbon, in addition, optimum pH value was 3-4. The adsorptive capacity would increase when temperature was higher, but the adsorption for phosphorus was a type of reaction of thermal relief.

The Langmuir adsorption theory states that no solid surface is even and smooth absolutely, there are a great quantity of convex points which attract ions. The atom and ion on the convex point have unsaturated chemical bond, and creat surface activated centers, which can adsorb the adsorbate. Every center trap only one adsorbate

Table 3. Adsorption experimental result for phosphorus by silica sand.

Initial concentration $C_i(\mu g/L)$	Equilibrium concentration $C_e(\mu g/L)$	Adsorptive capacity $q_e(\mu g/g)$	C_e/q_e
100	79.25	4.15	19.09
200	162.32	7.54	21.54
300	247.89	10.42	23.78
500	423.53	15.29	27.69
800	689.02	22.20	31.04
1000	879.98	24.00	36.66

Table 4. Adsorption experimental result for phosphorus by anthracite coal.

Initial concentration $C_i(\mu g/L)$	Equilibrium concentration $C_e(\mu g/L)$	Adsorptive capacity $q_e(\mu g/g)$	C_e/q_e
50	1.59	9.68	0.16
100	3.29	19.34	0.17
200	11.74	37.65	0.31
300	46.04	50.79	0.91
500	148.11	70.38	2.10
1000	518.76	96.25	5.39

molecule. When surface activated centers were occupied completely, the adsorptive capacity reach the highest, so generally there is one layer absorbate molecule on the surface of adsorbent. Hua [9] indicated that when activated alumina was saturated, all of surface of micropore was deposited by adsorbate particle closely and tightly. Almost all micropores were not in conjunction longer and activated alumina would lose activation after saturation. Comparison of new and used activated alumina showed that new activated alumina had much more micropores and surface area than used.

The order of activated alumina adsorptive force for anion in water is followed:

$$OH^->PO_4^{3-}>F^->SO_3^->Fe(CN)_6^{4-}>CrO_4^{2-}>SO_4^{2-}>Fe(CN)_5^{3-}>Cr_2O_7^{2-}>I^->Br^->Cl^->NO_3^->MnO_4^->ClO_4^->S^{2-}$$
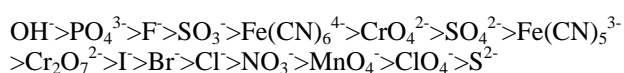
It is apparent that activated alumina adsorptive force for phosphate anion is stronger than other anions, such as SO_4^{2-} and Cl^-, so activated alumina adsorb phosphate anion in predominance.

4.2. Filter Media Comparison

According to adsorptive experiment, the adsorptive capacity of activated alumina, silica sand and anthracite coal were 3333µg/g, 49µg/g and 100µg/g respectively. Characteristic difference of three filter media are analyzed as follows, and represented in Table 5.

Porosity: It is different for every filter media. The porosity just represents the space between granules, not including inner micropore. It is micropore performing main adsorptive function instead of space between granules, so it is insignificant to compare the porosity of filter media to analyze the adsorptive capacity.

Micropore volume and pore size: The quantity of micropore decides the inner surface area, and pore size limit the dimension of attached molecules. Silica sand and anthracite coal have little inner micropore, therefore they don't have inner adsorption efficiency for phosphorus.

Surface area: In Table 5, adsorptive capacity is correlative to surface area. The specific surface area of activated alumina was larger than that of silica sand and anthracite coal. Xie [10] reported that when specific surface area was large, the adsorptive capacity would be large. Additionally it was proved that even if absorbent was the same species, the adsorptive capacity would differ because of specific surface area.

The adsorptive efficiency of silica sand or anthracite coal was very low for soluble ortho-phosphate, because they were all pure solid without micropore. The adsorptive property was only influenced by outer surface area for these two materials. Xie [11] reported that silica sand with diameter from 0.5mm to 1.2mm had a little surface area, and the surface was charged negatively. The outer surface of them was flat without micropore under the test of EM reported by Zhang [12], so the adsorptive function was not considered when they were applied to water treatment process.

Surface charge: Surface of mineral and clay was charged negatively, so they can not adsorb the anion in water. But activated alumina surface attach numerous anion OH^-, so the surface isoelectric pH value is higher than 7, and it has capacity of ion exchange. The surface isoelectric pH value of silica sand is less than 7, reportedly it is 0.7~2.2 [13], so it is charged negatively. This is the part reason for these three filter media holding different adsorptive capacity for phosphorus.

5. Conclusions

Adsorptive experiments of activated alumina, silica sand and anthracite coal were conducted for phosphorus removal, and result showed that adsorptive capacity of activated alumina, silica sand and anthracite coal were 3333µg/g, 49µg/g and 100µg/g respectively.

Effective adsorptive property of activated alumina for phosphorus results from three factors, firstly there are many inner micropore that silica sand and anthracite coal do not have. The second factor is that surface area of activated alumina is approximate $300m^2/g$ and much larger than that of silica sand and anthracite coal. Finally the surface isoelectric pH value is higher than 7, but those of silica sand and anthracite coal are far less than 7.

For the biological stabilization of tap water, in order to improve removal of phosphorus, the activated alumina could be considered as effective material to replace the traditional filter media, because in filtration process the activated alumina can remove more phosphorus relying on the adsorptive capacity. But undesirable factors exist for applicable feasibility of activated alumina, such as the frangibility, the difficulty of regeneration and high cost in running process.

6. Acknowledgement

Table 5. Comparison of every adsorbent.

Filter media	Pore volume (mL/g)	Pore size (nm)	Surface isoelectric pH	Specific surface area (m²/g)
Activated alumina	>0.39	1-100	9.5	>300
Silica sand	0	--	0.7~2.2	0.04
Anthracite coal	0	--	4~5	0.23

laboratory staffs of the laboratories of School of Environment and Energy of BUCEA.

7. References

[1] M. J. Lehtola, I. T. Miettinen, T. Vartiainen, T. Myllykangas and P. J. Martikainen, "Microbially available organic carbon, phosphorus and microbial growth in ozonited drinking water," Water Research, Vol. 35, No. 7, pp. 1635–1640, July 2001.

[2] J. Q. Sang, G. Z. Yu, X. H. Zhang and Z. S. Wang, "Relation between phosphorus and bacterial regrowth in drinking water," Chinese Journal of Environmental Science, Vol. 24, No. 4, pp. 81–84, April 2003.

[3] A. Dietze, U. Wiesmann and R. Gnirss, "Phosphorus removal with membrane filtration for surface water treatment," Water Science and Technology: Water Supply, Vol. 3, No. 5, pp. 23–30, May 2003.

[4] W. Nishijima, E. Shoto and M. Okada, "Improvement of biodegradation of organic substance by addition of phosphorus in biological activated carbon," Water Science and Technology, Vol. 36, No. 12, pp. 251–257, December 1997.

[5] D. L. Jiang, and X. J. Zhang, "Relationship between phosphorus and bacterial regrowth in drinking water," Chinese Journal of Environmental Science, Vol. 25, No. 5, pp. 57–60, May 2004.

[6] D. L. Jiang and X. J. Zhang, "Phosphorus in drinking water and it's removal in conventional treatment process," Chinese Journal of Environmental Science, Vol. 24, No. 5, pp. 796–801, May 2004.

[7] Q. Y. Feng, "Study on advanced treatment technique of phosphorus removal in drinking water," Master Dissertation, Beijing University of Technology, Beijing, 2007.

[8] P. Ning, C. L. Deng, H. P. Pu and L. M. Niu, "Adsorption of phosphate from water with activated alumina," Nonferrous metal, Vol. 54, No. 1, pp. 37–39, January 2002.

[9] N. B. Hua and Y. Z. Ruan, "Microstructures of active alumina reproduction by heat-treatment method," Journal of Fuzhou University (Natural Science Edition), Vol. 35, No. 1, pp. 81–84, January 2007.

[10] H. Xie, W. B. Jia and Z. G. Wu, , "Performance of activated aluminum oxide as a fluorine-removal agent," Journal of Huazhong University of Science and Technology (medical sciences), Vol. 34, No. 5, pp. 644–646, May 2005.

[11] S. B. Xie, J. S. Lou, Z. W. Xiong and Y. Q. Wang, , "Research on phenol removal by silica sand filter," China Water and Wastewater, Vol. 16, No. 8, pp. 8–11, August 2000.

[12] X. H. Zhang, X. C. Xiang and Q. Y. Meng, "Study on a new filtration medium-activated anthracite coal and its filtration process," Water Purification Technology, Vol. 26, No. 1, pp. 54–57, July 2007.

[13] M. M. Benjiamin, R. S. Sletten, R. T. Bailey and T. Bennett, "Sorption and filtration of metals using iron-oxide coated sand," Water Research, Vol. 30, No. 11, pp. 2609–2620, November 1996.

Scientific Research

Research on Plane 2-D Sediment Model of a Watercourse on Yangtze River

Yong FAN

Water Conservancy and Hydropower Institute of Hohai University, Nanjing, China
E-mail: fyhhu@126.com

Abstract

To provide basis for sand excavation of hydraulic fill and land forming in Daohukou region in a watercourse (Wuhan reach) on Yangtze River, a 2-D water-sand mathematic model of this river reach is established. The variation of water levels of this reach and the back silting of watercourse after sand excavation are calculated. The rationality of the results calculated by this model and the measured data are validated and analyzed. The results show that, this model is reasonable and reliable.

1. Introduction

To comprehensively renovate and exploit the flood control and environment of the new and old Wujin dike inner section in Daohuhou region of Wuchang District, hydraulic fill and land forming project is constructed by the government of Wuhan City. The main sand source region is located at the right of Yangsiji channel bar, Heposhan point bar, and the right of Baishazhou tail. Engineering hydraulic fill and sand excavation is mainly utilized. According to the landform data of the hydraulic fill area provided by Wuhan City, this area is relatively low with some fish ponds and cultivated land, including some residential area, etc. The land elevation varies from 23.0 to 27.0mm, and the area is about 0.65km^2. This project is located at the urban area of Wuhan, so the source of soil materials in surrounding areas is very tense. The transportation distance from the soil field is far and the cost is high. To solve this problem, lower the engineering cost and reduce the impact to surrounding ecology and environment, sand will be excavated from the river in Wuhan reach on Yangtze River for hydraulic fill. It is estimated that about 2 million cubic meters of sand will have to be filled for this area. After sand excavation, the river regime of this river reach will be adjusted and the riverbed scouring and silting will be changed. Potential adverse effects may be brought to the flood control safety, navigation safety, water ecology, environment, and others of this reach. To reduce these adverse effects, the sand excavation location, scheme and countermeasures should be reasonably determined on the basis of analyzing and predicating the evolution law and development trend of watercourse of the sand excavation reach. Therefore, the feasibility of this sand excavation project should be demonstrated to provide referencing basis for the examination and approval by the water administrative department.

On the basis of considering the synchronous impact and continuous effect for riverbed evolution by sand excavation, mathematic control equations, which describe the water-sand movement in river in detail, are introduced. The mathematic model of plane 2-D sediment of the sand excavation river is established. The variation of water-sand movement in the sand excavation river is simulated in detail. Except specially noted, the Beijing coordinate system in 1954 will be used as the plane coordinates. The elevation standard in 1985 is used as the elevations of water levels and landform.

2. Calculation and Analysis of Plane 2-D Sediment Model

Through comprehensively considering the river regime, engineering study contents, hydrology data, and other factors, the scope of calculated reach of the 2-D mathematic model is selected as: Xiaojunshan is selected as the inlet section on the upstream, Yangluo is selected as the outlet control section on the downstream, and the total length is about 55km; and the influx of Hanjiang River is considered.

2.1. Plane 2-D Sediment Mathematic Model

Plane 2-D current and sediment equations under orthogonal curvilinear coordinate system are adopted.

1) Continuity equation and motion equation of current:

$$\frac{\partial C_\xi C_\eta Z}{\partial t} + \frac{\partial (C_\eta HU)}{\partial \xi} + \frac{\partial (C_\xi HV)}{\partial \eta} = 0 \tag{1}$$

2) Motion equation [1,2] of current:

$$\frac{\partial (C_\xi C_\eta HU)}{\partial t} + [\frac{\partial}{\partial \xi}(C_\eta HU \cdot U) + \frac{\partial}{\partial \eta}(C_\xi HV \cdot U)$$

$$+ HVU \frac{\partial C_\xi}{\partial \eta} - HV^2 \frac{\partial C_\eta}{\partial \xi}]$$

$$+ C_\eta gH \frac{\partial Z}{\partial \xi} = -\frac{C_\xi C_\eta n^2 gU\sqrt{U^2+V^2}}{H^{1/3}} + C_\zeta C_\eta fHV$$

$$+ [\frac{\partial}{\partial \xi}(C_\eta H\sigma_{\xi\xi}) + \frac{\partial}{\partial \eta}(C_\xi H\sigma_{\eta\xi}) + H\sigma_{\xi\eta}\frac{\partial C_\xi}{\partial \eta} - H\sigma_{\eta\eta}\frac{\partial C_\eta}{\partial \xi}] \tag{2}$$

$$\frac{\partial (C_\xi C_\eta HV)}{\partial t} + [\frac{\partial}{\partial \xi}(C_\eta HU\cdot V) + \frac{\partial}{\partial \eta}(C_\xi HV\cdot V) + HUV\frac{\partial C_\eta}{\partial \xi}$$

$$- HU^2\frac{\partial C_\xi}{\partial \eta}] + C_\xi gH\frac{\partial Z}{\partial \eta} = -\frac{C_\xi C_\eta n^2 gV\sqrt{U^2+V^2}}{H^{1/3}} - C_\zeta C_\eta fHU$$

$$+ [\frac{\partial}{\partial \xi}(C_\eta H\sigma_{\xi\eta}) + \frac{\partial}{\partial \eta}(C_\xi H\sigma_{\eta\eta}) + H\sigma_{\xi\eta}\frac{\partial C_\eta}{\partial \xi} - H\sigma_{\xi\xi}\frac{\partial C_\xi}{\partial \eta}] \tag{3}$$

Where, U and V represent the velocity components in ξ and η directions; Z represents the water level; g represents the acceleration of gravity; $\sigma_{\xi\xi}$, $\sigma_{\eta\eta}$, $\sigma_{\xi\eta}$, $\sigma_{\eta\xi}$ are stresses, which expressions are as follows:

$$\sigma_{\xi\xi} = 2\upsilon_t[\frac{1}{C_\xi}\frac{\partial U}{\partial \xi} + \frac{V}{C_\xi C_\eta}\frac{\partial C_\xi}{\partial \eta}] \tag{4}$$

$$\sigma_{\eta\eta} = 2\upsilon_t[\frac{1}{C_\eta}\frac{\partial V}{\partial \eta} + \frac{U}{C_\xi C_\eta}\frac{\partial C_\eta}{\partial \xi}] \tag{5}$$

$$\sigma_{\xi\eta} = \sigma_{\eta\xi} = \upsilon_t[\frac{C_\eta}{C_\xi}\frac{\partial}{\partial \xi}(\frac{V}{C_\eta}) + \frac{C_\xi}{C_\eta}\frac{\partial}{\partial \eta}(\frac{U}{C_\xi})] \tag{6}$$

C_ξ, C_η are Lame coefficients in the physical orthogonal curvilinear coordinate system:

$$C_\xi = \sqrt{x_\xi^2 + y_\xi^2}, \quad C_\eta = \sqrt{x_\eta^2 + y_\eta^2} \tag{7}$$

3) Suspended sediment transport equation:

$$\frac{\partial (C_\xi C_\eta HS_i)}{\partial t} + [\frac{\partial}{\partial \xi}(C_\eta HU \cdot S_i) + \frac{\partial}{\partial \eta}(C_\xi HV \cdot S_i)$$

$$= [\frac{\partial}{\partial \xi}(\frac{\varepsilon_\xi C_\eta}{C\xi}\frac{\partial HS_i}{\partial \xi}) + \frac{\partial}{\partial \eta}(\frac{\varepsilon_\eta C_\xi}{C_\eta}\frac{\partial HS_i}{\partial \eta})] + C_\xi C_\eta \alpha_i \omega_i(S_i^* - S_i) \tag{8}$$

Where, i represents the group of sediment; S_i and S_i^* represent the sediment concentration and sediment carrying capacity; ε_ξ and ε_η represent the sediment diffusion coefficient in coordinate direction.

The grouping sediment carrying capacity $S_i^* = P_i^* \cdot S^*$, is controlled by current strength and bed sand gradation. S^* represents the sediment carrying capacity of current with the average settling speed of ω_m; P_i^* represents the gradation of grouping sediment carrying capacity [3].

4) Riverbed deformation equation [4,5] is:

$$\gamma_s^{'}\frac{\partial Z_b}{\partial t} + \frac{1}{C_\xi}\frac{\partial g_{b\xi}}{\partial \xi} + \frac{1}{C_\eta}\frac{\partial g_{b\eta}}{\partial \eta} = \sum_{i=1}^{n}\alpha_i\omega_i(S_i - S_i^*) \tag{9}$$

2.2. Model Numerical Method and Calculation Program

While solving the differential equation, finite volume method is adopted for the numerical discrete of control Equations (1–9). The solution of discrete equations is based on SIMPLEC arithmetic. The Gauss-Seidel iteration is used as the main iterative algorithm in the solution process. Over-relaxation and under-relaxation techniques [6] are used.

2.3. Treatment of Problems Relevant to Mathematical Calculation

2.3.1. Division of Calculating Grid
Body-fitted orthogonal curvilinear grid at the boundary of watercourse is adopted as the 2-D calculating grid. The quantity of grid nodes is 289×70. The space between grids in the direction of the current varies from 60 to 300m, and the space in the direction vertical to the current varies from 10 to 80m.

2.3.2. Treatment of Moving Boundary
According to the depths of water calculated in each time, distinguish the calculating nodes of water area and land area; boundary partition wall method is adopted for the treatment of calculating nodes at bank boundary; a small keel clearance is maintained for the calculating nodes at bank boundary to make the calculation possible; water level extension [7] at alongshore water area is adopted by the land area water level.

2.3.3. Roughness, and Other Parameters and Coefficients
The roughness in the calculating river reach is reversely calculated by using the measured hydrological data in general. According to the local landform, it is debugged in blocks according to the element. The calculated roughness coefficient in this paper varies from 0.018 to 0.022 in riverbed part and from 0.022 to 0.035 in bottomland.

The turbulent viscosity coefficient νt of the current is related to the turbulent stress in the current. In general situations, equation with constant coefficients is used to simplify the calculation. Its empirical correlation is νt= cu*h, where c represents the empirical constant (the value range is from 0.25 to 1.0) [8,9]. In this calculation, c is taken as 1.0. For sediment turbulent diffusion coefficient, its value is generally taken as the same of current turbulent viscosity coefficient, that is to say εx, εy=νt.

2.3.4. Model Definite Conditions

The definite conditions of the model include boundary conditions and initial conditions. Constant flow boundary conditions are adopted. Flux, sediment concentration, gradation, and others are provided for the upper reach; water level is provided for the lower reach; the velocity and sediment concentration at bank boundary are taken as zero. The initial landforms of riverbed and bed sand gradations of the calculated river reach are given.

Initial conditions: the initial velocity field is given as zero, and the initial water level is given according to the water surface profile gradient ratio. The errors brought by the initial values will be disappeared soon in the calculation.

3. Analysis of Mathematic Modes Calculation under the Influence of Sand Excavation

The influences to flood control, deposition, and others of Yangtze River by this project are evaluated through the calculation of variations of water levels, velocities, flow regimes, riverbed sediment depositions before and after the sand excavation project in this section.

3.1. Analysis for the Variation of Plane Velocity Field and Flow Regime

The main streamlines of the river reach of this project before and after the excavation of sand are compared in Figure 1. The engineering local flow fields before and after the excavations of sand are shown in Figure 2 and Figure 3. From Figure 1 to Figure 3 we can see that, the main streamlines of this engineering river reach are
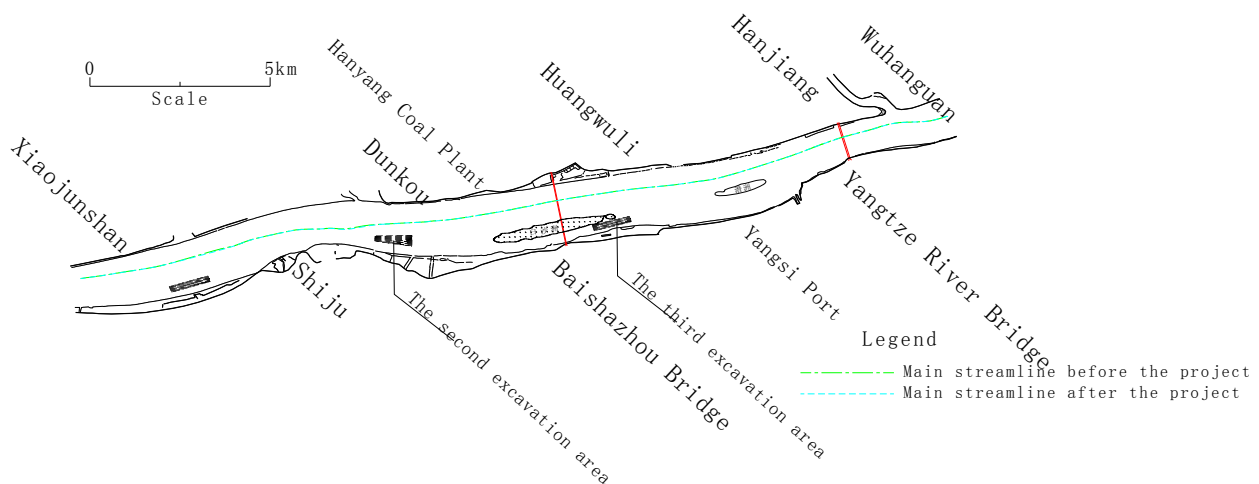

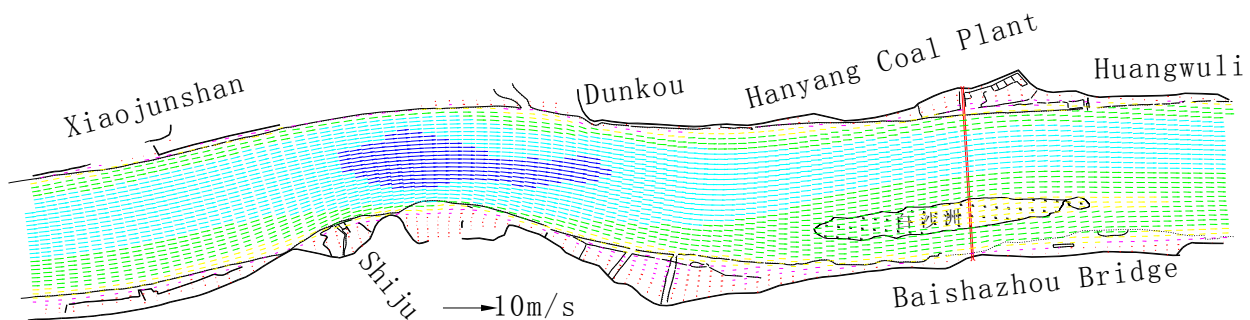**Figure 1. Comparison of mainstreams before and after.**

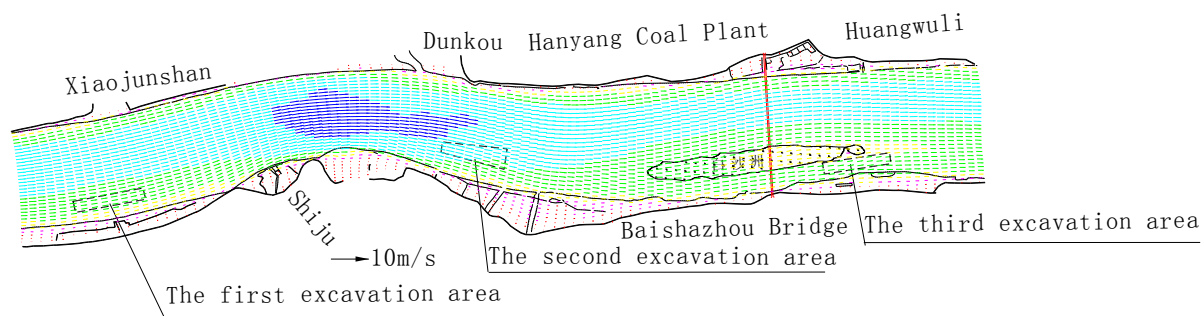**Figure 2. Local flow field before implementing this project (Q=76,100m³/s).**

JWARP

Figure 3. Local flow field after implementing this project (Q=76,100m³/s).

straightening with the increasing of flux, and are restricted by the river channel, both banks' embankment revetment works and river beach. Except the area of this project, the positions of main streamlines are not changed obviously before and after the excavation of sand. The plane velocity field and flow regime of the engineering river reach are not changed obviously.

3.2. Analysis of Water Level Variation

To compare and analyze the water levels before and after implementing this project, 40 water level analyzing points are selected and arranged near the water area of this planned sand excavation project to plot the contour map for the variation of water levels before and after implementing this project. Through analyzing the variation of water levels of all analyzing points and the contour map for the variation of water levels of this river reach, the potential influences to the water levels of the watercourse by the sand excavation project are studied. The calculating results are shown in Figure 4 (variation of water level field). The calculating results show that, the variation of water levels is different quantitatively but consistent qualitatively after the implementing of this project.

3.3. Analysis of Sediment Back Silting Quantity in Sand Excavation Area

The back silting of sediment is calculated by selecting the water-sand data in three typical years of 2004 (medium flow and less sand). From the calculating results (Figure 5) we can see that, the back silting rates under different incoming water and incoming sediment conditions of the excavation areas vary greatly. Generally, the larger of the incoming sediment is, the higher the back silting rate will be. The first excavation area is located at the broadening section between Junshan Longchuanji node and Shiju node. The annual back silting rate of this area basically maintains at 54.9 to 79.8% in the year with large incoming sediment from the upper reach. And it can also maintain at about 27% in the year with small sediment. The second excavation area is located at the upper of the broadening section at the downstream of Shiju node. This area is greatly influenced by the swing of mainstream. The back silting rate in the year with medium flow and medium sediment will reach to 41.5%, and it will be below 15% in other years in general. The third excavation area is located at the slack water area at the tail of the right branch of Baishazhou. Compared with the two other areas at the upper reach, the variation of annual back silting rate is small even if the incoming water and sediment conditions are changed. It can maintain at 24.4 to 39.4% in general.
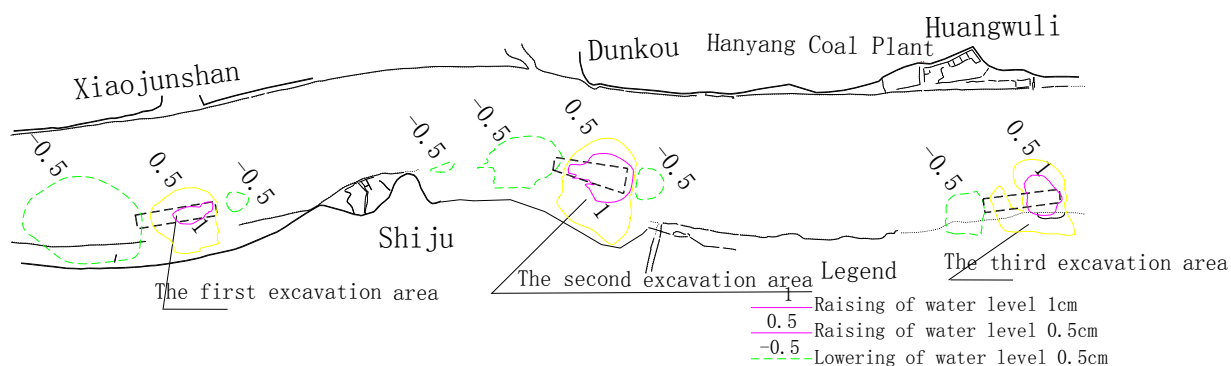

Figure 4. Variation scope of water levels after the implementing of sand excavation project (Q=76,100m³/s).
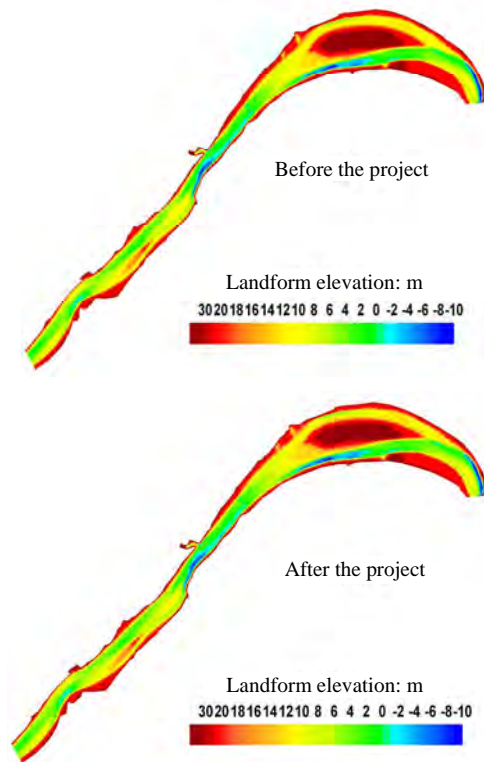
Figure 5. Comparison of landform of the engineering river reach after scouring and silting before and after the excavation of sand (2004).

4. Conclusions

We can see from the calculation results of the above model that:

1) If the incoming water, incoming sediment and boundary conditions are not varied greatly, Wuhan reach can still maintain the current river regime pattern. Due to the control of both banks by the nodes and the construction of revetment works on Wuhan reach, the current general river regime is relatively stable, which provides favorable river regime conditions for the excavation of sand.

2) The selected excavation area is far from the Yangtze River embankment and shoreline. The nearest distance to the embankment is 340m. There are wide high floodplains outside the embankment. The calculation results of the mathematic model show that, the positions of the mainstream line are not changed obviously before and after the sand excavation, except slight change in the engineering area. There are basically no significant changes in the plane velocity field and flow state of the engineering river reach. After the implementation of sand excavation project, the influence to the diversion ratio between Baishazhou inlet and Qianzhou channel is small, and the diversion ratio

of Tianxingzhou inlet is not affected. After the implementation of sand excavation project, the velocity values in the excavation area are all reduced, and the overall performance of the water level is slightly banked-up. The maximum banked-up value of water level occurs at the lower reach of the excavation area. However, the maximum bank-up value of all three-excavation areas is not exceeding 2.3cm. The implementation of the sand excavation project causes the redistribution of wetted cross-section unit width flux. The velocities a the left and right of the excavation area are reduced, while the velocities within certain scope of the upper reach and lower reach of the excavation area are slightly increased. After the implementation of sand excavation project, the changes of riverbank near embankment at the left of this project, the water level in coastal water, and the velocity are small (slightly reduced). The influences to the water level and velocity are mainly concentrated at local coastal segments at the right near this project. The influence is limited because the sand excavation area is far from the main water-related project in the engineering river reach.

Through rating and validation of measured water levels along Wuhan reach, the rating and validation of velocity distribution and sediment distribution in typical cross sections, the validation results of scouring and silting amount and distribution of the riverbed, we can see that, the adopted plane 2-D water-sand mathematic model and the treatment of its parameters and coefficients are reasonable and feasible. The model can preferably reflect the movement characters of water and sediment in the river reach, as well as the scouring and silting variation law of riverbed. Therefore, this model can be used for calculating and analyzing the impact to watercourse current and river regime by the excavation of sand.

5. References

[1] X. L. Liu, L. Xun and Q. Zheng, "Computational fluid dynamics," Harbin: Harbin Press, 1998.

[2] D. SilvaA, "Turbulent flow in sine generated meandering channel," Queen's University, Kingston, Ontario, Canada, March 1995.

[3] A. Vanoni, "Sediment engineering," Beijing: Water Conservancy Press, 1981.

[4] T. Y. Li, "Research and preliminary application of sediment mathematic model in fluctuating backwater area of Three Gorges Reservoir [M]," Wuhan: Wuhan Industrial Press, 1993.

[5] Z. L. Wei, "A finite element solution of current and sediment problems in watercourse [J]," Journal of Wuhai Water Conservancy and Hydroelectric Power, 1990.

[6] J. H. Xie. "River simulation [M]," Beijing: Water Conversancy & Power Press, 1990.

[7] Y. L. Zhao and X. F. Zhang, "Hydrology [M]," Beijing: China Architecture & Building Press, 2001.

[8] X. Q. Zhou, "Computational Hydraulics [M]," Beijing: Tsinghua University Press, 1995.

[9] Y. C. Chang, "Lateral mixing in meandering channels," PhD dissertation, The Department of mechanics and Hydraulics, University of Iowa, 200.

Scientific
Research

Multi Objective Multireservoir Optimization in Fuzzy Environment for River Sub Basin Development and Management

D. G. REGULWAR[1,*], P. Anand RAJ[2]

[1] *Department of Civil Engineering, Government College of Engineering, Aurangabad, India*
[2]*Water & Environment Division, Department of Civil Engineering,*
National Institute of Technology, Warangal, India
E-mail: *dgregulwar@rediffmail.com*
Received June 19, 2009; *revised July* 19, 2009; *accepted July* 22, 2009

Abstract

In this paper, a multi objective, multireservoir operation model is proposed using Genetic algorithm (GA) under fuzzy environment. A monthly Multi Objective Genetic Algorithm Fuzzy Optimization (MOGAFU-OPT) model for the present study is developed in 'C' Language. The GA parameters i.e. population size, number of generations, crossover probability, and mutation probability are decided based on optimized values of fitness function. The GA operators adopted are stochastic remainder selection, one point crossover and binary mutation. Initially the model is run for maximization of irrigation releases. Then the model is run for maximization of hydropower production. These objectives are fuzzified by assuming a linear membership function. These fuzzified objectives are simultaneously maximized by defining level of satisfaction (λ) and then maximizing it. This approach is applied to a multireservoir system in Godavari river sub basin in Maharashtra State, India. Problem is formulated with 4 reservoirs and a barrage. The optimal operation policy for maximization of irrigation releases, maximization of hydropower production and maximization of level of satisfaction is presented for existing demand in command area. This optimal operation policy so determined is compared with the actual average operation policy for Jayakwadi Stage-I reservoir.

Keywords: Optimization, Multi Objective Analysis, Multireservoir, Genetic Algorithms, Fuzzy Logic, Reservoir Operation

1. Introduction

In river basin studies, reservoir systems have their unique aspects and a variety of mechanisms are used in defining their operating rules [1]. Most of the water resources optimization problems involve conflicting objectives. The operation of a multi-purpose, multireservoir system consists of conflicting goals and requirements and consequently, several practical operating scenarios may exist. However, there are no standard operating rules, which are applicable to all situations. The successful management and operation of any reservoir system, therefore, lies in the ability to select the appropriate operating policy from amongst the available set of policies. Yeh [2] reviewed reservoir management and operation models. Optimal coordination of the many facets of reservoir systems requires the assistance of computer modeling tools to provide information for rational management and operational decisions. Labadie [3] has reviewed state-of-the-art in optimization of multi reservoir systems.

Genetic algorithms are search algorithms based on the mechanism of natural selection and natural genetics. It is originated in mid 1970s [4,5] and has developed into an effective optimization approach. Oliveira and Loucks [6] have presented operating rules for multireservoir systems by using genetic search algorithms. Using simulation they have evaluated each policy to compute performance index for a given flow series. Wardlaw and Sharif [7] have presented several alternative formulations of a genetic algorithm for reservoir system. Multireservoir systems optimization has been studied by Sharif and Wardlaw [8]. A genetic algorithm approach has been presented by considering the existing development situation in the basin and two future water resource development

scenarios. Chang and Yang [9] have presented optimizing the rule curves for multi-reservoir operations using a genetic algorithm and HEC-5. Srinivasa Raju and Nagesh Kumar [10] have discussed application of genetic algorithms for irrigation planning. GA was used to determine optimal cropping pattern for maximizing benefits for an irrigation project. Juran Ali Ahmed and Arup kumar Sarma [11] have demonstrated genetic algorithm model for finding the optimal operating policy of a multipurpose reservoir. Multireservoir operation planning using hybrid GA and linear programming have been presented by Reis *et al*. [12].They have proposed a new approach using GA and LP to determine operational decisions for reservoirs of a hydro system throughout a planning period, with the possibility of considering a variety of equally likely hydrologic sequences representing inflows. Jothiprakash and Ganeshan Shanthi [13] have developed GA model and applied to Pechiparai reservoir in Tamil Nadu, India to derive the optimal operational strategies. The fundamental guidelines for GA to optimal reservoir dispatching have been presented by Chang Jian-Xia *et al*. [14]. They have concluded that with three basic operators selection, crossover and mutation GA could search the optimum solution or near-optimal solution to a complex water resources problem. They have also considered alternative formulation schemes of GA. Reis *et al*. [15] have demonstrated a hybrid method using GA and linear programming to determine operational decisions for a reservoir system over the optimization period. A multi-objective Evolutionary Algorithm (MOGA) to derive a set of optimal operation policies for a multipurpose reservoir system have been presented by Janga Reddy and Nagesh Kumar[16]. One of the main goals in multiobjective optimization was to find a set of well distributed optimal solutions along the pareto front.

Anand Raj [17] has presented multicriteria methods in river basin planning. ELECTRE-I and ELECTRE-II techniques were applied for water resources planning to Krishna river basin, India. Anand Raj and Nagesh kumar [18] have presented ranking of river basin alternatives using ELECTRE. Anand Raj and Nagesh kumar [19] have presented planning for sustainable development of a river basin using fuzzy logic. Simonovic [20] discussed tools for water management. He discussed the complexity of water resources domain and the complexity of the modeling tools in an environment characterized by continuous rapid technological development. Bender and Simonovic [21] have presented a fuzzy compromise approach to water resource systems planning under uncertainty. Panigrahi and Mujumdar [22] have developed fuzzy rule based model for the operation of a single purpose reservoir. The steps involved in the development of the model include construction of membership functions for the inflow, storage, demand and the release, formulation of fuzzy rules, implication and defuzzification. They

have applied this methodology to the Malaprabha irrigation reservoir in Karnataka, India. Nagesh Kumar *et al*. [23] have presented optimal reservoir operation using fuzzy approach. Comparison of fuzzy and nonfuzzy optimal reservoir operating policies have presented by Tilmant *et al*. [24]. Srinivasa Raju and Duckstein [25] have presented multiobjective fuzzy linear programming for sustainable irrigation planning. This MOFLP model have been formulated for the evaluation of management strategy for the case study of Jayakwadi irrigation project, Maharashtra State, India. Regulwar and Anand Raj [26] have presented development of 3-D optimal surface for obtaining operation policies of a multireservoir in fuzzy environment using genetic algorithm.

With respect to the literature review, it can be said that multiobjective multireservoir optimization gives better operating policies for reservoirs under fuzzy environment. Therefore this work is undertaken for presenting operating policies for a case study to utilize the water resource optimally and also to present maximized level of satisfaction and corresponding operating policy. Also the entire range of optimal operation policies, for different levels of satisfaction i.e., λ (ranging from 0 to 1), are determined.

2. System Description

The multireservoir system in Godavari river sub basin taken for present study consists of Jayakwadi project Stage-I across river Godavari, Jayakwadi project Stage-II across river Sindaphana, Yeldari project and Siddeshwar project across river Purna, and Vishnupuri barrage across river Godavari in Maharashtra state, India. The salient features of reservoirs are presented in Table 1. The schematic representation of the physical system is shown in Figure 1. The irrigation demand and inflow is presented in Table 2.

3. Model Development

The objective of the study is to develop optimal operation policies for a multireservoir in a river sub basin. For this a monthly Multi Objective Genetic Algorithm Fuzzy Optimization (MOGAFUOPT) model is developed. The two objectives considered in this study are:

1. Maximization of irrigation releases (i.e., IR)
2. Maximization of hydro-power production (i.e., HP)

$$\text{Max } Z = \sum_i \sum_t (\text{IR})_{it} \qquad \forall \, i = 1,2,3,4 \qquad \textbf{(1)}$$

$$\text{Max } Z = \sum_i \sum_t (\text{HP})_{it} \qquad \forall \, t = 1,2,3,\ldots\ldots,12 \qquad \textbf{(2)}$$

Where i is number of reservoirs and t is number of time steps. In the problem formulation, four reservoirs are
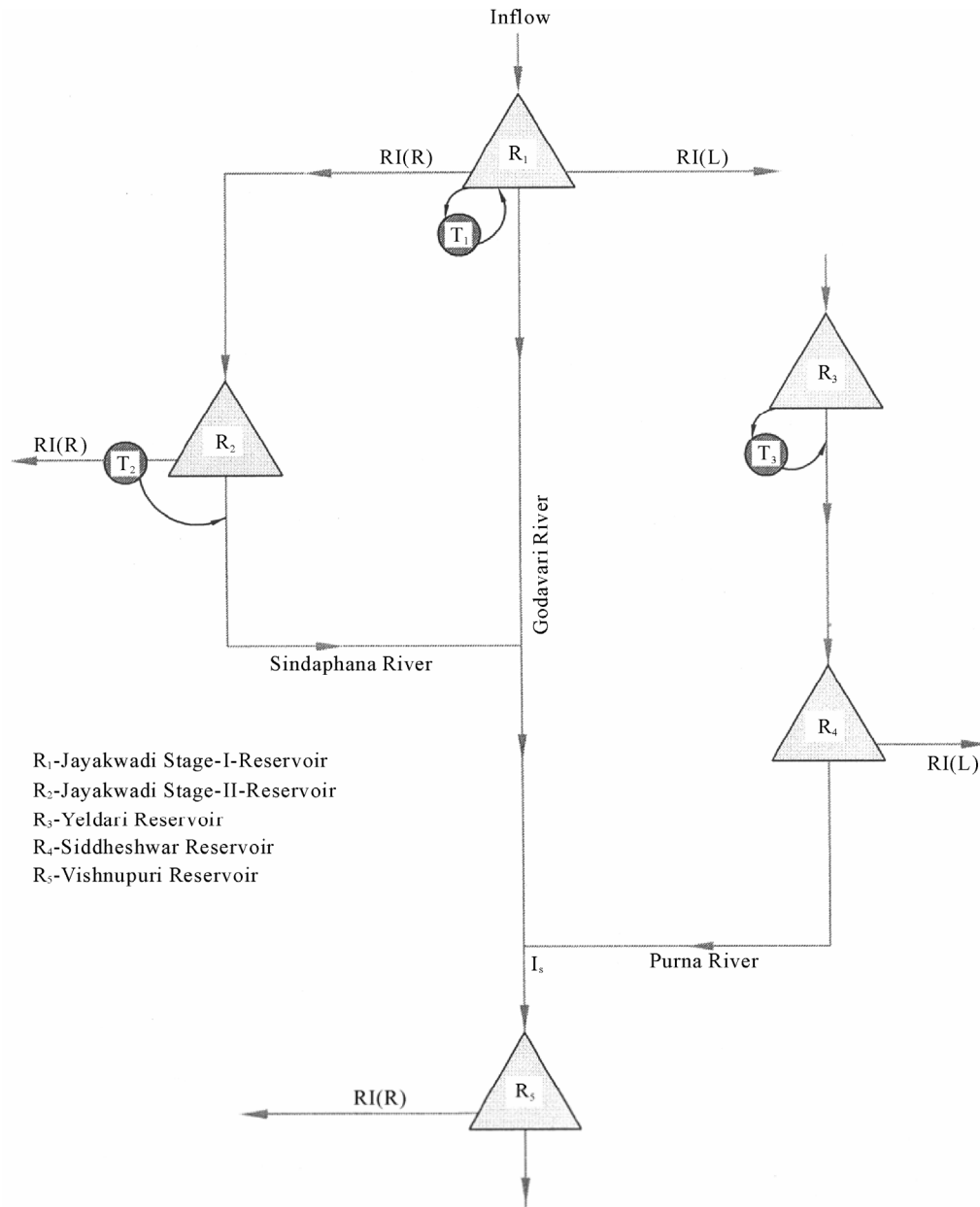
Figure 1. Schematic representation of the physical system.

Table 1. Salient features of reservoirs.

Sr. No.	Salient Features	Reservoirs				
		Jayakwadi Stage-I (R$_1$)	Jayakwadi Stage-II (R$_2$)	Yeldari (R$_3$)	Siddheshwar (R$_4$)	Vishnupuri (R$_5$)
1	River	Godavari	Sindaphana	Purna	Purna	Godavari
2	State/Country	Maharashtra State, India	Maharashtra State, India	Maharashtra State, India	Maharashtra State, India	Maharashtra State, India
3	Catchment Area (km^2)	21750	3840	7330	7770	13870
4	Gross Storage (Mm^3)	2909	453.64	934.44	250.85	83.85
5	Live Storage (Mm^3)	2171	311.30	809.77	80.96	81.67
6	Installed Capacity for hydro-power generation (MW)	12.0 (Pumped storage plant)	2.25 (Canal power house)	15.0	--	--
7	Irrigable command area (km^2)	1416.40	938.85	--	615.60	337.24

Table 2. Maximum irrigation demand and inflow in reservoirs in Mm³.

Month	Jayakwadi Stage-I (R_1)		Jayakwadi Stage-II (R_2)		Yeldari (R_3)		Siddheshwar (R_4)		Vishnupuri (R_5)	
	Irrigation Demand	Inflow	Irrigation Demand	Inflow	Irrigation Demand	Inflow	Irrigation Demand	Inflow	Irrigation Demand	Inflow
Jun	18.55	148.76	7.12	20.98	0	72.83	33.10	7.71	35.91	16.42
Jul	26.70	408.25	20.83	43.46	0	141.09	35.23	2.21	22.97	35.96
Aug	25.43	610.66	37.64	96.88	0	200.36	35.23	11.97	31.69	107.32
Sep	85.79	600.0	46.02	144.17	0	160.77	93.46	9.18	31.49	246.07
Oct	267.86	287.75	132.01	75.52	0	123.10	77.60	1.29	31.95	79.00
Nov	228.74	196.46	127.05	10.24	0	49.48	74.68	0.57	22.68	9.91
Dec	210.88	125.53	89.43	4.27	0	35.58	65.14	0.89	35.09	7.93
Jan	230.34	37.65	100.68	0.37	0	32.18	65.14	1.00	38.46	1.13
Feb	85.23	21.46	30.02	0.37	0	24.23	35.50	0.39	23.65	0.00
Mar	70.06	19.56	28.98	0.16	0	23.54	37.40	1.00	14.50	0.00
Apr	85.49	25.50	35.58	0.12	0	13.15	30.50	0.40	19.06	0.00
May	58.20	46.58	25.88	0.06	0	13.86	22.30	0.40	28.07	0.00
Total	1393.2	2528.17	681.24	396.60	0	890.17	605.2	37.01	335.5	503.74

taken for optimization. The fifth reservoir is considered as downstream control and is incorporated as a constraint in the model. These objectives are subjected to the following constraints:

3.1. Turbine Release Constraints

The releases into turbines for power production, should be less than or equal to the flow through turbine capacities for all the months. Also, power production in each month should be greater than or equal to the firm power. These constraints can be written as:

$$HPR(i,t) \leq TCR(i) \qquad \forall \quad i=1,2,3,4 \qquad (3)$$

$$HPR(i,t) \geq FPR(i) \qquad \forall \quad t=1,2,3,.........,12 \qquad (4)$$

3.2. Irrigation Release Constraints

The irrigation releases should be less than or equal to the irrigation demand on all reservoirs for all the months and should be greater than or equal to the minimum irrigation demand (ID_{min}). Mathematically this constraint is given as:

$$ID_{min}(i,t) \leq IR(i,t) \leq ID_{max}(i,t) \qquad \forall \quad i=1,2,3,4$$
$$\forall \quad t=1,2,3,.........,12 \qquad (5)$$

3.3. Reservoir Storage Constraints

The storage in the reservoirs should be less than or equal to the capacity of reservoir and greater than or equal to the dead storage for all months. Mathematically this constraint is given as:

$$S_{min}(i) \leq S(i,t) \leq S_{max}(i) \qquad \forall \quad i=1,2,3,4$$
$$\forall \quad t=1,2,3,...............,12 \qquad (6)$$

3.4. Hydrologic Continuity Constraints

These constraints relate to the turbine releases, irrigation releases, release for drinking and industrial water supply which is taken as a constant, reservoir storage, inflows into the reservoirs, Losses from the reservoirs for all months. The hydrologic continuity constraints for all the reservoirs is stated as:

1) Reservoir (R_1)

$$(1+a_t(1,t))S(1,t+1) = (1-a_t(1,t))S(1,t)+IN(1,t)-HPR(1,t)-IR(1,t)$$
$$-SPILL(1,t)-WSR(1,t)-FCR(1,t)+\alpha_1 HPR(1,t)-A_0 e_t(1,t)$$
$$\forall \, t=1,2,3,...............,12 \qquad (7)$$

2) Reservoir (R_2)

$$(1+a_t(2,t))S(2,t+1) = (1-a_t(2,t))S(2,t)+IN(2,t)+\alpha_2 FCR(1,t)-HPR(2,t)$$
$$-IR(2,t)-SPILL(2,t)-WSR(2,t)-A_0 e_t(2,t)$$
$$\forall \, t=1,2,3,............,12 \qquad (8)$$

3) Reservoir (R_3)

$$(1+a_t(3,t))S(3,t+1) = (1-a_t(3,t))S(3,t)+IN(3,t)-HPR(3,t)$$
$$-SPILL(3,t)-WSR(3,t)-A_0 e_t(3,t)$$
$$\forall \, t=1,2,3,..............,12 \qquad (9)$$

4) Reservoir (R_4)

$$(1 + a_t(4, t))S(4, t+1) = (1 - a_t(4, t))S(4, t) + IN(4, t) + \alpha_3 SPILL(3, t)$$
$$+ \alpha_4 HPR(3, t) - IR(4, t) - WSR(4, t) - SPILL(4, t) - A_0 e_t(4, t) \tag{10}$$
$$\forall\, t = 1,2,3,.... \,...........,12$$

5) Reservoir (R_5)

$$DSR(t) = C_1 * SPILL(1,t) + C_2 * SPILL(2,t) + C_3 * SPILL(4,t)$$
$$+ DSIN(t) + \alpha_5 HPR(2,t) \tag{11}$$

$$\forall\, t = 1,2,3,...........,12$$
$$S(i,1) = S(i,13) \tag{12}$$

The transition loss for pumping turbine releases back into the reservoir for R_1, feeder canal release (FCR) from R_1 to R_2, Spills from R_3 to R_4, turbine releases (HPR) from R_3 to reach to R_4, turbine releases from R_2 to reach R_5, Spills from R_1 to reach to R_5, Spills from R_2 to reach to R_5, Spills from R_4 to reach to R_5 is taken as 10 % in the model. Water supply releases is taken as constant for reservoir R_1 as 31.63 Mm^3, 3.55 Mm^3 for R_2, and 2 Mm^3 for R_3 and R_4 for all months.

4. Results and Discussions

For developing optimal operating policies for a multireservoir in a river sub basin a monthly MOGAFUOPT model is developed. By using MOGAFUOPT, the irrigation releases, hydropower production and level of satisfaction (λ) is maximized. For this the GA operators used are stochastic remainder selection, one point crossover and binary mutation. For selection of population size, crossover probability, mutation probability and optimal generations, a thorough sensitivity analysis is carried out. The system performance is estimated by taking crossover probability between 0.7 to 1.0 with a increment of 0.05 and mutation probabilities between 0.3 to 0.001 with a decrement of 0.1 up to 0.01 and then the decrement is taken as 0.001. The population size is varied from 20 to 150 and generation from 20 to 500. Based on the system performance the optimal population size and optimal number of generations are 130 and 500 respectively. When one of the objectives: Z_1 (irrigation releases) is maximized, giving no preference to second objective: Z_2 (hydropower production), the comparison shows that for

crossover probability 0.7 and mutation probability 0.1, the maximization (i.e., maximum value of Z_1: Z_1^+) is achieved. The variation of maximized irrigation releases with respect to different mutation probabilities for selected crossover probability is shown in Figure 2. When Z_2 is maximized, giving no preference to Z_1, the comparison shows that for crossover probability 0.9 and mutation probability 0.1, the maximization (i.e., maximum value of Z_2: Z_2^+) is achieved. The variation of maximized hydropower production with respect to different mutation probabilities for selected crossover probability is shown in Figure 3. In fuzzy optimization model, when λ (level of satisfaction) is maximized, the comparison shows that for crossover probability 1.0 and mutation probability 0.004, the maximization (i.e., maximization of both the objectives simultaneously) is achieved. The variation of maximized λ (level of satisfaction) with respect to different mutation probabilities for selected crossover probability is shown in Figure 4.

The MOGAFUOPT model is developed for multireservoir system as shown in Figure 1 with the objectives 1) to maximize irrigation releases and 2) to maximize hydropower production. The best and worst values for both the objectives i.e., Z_1 for irrigation releases (Z_1^+ and Z_1^-) and Z_2 for hydropower production (Z_2^+ and Z_2^-) are determined by considering one objective at a time, ignoring the other. When Z_1 is maximized, the corresponding value of Z_2 is considered to be the worst and vice versa. These values are given in Table 3. These objectives are fuzzified by considering linear membership function. The membership functions for irrigation releases and hydropower production are presented in Equations 13 and 14 respectively.

$$\mu_{Z_1}(x) = \begin{cases} 0 & Z_1 \leq 1807.97 \\ \dfrac{(Z_1 - 1807.97)}{(2218.36 - 1807.97)} & 1807.97 \leq Z_1 \leq 2218.36 \\ 1 & Z_1 \geq 2218.36 \end{cases} \tag{13}$$

$$\mu_{Z_2}(x) = \begin{cases} 0 & Z_2 \leq 85591654.2 \\ \dfrac{(Z_2 - 85591654.2)}{(117394536.3 - 85591654.2)} & 85591654.2 \leq Z_2 \leq 117394536.3 \\ 1 & Z_2 \geq 117394536.3 \end{cases} \tag{14}$$
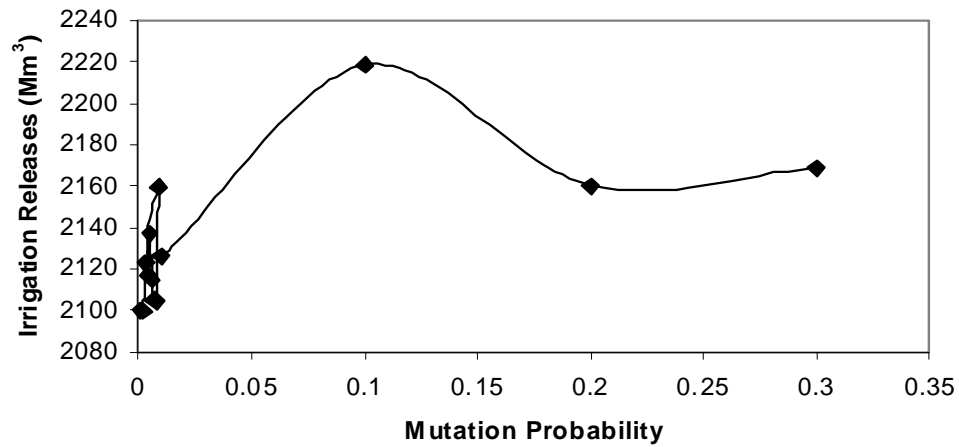
D. G. REGULWAR *ET* *AL.*

Figure 2. Variation of irrigation releases corresponding to mutation probability for crossover probability 0.7.
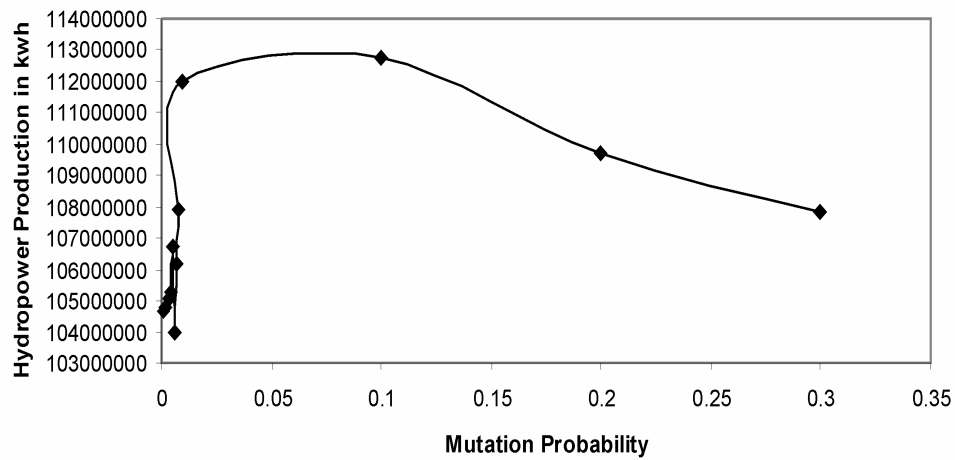

Figure 3. Variation of hydropower production corresponding to mutation probability for crossover probability 0.9.
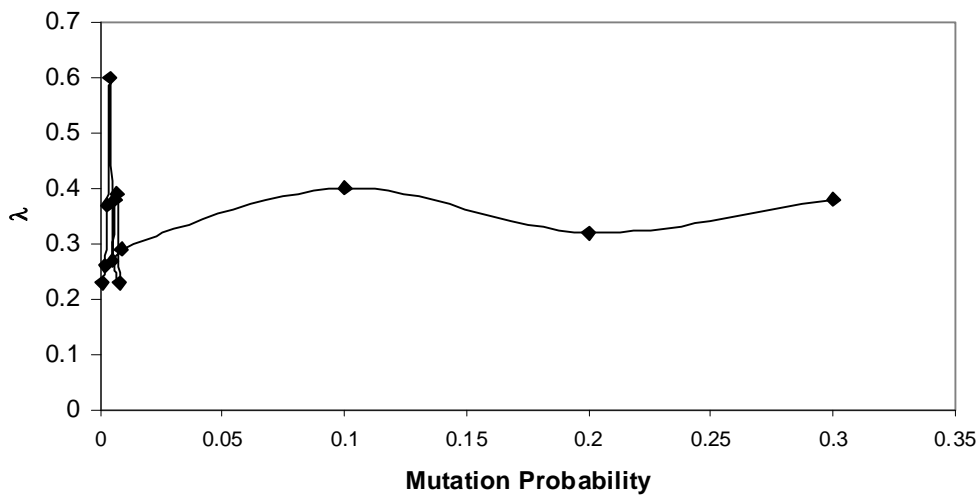

Figure 4. Variation of λ corresponding to mutation probability for crossover probability 1.0.

**Table 3. Best and worst values for objective functions.**

Objective Function (Maximization)	Best value Z^+	Worst value Z^-
Irrigation releases (Z_1) Mm^3	2218.36	1807.97
Hydro-power production (Z_2) mwh	117394.5	85591.7

These fuzzified objectives are simultaneously maximized by defining level of satisfaction (λ) and then maximizing it. The λ (Maximum level of satisfaction) was found to be 0.60. The irrigation releases (Z_1^*) and hydropower produced (Z_2^*) corresponding to maximum level of satisfaction are 2054.22 Mm^3 and 104755.5 mwh respectively. Monthly optimized irrigation releases from reservoirs are shown graphically in Figure 5. Monthly optimized hydropower production from reservoirs is presented in Figure 6.

Decision maker may adopt λ value as it is or he may demand different λ value. For this, λ can be changed for both the objectives as per preferences of decision maker

and run the model again to obtain respective solution. For this purpose, the whole range of operation policies with satisfaction levels ranging from 0 to 1, for both the objectives, are determined. These policies are presented in Table 4.

The comparison between existing operation policy and optimized operation policy is prepared for Jaykwadi stage-I reservoir (R_1). The results of MOGAFUOPT shows that the annual maximized irrigation releases for Jayakwadi stage-I reservoir (R_1) is 1166.20 Mm^3. The annual maximum irrigation demand for this reservoir is 1393.2 Mm^3 as per data presented in Table 2. The historical outflow data of reservoir R_1 for 30 years is analyzed and monthly average outflow for irrigation releases is worked out. Average of 30 years outflow data is taken and it works out to be 1295.6 Mm^3. The comparison of average existing operation policy and optimized operation policy derived by GA under fuzzy environment is promising. The historic data of existing operation policy for other reservoirs is not obtained. Hence comparison is presented for Jaykwadi stage-I reservoir (R_1) in Figure 7.
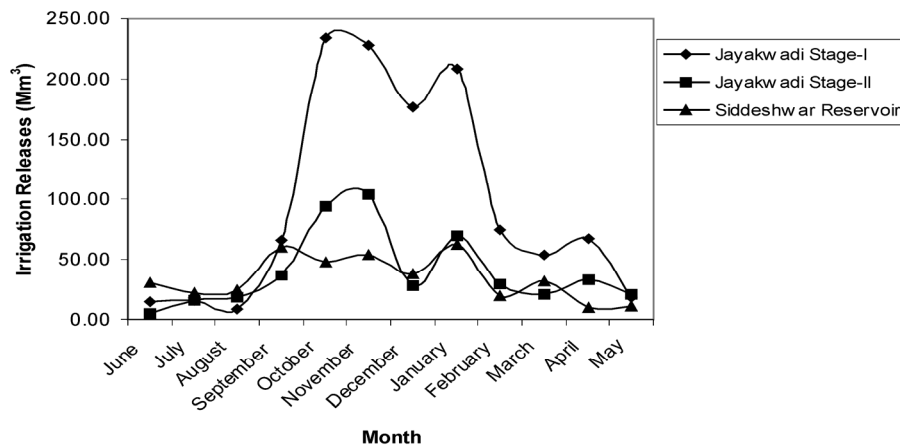
Figure 5. Monthly optimized irrigation releases from reservoirs.
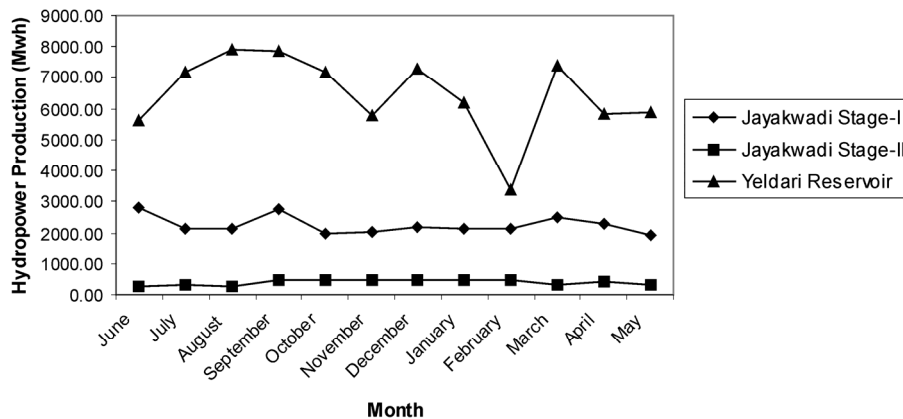
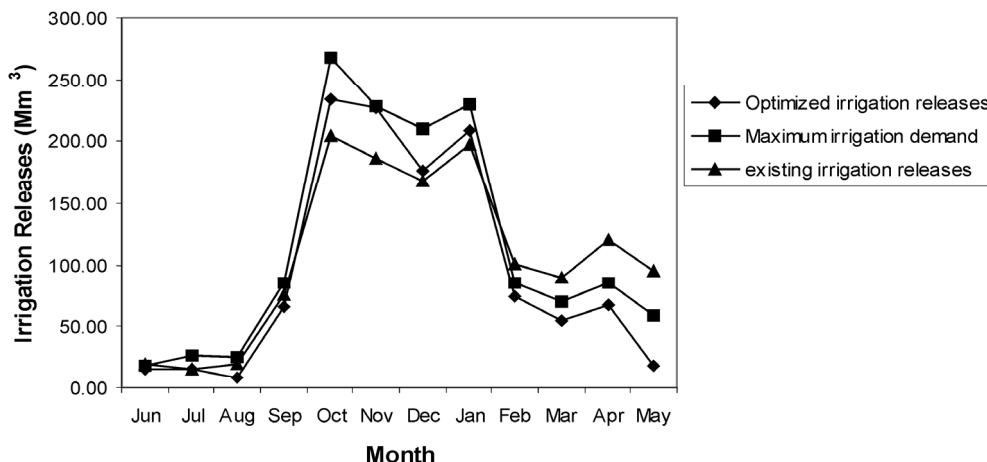**Figure 6. Monthly optimized hydropower production (mwh).**

Figure 7. Comparision of irrigaion releases for jayakwadi stage-I project.

Table 4. Solutions of MOGAFUOPT for Different Values of λ.

Sr. No.	Degree of Satisfaction (λ)		Objective Value	
	λ_1	λ_2	Z_1 (Mm^3)	Z_2 (mwh)
1	0	1.00	1807.99	117394.5
2	0.1	0.81	1849.03	111304.5
3	0.2	0.77	1890.07	110187.9
4	0.3	0.70	1931.11	107869.6
5	0.4	0.68	1972.15	107285.8
6	0.5	0.66	2012.18	106526.5
7	0.6	0.60	2054.22	104755.5
8	0.7	0.50	2095.26	101575.2
9	0.8	0.40	2136.30	98394.9
10	0.9	0.30	2177.34	95214.6
11	1.0	0.20	2218.38	92034.3

5. Summary and Conclusion

Multiobjective, multireservoir optimization in fuzzy environment by using GA is explored in this study. A multireservoir system in Godavari river sub basin in Maharashtra State, India is considered. A MOGAFU-OPT model is developed and applied to the case study. The objective function of the GA model was set to maximize irrigation releases, hydropower production and level of satisfaction (λ). The sensitivity analysis for deciding crossover probability, mutation probability, population size and number of generations are presented in the result for this case study. By adopting these GA parameters, irrigation releases, hydropower production and level of satisfaction are maximized and results are presented. The maximum level of satisfaction (λ^*) achieved by maximizing both the objectives simultaneously is 0.60. The corresponding irrigation releases and hydropower production are 2054.22 Mm^3 and 104755.5 mwh respectively. The whole range of operation policies with satisfaction levels ranging from 0 to 1 for both the objectives are determined. Monthly optimized irrigation releases and hydropower produc-

tion from reservoirs are presented. The comparison of average existing operation policy and optimized operation policy derived by GA under fuzzy environment is promising. The application of proposed MOGAFUOPT model can be extended to the other river basins with little modifications taking physical features and the constraints of the basin into consideration. This study shows that MOGAFUOPT model has significant potential in application to multiobjective, multireservoir system in a river basin.

6. Acknowledgement

7. References

[1] R. A. Wurbs, "Modelling and analysis of reservoir system operation," NJ: Prentice Hall PTR, Prentice-Hall Inc., 1996.

[2] W. W-G. Yeh, "Reservoir management and operations models: A state-of-the-art review," Water Resour. Res., Vol. 21, No. 12, pp. 1797–1818, 1985.

[3] J. W. Labadie, "Optimal operation of multireservoir systems: State-of-the-art review," J. Water Resour. Plan. and Manage., Vol. 130, No. 2, pp. 93–111, 2004.

[4] J. H. Holland, "Adaptation in natural and artificial systems," University of Michiyan Press annarbov, Cambridge Mass, 1975.

[5] D. E. Goldberg, "Genetic algorithms in search, optimization and machine learning," Addison-Wesley Publishing Co., Inc., Reading MA, 1989.

[6] R. Oliveira and D. P. Loucks, "Operating rules for multi-reservoir systems," Water Resour. Res., Vol. 33, No. 4, pp. 839–852, 1997.

[7] R. Wardlaw and M. Sharif, "Evaluation of genetic algorithm for optimal reservoir system operation," J. Water Resour. Plan. and Manage., Vol. 125, No. 1, pp. 25–33, 1999.

[8] M. Sharif and R. Wardlaw, "Multireservoir systems optimization using genetic algorithms: Case study," J. Compu. in Civil Engrg., Vol. 14, No. 4, pp. 255–263, 2000.

[9] L. C. Chang and C. C. Yang, "Optimizing the rule curves for multi-reservoir operations using a genetic algorithm and HEC-5," J. Hydrosci. and Hydra. Engrg., Vol. 20, No. 1, pp. 59–75, 2002.

[10] K. Srinivasa Raju and D. Nagesh Kumar, "Irrigation planning using genetic algorithms," Water Resour. Manage., Vol. 18, pp. 163–176, 2004.

[11] J. A. Ahmed and A. K. Sarma, "Genetic algorithm for optimal operating policy of a multipurpose reservoir," Water Resour. Manag., Vol. 19, pp. 145–161, 2005.

[12] L. F. R. Reis, G. A. Walters, D. E. Savic, and F. H. Chaudhry, "Multi-reservoir operation planning using hybrid genetic algorithm and linear programming (GA-LP): An alternative stochastic approach," Water Resour. Manag., Vol. 19, pp. 831–848, 2005.

[13] V. Jothiprakash and Ganesan Shanthi, "Single reservoir operating policies using genetic algorithm," Water Resour. Manag., Vol. 20, pp. 917–929, 2006.

[14] J. X. Chang, G. Huang, and Y. M. Wang, "Genetic algorithms for optimal reservoir dispatching," Water Resour. Manag., Vol. 19, pp. 321–331, 2005.

[15] L. F. R. Reis, F. T. Bessler, G. A. Walters, and D. Savic, "Water supply reservoir operation by combined genetic algorithm-linear programming (GA-LP) approach," Water Resour. Manag., Vol. 20, pp. 227–255, 2006.

[16] M. Janga Reddy, and D. Nagesh Kumar, "Optimal reservoir operation using multi-objective evolutionary algorithm," Water Resour. Manag., Vol. 20, pp. 861–878, 2006.

[17] P. Anand Raj, "Multicriteria methods in river basin planning-A case study," Water Sci. and Techno., Vol. 31, No. 8, pp. 261–272, 1995.

[18] P. Anand Raj and D. Nagesh Kumar, "Ranking of river basin alternatives using ELECTRE," J. Hydrol. Sci., Vol. 41, No. 5, pp. 697–713, 1996.

[19] P. Anand Raj, and D. Nagesh Kumar, "Planning for sustainable development of a river basin using fuzzy logic," in Proce. of Int. Conf. on Civil Engrg. for Sustainable Development, Roorkee, India, pp. 173–182, 1997.

[20] S. P. Simonovic, "Tools for water management: One view of the future," Water International, IWRA, Vol. 25, No. 1, pp. 76–88, 2000.

[21] M. J. Bender and S. P. Simonovic, "A fuzzy compromise approach to water resource systems planning under uncertainty," Fuzzy Sets and Systems, Vol. 115, pp. 35–44, 2000.

[22] D. P. Panigrahi and P. P. Mujumdar, "Reservoir operation modeling with fuzzy logic," Water Resour. Manag., Vol. 14, pp. 89–109, 2000.

[23] D. Nagesh Kumar, D. S. V. Prasad, and K. Srinivasa Raju, "Optimal reservoir operation using fuzzy approach," in Proce. of Int. Conf. on Civil Engrg., Banglore, India, Interline Publishing, pp. 377–384, 2001.

[24] A. Tilmant, M. Vanclooster, L. Duckstein, and E. Persoons, "Comparision of fuzzy and nonfuzzy optimal reservoir operating policies," J. Water Resour. Plan. and Manage., Vol. 128, No. 6, pp. 390–398, 2002.

[25] K. Srinivasa Raju and L. Duckstein, "Multiobjective fuzzy linear programming for sustainable irrigation planning: An Indian case study," Soft Computing, Vol. 7, pp. 412–418, 2003.

[26] D. G. Regulwar and P. Anand Raj, "Development of 3-D optimal surface for operation policies of a multireservoir in fuzzy environment using genetic algorithm for river basin development and management," Water Resour. Manag., Vol. 22, pp. 595–610, 2008.

Appendix: notation

The following symbols are used in this paper

DSR (t)   =Downstream requirement during month t;
DSIN (t)   = Downstream inflow during month t;
FCR(i,t)   = Feeder Canal Releases during month t from reservoirs i;
FPR(i)   = Flow for firm power release from reservoirs i;
$ID_{max}(i,t)$ =Maximum irrigation demand during month t from reservoirs i;
$ID_{min}(i,t)$ =Minimum irrigation requirement during month t from reservoirs i;
IN(i,t)   =Monthly inflow into the reservoir during month t from reservoirs i;
SPILL(i,t)   =Spills during month t from reservoirs i;
HP(i,t)   =Hydropower produced during month t from reservoir i;
IR(i,t)   =Irrigation releases during month t from reservoirs i;
HPR(i,t)   =Releases for hydropower production in month t from reservoirs i;
WSR(i,t)   =Water supply releases during month t from reservoirs i;
S(i,t)   =Storage in the reservoir during month t from reservoirs i;
$S_{min}(i)$ =Minimum storage capacity for i^{th} reservoir;
$S_{max}(i)$ =Maximum storage capacity for i^{th} reservoir;
T_1, T_2, T_3 =Turbines for reservoirs R_1, R_2 and R_3;
TCR(i)   =Flow for maximum capacity of turbine from reservoirs i;
$\mu_i(x)$ =Membership function;
λ =Level of satisfaction;
λ^* =Maximum degree of overall satisfaction;
λ_1 =Level of satisfaction for irrigation releases;
λ_2 =Level of satisfaction for hydropower produced;
$\alpha_1, \alpha_2, \alpha_3, \alpha_4, \alpha_5$ =Constants; and
C_1, C_2, C_3 =Constants.

Scientific
Research

Study on Reducing Leachate Production by Saw Powder Adding

Jun YIN[1], Baojun JIANG[1], Xiaoyan WU[2], Liang LIANG[2], Xue LIU[2]

[1]*School of Municipal and Environmental Engineering, Harbin Institute of Technology, Harbin, China.*
[2]*Jilin Province Key Laboratory of Water Pollution Control and Resources Reuse, Jilin Architectural
and Civil Engineering Institute, Changchun, China*
E-mail: *hitjunyin@163.com*

Abstract

In order to study the effect of saw powder on leachate production, degradation of rubbish, COD and NH_3-N concentration of leachate, three cylinder reactors for anaerobic landfill disposal were built to simulate the operation of landfill. In this experiment, leachate quantity, settling height of rubbish layer, COD and NH_3-N concentration were monitored. The results come from experiment data analyses indicate that saw powder has strong effect on reducing leachate quantity and accelerating degradation of rubbish. In 60 days, saw powder mixed in rubbish layer can reduce 1200-1300mL leachate every liter rubbish, moreover, rubbish layer with saw powder mixed in settled more leachate than rubbish layer with no saw powder mixed in for 5cm. The experimental results indicate that saw powder can reduce COD concentration of leachate and adsorb NH_3-N, too.

1. Introduction

Nowadays, people take ground water as drinking water resource in many regions of China, and it is closely related with people's health, however, the ground water could be polluted by leachate seriously. As a kind of organic wastewater with complex integrant, its COD concentration is regular at 2000-80000mg/L, which is several hundred times higher than COD concentration of domestic sewage and industrial effluents; NH_3-N concentration of leachate is usual at 1000-6000mg/L, which is 20-40 times higher than domestic sewage's and industrial effluent's [1]. Furthermore, there are more than ten kinds of heavy metal ions in leachate, so it is a difficulty for leachate treatment all over the world. Nowadays, many researchers have done widely study in leachate treatment field, and a lot of useful results have been obtained [2]. However, little research has been done in leachate reduction. Obviously, the costs of leachate treatment is higher than the cost of sewage and industrial wastewater treatment, therefore, if developing a operated easily and cost lower to reduce leachate quantity technology, the burden of dealing with leachate can be reduced and the costs of leachate treatment can be lowered too. Saw powder is a kind of scrap which comes from timber processing, and physical characters are bulk den-

sity $0.19kg/cm^3$, total pore volume 78.3%, big pore volume 34.5%, small pore volume 43.8% [3–8], so saw powder has perfect absorption ability because of this nature. Saw powder was added in rubbish as absorbent and filler in this experiment, a rubbish column no saw powder added in was taken as contrast reactor. The research contents are that the effect and mechanism of saw powder reducing leachate quantity; the effect of saw powder on rubbish degradation; the effect of saw powder on COD and NH_3-N concentration of leachate and the effect of saw powder on pollutant stripping.

2. Materials and Methods

2.1. Experimental Device

The experimental device consists of three cylinder organic glass columns with the size of 0.1 meters in diameter and 1.0 meters in height. The first column was used as comparative reactor, no saw powder added in, the second column was used as reactor saw powder mixed in rubbish in it, and the third column was used as reactor saw powder added on the bottom of rubbish in it. The rubbish used in the experiment taken from Sandao landfill in Changchun city, all the rubbish was fresh domestic refuse. Saw powder with 5 centimeters thickness

was added on the bottom of the third reactor, the same quantity saw powder was mixed homogeneously in rubbish in the second reactor. The rubbish layer was 0.76 meters in height in the first and third reactor, considering saw powder occupation of some volume, the rubbish layer was 0.80 meters in height in the second reactor (but still measured as 0.76 meters in rubbish height), soil layer with 0.05 meters thickness was covered on the top of the rubbish layer in three reactors. The total volume of rubbish compacted in every reactor was 5.8875 liters. Leachate was collected by the beaker on the bottom of the experimental device. The organic glass columns used in the experimental cannot take any reactions with leachate. The experimental device was presented as Figure 1.

2.2. Experimental Methods

In the experiment, 300mL tap water was sprayed on the head of the reactors homogeneously every 5 days to simulate raining. Then, the volume of leachate produced from rubbish layer in the reactors and heights of rubbish layer were measured every 24 hours, COD concentration of leachate was measured every 48 hours, NH_3-N concentration of leachate was measured every 120 hours. COD measure method used in the experiment was Potassium dichromate method (GB11914-89), NH_3-N measure method used in the experiment was Nessler's Reagent Colorimetric method (GB7479-87).

3. Results and Disdussion

3.1. The Effect of Adding Saw Powder on Leachate Reduction

Figure 2 is shown the variation of leachate quantity producing from rubbish layers in three reactors with time. Every abscissa represents days of experiment, every ordi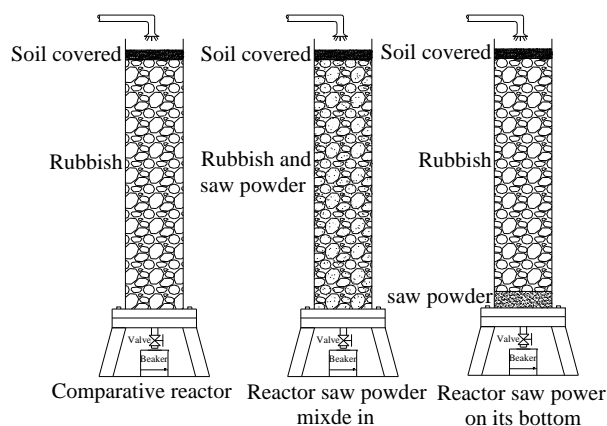nate represents the ratio of total leachate volume pro-ducing from the beginning of the experiment to the day abscissa corresponding and rubbish volume. The curved lines shows that leachate quantity of the second and the third reactors was always shorter than leachate quantity of the first reactor, moreover, leachate quantity of the second reactor was shorter than leachate quantity of the third reactor. In the first 25 days, the trend that leachate quantity of the second and the third reactors were shorter than leachate quantity of the first reactor wasn't obvious, then, leachate quantity of reactors with saw powder added began to be shorter than leachate quantity of comparative reactor obviously, leachate quantity of the second reactor was 1000-1400mL shorter than leachate quantity of the first reactor every liter rubbish, 1200-1300mL shorter in mostly time; leachate quantity of the third reactor was 700-1100mL shorter than leachate quantity of the first reactor every liter rubbish, 900-1000mL shorter in mostly time. The reduction effect of saw powder on leachate became more and more obvious. The results of the experiment also indicate that the re-duction result is better of saw powder mixed in rubbish than saw powder added on the bottom of rubbish. After 50 days, saw powder in the third reactor began to become black step by step and settled a little, which showed that saw powder had begun to degrade obviously.

The authors think that there are two phases to complete the reduction of saw powder on leachate. In the first phase, it mainly depends on adsorption water effect of saw powder. A fraction of water is adsorbed by saw powder during the course of leachate flow the whole rubbish layer. In first 25 days, soil covered layer and rubbish layer don't reach their field moisture capacity, most sprayed water was absorbed by soil and rubbish, only a little water was absorbed by saw powder, so the reduction effect of saw powder on leachate wasn't obvious. After rubbish layer reached its field moisture capacity, saw powder absorbed water in rubbish layer fully, this reduced leachate quantity. On the condition of the same saw powder quantity was added, there were more
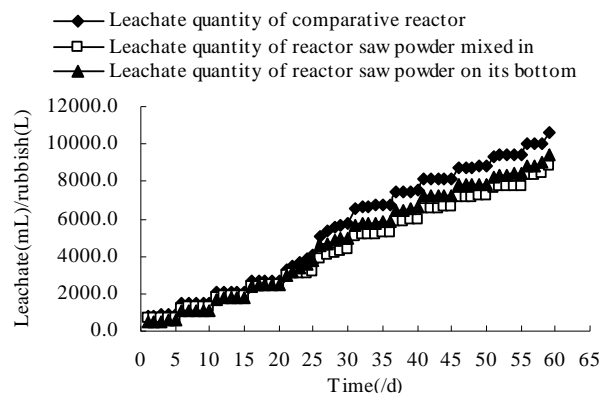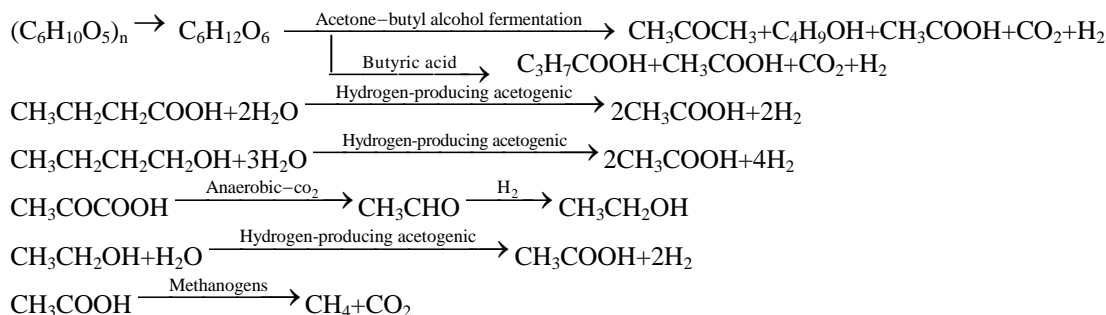

Figure 1. The chart of experimental device.

Figure 2. The variation of leachate quantity with time.

$$(C_6H_{10}O_5)_n \xrightarrow{} C_6H_{12}O_6 \xrightarrow{\text{Acetone}-\text{butyl alcohol fermentation}} CH_3COCH_3+C_4H_9OH+CH_3COOH+CO_2+H_2$$

$$\xrightarrow[\text{Butyric acid}]{} C_3H_7COOH+CH_3COOH+CO_2+H_2$$

$$CH_3CH_2CH_2COOH+2H_2O \xrightarrow{\text{Hydrogen-producing acetogenic}} 2CH_3COOH+2H_2$$

$$CH_3CH_2CH_2CH_2OH+3H_2O \xrightarrow{\text{Hydrogen-producing acetogenic}} 2CH_3COOH+4H_2$$

$$CH_3COCOOH \xrightarrow{\text{Anaerobic}-co_2} CH_3CHO \xrightarrow{H_2} CH_3CH_2OH$$

$$CH_3CH_2OH+H_2O \xrightarrow{\text{Hydrogen-producing acetogenic}} CH_3COOH+2H_2$$

$$CH_3COOH \xrightarrow{\text{Methanogens}} CH_4+CO_2$$

chances of touching saw powder for water in rubbish in the second reactor than water in rubbish in the third reactor when it flowed rubbish layer in seepage, therefore more water was absorbed and less leachate produced in the second reactor. In the second phase, it mainly depends on consumption water effect of saw powder during its degradation. Saw powder in the reactors was degraded by microorganisms in rubbish little by little with the extended rubbish landfill time. The main ingredient of saw powder is cellulose, the proportion of cellulose in saw powder is more than 50%. The degradation processing of cellulose can be showed as the following biochemical function:

It can be known from the functions that water in the rubbish cell be consumed during the course of degradation cellulose, hydrogen of consumed water becomes hydrogen element of methane, oxygen of consumed water becomes oxygen element of carbon dioxide, but there is not water produce during the whole course of saw powder degradation. A part of water consumed in the second phase comes from water absorbed by saw powder in the first phase, so the reduction effect of saw powder on leachate in the second phase is secondary to the reduction effect in the first phase. Furthermore, there are more microorganisms in rubbish layer than that in saw powder layer on the bottom of reactor, saw powder mixed in rubbish can be degraded more completely than saw powder on the bottom of the reactor, so more water is consumed and less leachate is produced.

3.2. The Effect of Adding Saw Powder on Rubbish Degradation Velocity

The variation curved lines of rubbish layer heights in three reactors with time are showed in Figure 3. The curved lines show that rubbish layers in first reactor and third reactor settled almost at the same velocity, however, rubbish in second reactor settled more quickly than rubbish in first reactor. After 41 days, rubbish layer height in fist and third reactor became 0.47 meters, rubbish layer height in fist and third reactor became 0.42 meters, this experimental result indicates that saw powder mixed in rubbish layer can accelerate rubbish degradation, but saw powder added on the bottom of rubbish layer hasn't

effect on velocity of rubbish degradation. Saw powder mixed in rubbish layer can take the action of filler, microorganisms attaching on surface of saw powder form biomembrane, moreover, water saw powder absorbing was utilized effectively by microorganisms, so rubbish surrounding saw powder could be degraded more quickly. But at the same time, saw powder absorbed and consumed water in rubbish layer during the course of degradation, lowered water content of rubbish, which decelerated rubbish degradation. Because water content is an important factor of influencing rubbish degradation, it is benefit to dissolve nutrients microorganisms needing if water content of rubbish is enough, then all kinds of biochemical reactions can take place normally and microorganisms can attain nutrients easily, it is benefit to microorganisms propagation, which accelerates rubbish degradation. On the contrary, water content of rubbish isn't enough will result in lowering rubbish degradation velocity. Generally speaking, as a kind of filler, saw powder still can accelerate rubbish degradation. The experimental data indicates that the settling height of rubbish layer with saw powder mixed in always 0.02~0.05 meters lower than the settling height of comparative rubbish layer in 41 days of rubbish degradation.

3.3. The Effect of Adding Saw Powder on COD of Leachate

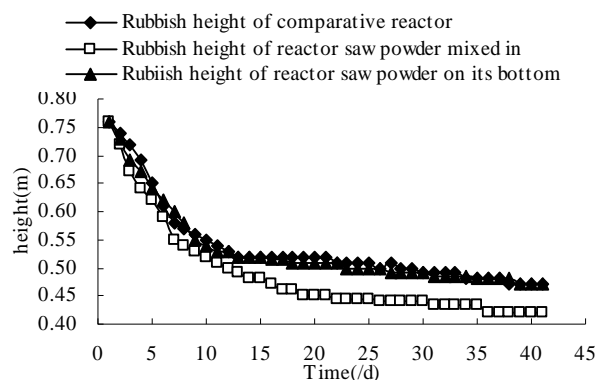The COD concentration variation of leachate with time is

Figure 3. The variation of rubbish layer height with time.

showed in Figure 4, the COD content variation of leachate with time is showed in Figure 5. COD content represents multiplication of COD concentration and leachate quantity produced that day. Curved lines in Figure 4 indicates that COD concentration of leachate produced in the first reactor was lower than COD concentration of leachate produced in the third reactor, but higher than that of the second reactor. Saw powder absorbed water in rubbish, which reduced leachate quantity, therefore COD concentration of leachate stripping from the third reactor was higher than COD concentration of leachate stripping from the first reactor. Water in rubbish was absorbed by mixed saw powder, which can result in COD concentration of leachate raise. But saw powder also takes the action of filler, which can accelerate rubbish degradation, so dissolved organisms in leachate produced in the second reactor can be degraded more completely than dissolved organisms in leachate produced in the first reactor, which result in COD content of stripping leachate from the second reactor was lower than COD content of stripping leachate from the first reactor, so COD concentration of leachate produced in the second reactor is lower than COD concentration of leachate produced in the first reactor. The experimental result
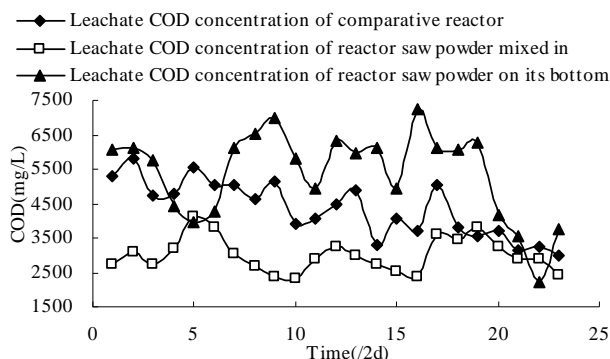
indicates that saw powder can reduce leachate quantity and lowering COD concentration of leachate. Saw powder on the bottom of rubbish layer don't touch rubbish completely and there were few microorganisms in saw powder layer, so it cannot take the action of accelerating rubbish degradation. Curved lines in Figure 4 indicate that pollutant quantity stripping from second reactor was shorter than pollutant quantity stripping from first reactor, however, the difference of pollutant quantity stripping from the third reactor and pollutant quantity stripping from first reactor isn't obvious, which proves the experimental result that saw powder mixed in rubbish can accelerate rubbish degradation and reduce pollutant quantity stripping from rubbish further.

3.4. The Effect of Adding Saw Powder on NH_3-N of Leachate

High concentration NH_3-N is a mainly character of leachate, and it is also a difficulty for leachate treatment, NH_3-N concentration of leachate produced from rubbish layer of first and second reactor were monitored in the experiment, the variation curved lines of NH_3-N concentration with time are showed in Figure 6, the variation
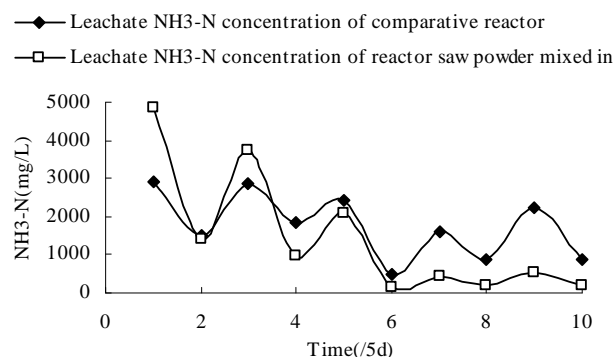

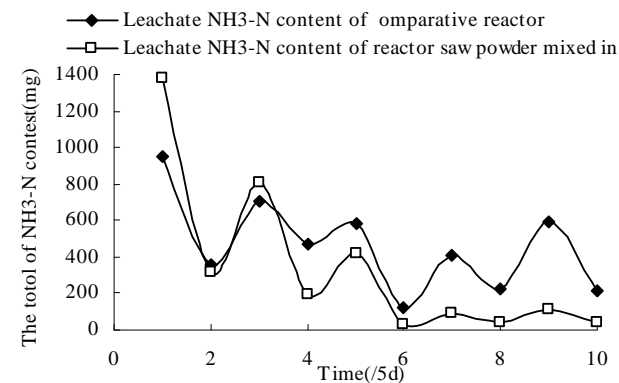**Figure 4. The COD concentration variation of leachate with time.**
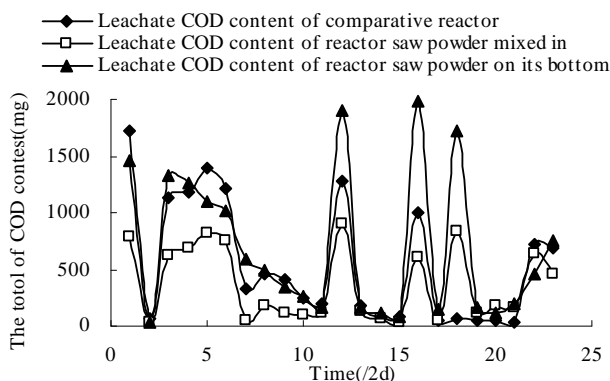
Figure 5. The COD content variation of leachate with time.

Figure 6. NH_3-N concentration variation of leachate with time.

Figure 7. NH_3-N content variation of leachate with time.

curved lines of NH$_3$-N content with time are showed in Figure 7, NH$_3$-N content represents multiplication of NH$_3$-N concentration and leachate quantity produced that day. The curved lines indicate that NH$_3$-N concentration variation of leachate produced from rubbish layer of first and second reactor was basically the same, because leachate quantity of rubbish layer in second reactor was shorter than leachate quantity of rubbish layer in first reactor and rubbish in second reactor degraded more rapidly than rubbish in first reactor, NH$_3$-N concentration of leachate produced in rubbish of second reactor should be higher obviously than NH$_3$-N concentration of leachate produced in rubbish of first reactor, but in fact NH$_3$-N concentration of leachate produced from first and second reactor were basically the same, this phenomenon proves that saw powder can adsorb NH$_3$-N. Adsorption of saw powder on NH$_3$-N prevented from NH$_3$-N concentration rising which probably happen because of the reduction and acceleration degradation effect of saw powder. Figure 7 shows that there wasn't too much difference of NH$_3$-N content stripping from rubbish layer of first reactor and that of second reactor, this experimental result proves that saw powder can adsorb NH$_3$-N further.

4. Conclusion

1) Saw powder has obvious reduction effect on leachate. Leachate quantity can be reduced 1200-1300mL for liter rubbish by mixing saw powder in rubbish; leachate quantity can be reduced 900-1000mL every liter rubbish by adding saw powder on the bottom of rubbish layer. According to this experimental result, less than 600m^3 leachate can be reduced every 500t rubbish during the course of degradation, which reduces greatly the burden of dealing with leachate, and it will bring many social benefits.

2) Saw powder can obviously accelerate rubbish degradation and mineralization. The experimental results indicate that rubbish layer mixed saw powder in settle 5cm more than rubbish layer no saw powder in 60 days.

3) Saw powder mixed in rubbish can lower COD concentration of leachate, but level of pollutant stripping from rubbish layer of second reactor and first reactor is almost the same. Saw powder has strong adsorption effect on NH$_3$-N.

5. Future Perspective

The reduction of leachate is still in the initial stage, a brief analysis and summary is done in the essay, there are masses of work should be carried out in the future, such as the best sawdust dosage, other filler (discarded newspaper, active carbon, zeolite), operation process, and so on.

6. References

[1] Z. Salem, K. Hamouri and R. Djemaa, "Evaluation of landfill leachate pollution and treatment," Desalination, Vol. 220, pp. 108–109, 2008.

[2] S. Bilgili, "COD fractions of leachate from aerobic and anaerobic pilot scale landfill reactors," Journal of Hazardous Materials, Vol. 1, No. 55, pp. 15–18, January 2008.

[3] X. Y. Shi, B. Xiao, J. F. Li, and X. Y. Yang, "Application of sawdust to heavy metal containing wastewater treatment," Industrial Water Treatment, Vol. 27, No. 4, pp. 12–15, April 2007.

[4] S. L. Huo, B. D. Xi, H. C. Yu, and L. S. He, "Characteristics of dissolved organic matter (DOM) in leachate with different landfill ages," Journal of Environmental Sciences, Vol. 20, pp. 492–498, 2008.

[5] E. Neczaj, M. Kacprzak, J. Lachc, and E. Okoniewska, "Effect of sonication on combined treatment of landfill leachate and domestic sewage in SBR reactor," Desalination, Vol. 204, pp. 227–233, 2007.

[6] C. Visvanathan, M. K. Choudhary, M. T. Montalbo, and V. Jegatheesan, "Landfill leachate treatment using thermopile membrane bioreactor," Desalination, Vol. 204, pp. 8–16, 2007.

[7] L. Zhu, "Landfill leachate treatment with anovel process: Anaerobic annonium oxidation (Anammox) combined with soil infiltration system," Journal of Hazardous Materials, Vol. 151, pp. 202–212, 2008.

[8] Z. Salem, K. Hamouri, R. Djemaa, and K. Allia, "Evaluation of landfill leachate pollution and treatment," Desalination, Vol. 220, pp. 108–114, 2008.

Scientific Research

Simultaneous Determination of Chemical Oxygen Demand (COD) and Biological Oxygen Demand (BOD₅) in Wastewater by Near-Infrared Spectrometry

Qiong YANG[1], Zhenyao LIU[1], Jidong YANG[1,2*]

[1]*School of Chemistry and Chemical EngineerWing, Southwest China University, Chongqing, China*
[2]*School of Chemistry and Chemical Engineering, Yangtze Normal University, Chongqing, China*
E-mail: *flyjd6400@sina.com*

Abstract

To rapidly determine the pollution extent of wastewater, the calibration models were established for determination of Chemical Oxygen Demand and Biological Oxygen Demand in wastewater by partial least squares and near infrared spectrometry of 120 samples. Spectral data preprocessing and outliers' diagnosis were also discussed. Correlation coefficients of the models were 0.9542 and 0.9652, and the root mean square error of prediction (RMSEP) were 25.24 mg·L^{-1} and 12.13 mg·L^{-1} in the predicted range of 28.40~528.0 mg·L^{-1} and 16.0~305.2 mg·L^{-1} for Chemical Oxygen Demand and Biological Oxygen Demand, respectively. By statistical significance test, the results of determination were compared with those of standard methods with no significant difference at 0.05 level. The method has been applied to simultaneous determination of Chemical Oxygen Demand and Biological Oxygen Demand in wastewater with satisfactory results.

Keywords: Near-Infrared Spectrometry, Wastewater, Biological Oxygen Demand, Chemical Oxygen Demand

1. Introduction

Chemical Oxygen Demand (COD) is the amount of oxygen consumed by the organic compounds and inorganic matter which were oxidized in water. Biological Oxygen Demand (BOD₅) is the amount of oxygen consumed by the organic and inorganic compounds which were oxidized by biological-oxidation effect in a certain condition. Both of them reflect the pollution degree of the water, and are the comprehensive index of the relative content of organics. As the main comprehensive index of the organic pollution, COD and BOD₅ are important in the control of the total content of pollution and the management of water environment. So it is significant to farther research and develop the simple and rapid method for the determination of COD and BOD₅.

At present, potassium dichromate method is generally used to determine the value of COD [1] at home and abroad and other methods like spectrophotometry [2] and coulometric method [3] were reported. The method of BOD₅ determination contains routine measurement,

biosensor measurement [4] and spectral analysis [5]. Some of these methods of determination COD and BOD₅ has secondary pollution as added toxical reagents for COD determination, some method need pretreatment for BOD₅ determination, most of them need long time as five days at least. While the NIRS has many advantages, such as without pretreatment and destroy the sample, no pollution, convenient and fast, on-line detection, simultaneity multi-component, good reproducibility, etc. Since 1990s, NIR spectrum was developed fast and became the most conspicuous spectral analysis technique. It has been the official authorized method in many fields such as agriculture and food. It has been widely used in textile, polymer, drugs, petrochemical industry, biochemistry and environmental protection [6]. COD and BOD₅ of wastewater was determined with the method in this experiment, chemical value of BOD₅ and COD on the basis of national standard method was determined as the base data. Calibration model of BOD₅ and COD was built with PLS1 and Unscrambler software. The pretreatment such as smoothing processing, first derivative and second derivative was compared, outliers diagnosis was also

discussed. Further, the model was externally inspected. By statistical significance test, the results of determination were compared with those of standard methods with no significant difference. The method has been applied to simultaneously determine of Chemical Oxygen Demand and Biological Oxygen Demand in wastewater with satisfactory results.

2. Experiment Part

2.1. Instrument

Hitachi U-4100, detector type: PbS; 1cm quartz sample cell; biochemical constant temperature incubator; The Unscrambler 9.7 of CAMO Company.

2.2. Collection of Wastewater

The sample of wastewater collected from domestic sewage in which the Organics consuming oxygen, degradable organics, reducible inorganics, ammonia nitrogen, etc are the main pollutants in Fuling (Chong Qing). 120 samples were collected with glassware in different place. The method was offered by environmental monitoring.

2.3. Experiment Method

2.3.1. Determination Chemical Value of BOD$_5$ and COD
120 samples (110 for calibration set and 10 for prediction set) were deposited for 15 min. The value of BOD$_5$ and COD was detected separately, and then the NIR spectrum was collected. Determination of COD value was 16.0~305.2 mg·L^{-1} was got by the method of reference [1], and Determination of BOD$_5$ value was 28.4~528.0 mg·L^{-1} was got by the method of reference [7].

2.3.2. Collection of Spectrum
The spectrum was collected in the condition of 1cm quartz sample cell with air as reference, wavelength range was 800~1800 nm, wavelength spacing was 2 nm, slit width is 2 nm. scanning speed is 1500 nm/s, every sample was scanned 3 times and got average value. NIR Spectra of wastewater is shown in Figure 1.

2.3.3. PLS Mode's Establishment
The NIR spectrum was transformed into JCAMP-DX format, and introduced into analyze software of the Unscrambler 9.7; then the spectrum was pretreated. Taking the chemical value of BOD$_5$ and COD into the software. Calibration model of BOD$_5$ and COD was built with PLS1 and Cross-validation.
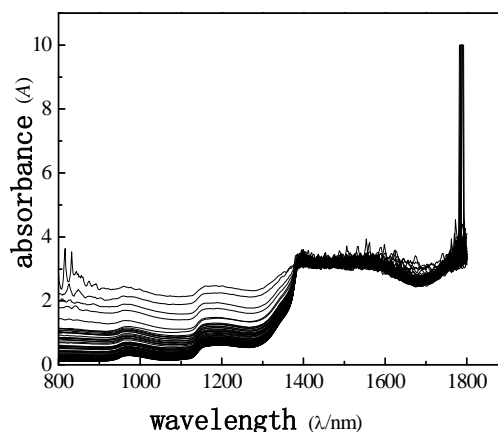

Figure 1. Near infrared spectra of 120 wastewater samples.

3. Results and Discussion

3.1. Choice of Model Algorithm

In the analysis of NIR spectrum, model algorithm includes MLR, PLS, PCA, ANN, TP, etc. The basic idea of model algorithm is that make use of total spectrum information of NIR spectrum, to eliminate influences of spectrum peak's overlap and complex background. PLS has been widely used in NIR spectrum analysis, and has been a common standard method. PLS method contains PLS1 and PLS2. To the complex system, PLS1 method optimizes each components, so the prediction results of PLS1 is generally better than the prediction results of PLS2 [8] through Cross-validation experiment shown. So, PLS1 method is used in this experiment.

3.2. Choice of Spectrum Pretreatment Method

Spectral signal that is determined by detector contains spectral information and several noises. Smoothing processing, first derivative and second derivative was compared in this experiment. Parameters of model are shown in the Table 1. From Table 1, the smoothing processing is best to BOD$_5$ and COD in the spectrum pretreatment.

3.3. Optimization of Model

As shown in Figure 1, spectra of wastewater is not concentrating, it shows that there are anomalous points in the spectra. So the anomalous points should be rejected when we build the model. This experiment use interactive check method, optimize the model step by step, determine the PCs, as far as get the best model. There are two methods for judging and rejecting anomalous points or influential point. The first is mahalanobis distance method, and the second method is

that the influence of model is investigated by Leverage [9], it is also called "reject one" cross-check method. It is combined diagnosed by Leverage and studentized residual, the influential point rejected step by step. This experiment use Leverage and Residual to reject the anomalous points of spectrum and chemical value. Leverage is set as 3.0, error of chemical value is 6.0%, optimize the model by rejecting anomalous points gradually, get the best PLS1 regression model of determining BOD_5 and COD. The correlation coefficient of best model about COD and BOD_5 are 0.9542 and 0.9652, respectively. The predicting relative deviation are 25.24 mg·L^{-1} and 12.13 mg·L^{-1}. The scatter plot of COD and BOD_5 between NIR predicted and measured values are shown in Figure 2 and Figure 3, the changes of residual variance with PCs are shown in Figure 4 and Figure 5.

3.4. Verification of Model

The estimated method is not only parameters' evaluating method of model itself, but also external check evaluating method of model by actual prediction. The 10 wastewater samples of prediction set were predicted about BOD_5 and COD, the results are shown in Table 2. Matched bilateral t test was made between prediction result and standard method by origin 6.0 software. The results are t_{COD}=0.6437, t_{BOD5}= 0.5297, p_{COD}= 0.6092, p_{BOD5}= 0.6092, p_{COD} and p_{BOD5} are much larger than 0.05. When significance level is larger than 0.05, two kinds of determination methods have not significant difference, which shows that there is no system error.

Table 1. Mathematical statistics results for calibration models of BOD$_5$ and COD.

Pretreatment method	COD			BOD$_5$		
	R	SEP (mg·L^{-1})	PCs	R	SEP (mg·L^{-1})	PCs
original	0.9031	35.56	2	0.9084	12.79	2
smoothing processing	0.9542	25.24	1	0.9652	12.13	1
first derivative	0.9256	26.83	1	0.8539	13.28	1
second derivative	0.8028	30.18	1	0.8448	19.46	1

Table 2. Predicted results of the prediction samples.

| NO.	COD				BOD$_5$			
	Standard method	NIR method	error	Relative Error (%)	Standard method	NIR method	error	Relative Error (%)
1	41.6	58.55	16.95	0.41	22.32	34.61	12.29	0.55
2	67.20	66.85	-0.35	-0.005	34.32	39.07	4.75	0.14
3	112.96	129.63	16.67	0.15	66.08	73.77	7.69	0.12
4	141.60	125.18	-16.42	-0.12	82.6	71.77	-10.83	-0.13
5	62.40	77.15	14.75	0.24	35.1	44.67	9.57	0.27
6	422.40	375.09	-47.31	-0.11	228.16	209.79	-18.37	-0.08
7	230.08	185.85	-44.58	-0.19	118.08	104.66	-13.42	-0.11
8	134.40	145.93	11.53	0.086	77.76	82.68	4.92	0.06
9	301.44	304.43	2.99	0.01	175.6	171.09	-4.51	-0.026
10	227.20	223.87	-3.33	-0.015	136.00	125.57	-10.43	-0.076
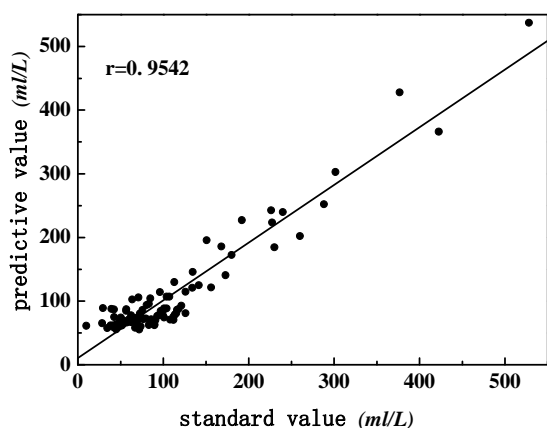
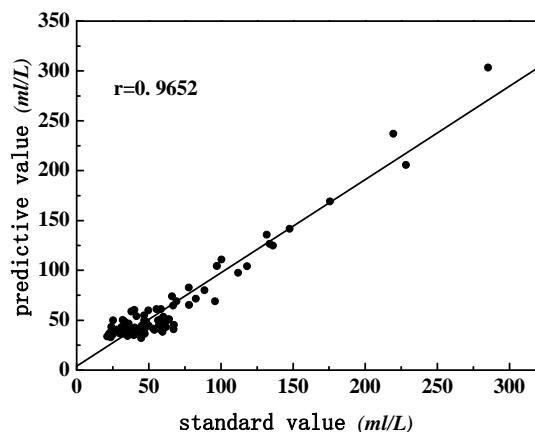**Figure 2. The scatter plot of COD between NIR predicted and measured values.**

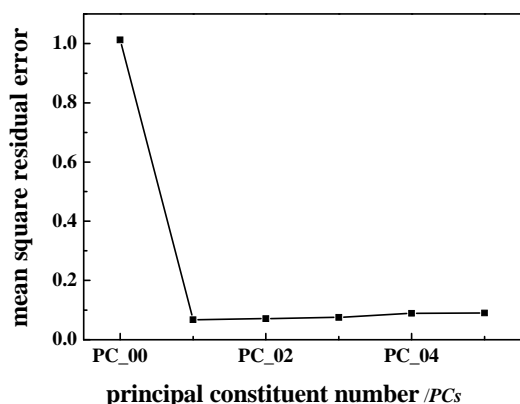**Figure 3. The scatter plot of BOD$_5$ between NIR predicted and measured values.**

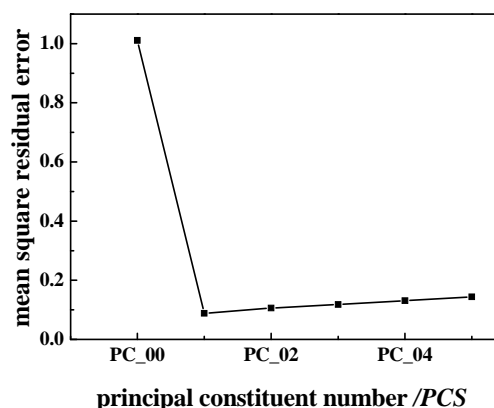Figure 4. The changes of residual variance with PCs.

Figure 5. The changes of residual variance with PCs.

3.5. Precision Test

Precision test has been made in this experiment for checking the stability of instrument and repeatability of samples' results. One sample was scanned 10 times, So, 10 NIR spectra were got, and then these 10 spectra were predicted by the model built already. RSD (n=10) of prediction (BOD_5 and COD) are 1.48% and 1.66%, respectively, the precision is good enough. The result indicates that the repeatability of samples' determination is very good.

The result indicates that the prediction effect of simultaneous determination about BOD_5 and COD by calibration model is very good. But temperature and turbidity maybe influence the prediction result in the actual experiment. Nonlinear problem should be noticed, only the linear correction method as PLS is hard to set a model that it meet requirements of analysis index. We could try some nonlinear correction method as artificial neural network method to compare with linear correction method as PLS. All the works above need further study.

4. References

[1] Chinese government standard GB11914-1989, "Determination of COD in water by dichromate titration method [S]."

[2] J. G. Zhan, G. Wei, and R. C Xiong, "Quick evaluation of chemical oxygen demand based on spectrophotometric and multi-linear analysis [J]," Journal of Beijing University of Chemical Technology (Natural Science Edition), Vol. 34, No. 7, pp. 389–392, 2007. (In Chinese).

[3] H. B. Yu, H. Wang, *et al.*, "Amperometric determination of chemical oxygen demand using boron-doped diamond (BDD) sensor [J]," Electrochemistry Communications, Vol. 9, No. 9, pp. 2280–2285, 2007.

[4] Kwok Nga-Yan, S. J. Dong, and W. H. Lo, "An optical biosensor for multi-sample determination of biochemical oxygen demand (BOD) [J]," Sensors and Actuators B: Chemical, Vol. 110, No. 2, pp. 289–298, 2005.

[5] D. M. Reynolds and S. R. Ahmad, "Rapid and direct determination of wastewater BOD values using a fluorescence technique [J]," Water Research, Vol. 31, No. 8, pp. 2012–2018, 1997.

[6] Y. L. Yan, "Basic and application of Near Infrared Spectra [M]," Beijing: China light industry publishing company, Vol. 3, 2005.

[7] Chinese government standard GB7488-1987, "Determination of BOD_5 in water by dilute and inoculation method [S]."

[8] L. Xu and X. G. Shao, "Chemomtrics [M]," Beijing: Science publishing company, Vol. 258, 2004.

[9] S. Weisberg, "Applied Linear Regression [M]," New York: John Wiley & Sons. Vol. 168, 1985.

Scientific
Research

Synthetic Detergents (Surfactants) and Organochlorine Pesticide Signatures in Surface Water and Groundwater of Greater Kolkata, India

Naresh C. GHOSE[1], Dipankar SAHA[2]*, Anjali GUPTA[3]

[1]*Department of Geology, Patna University, Patna, India*
[2]*Central Ground Water Board, Patna, India*
[3]*Department of Chemistry, B. S. College, Danapur, India*
E-mail: dsaha002@yahoo.com

Abstract

An assessment on the concentration of surfactants and pesticides of chlorinated hydrocarbon group in surface and groundwater, is made from Greater Kolkata located in the Western Ganga Delta, one of the largest urban agglomerate in Asia. Concentration of both anionic synthetic detergents and organochlorine pesticide residues analysed from 54 and 19 sampling stations covering groundwater and surface water sources respectively, are generally found to be within the tolerance limit for human consumption. The concentration of synthetic detergent ranges from 0.084 to 0.425mg/l. Residues of organochlorine pesticides are analysed from different sources like tanks, lakes, rivers and groundwater. Lindane (0.01-0.43µg/l) and DDT (0.03-0.65 µg/l) are the most widely detected pesticide residues. Howerer, the two have not exceeded the limits for drinking anywhere. High value of aldrin and dieldrin (0.9µg/l) is obtained in the river Hugli at Barakpur-Seoraphuli, 20 km north of Kolkata. Likewise high value of Heptachloreis detected in a canal water sample at Palta (0.05 µg/l), a suburban area. Seasonally, the pesticide concentration in surface water is maximum during winter due to their higher application and minimum during monsoon. In groundwater, however, this relationship is reverse due to higher infiltration of surface water during monsoon.

Keywords: Kolkata, Ganga Delta, Surface Water, Groundwater, Surfactants, Organochlorine Pesticides

1. Introduction

The synthetic detergents (or surfactants) and pesticides are the two most common group of chemical compounds that are increasingly being used in modern civilization. Surfactants are common contaminants of aquatic environments due to their large consumption in all types of washing and cleaning operations. Surfactants are chemical compounds that affects (usually reduces) surface tension when dissolved in water. As the production and human use of surfactants have increased manifolds in recent years, scientific studies have been intensified for better understanding on the transportation, toxicity and their chemical evolution process in aquatic environment.

Surfactants are synthetic compounds, characterised by a hydrophilic head and a lipophilic tail consisting of a C-based linear or branched chain. The synthetic detergents prepared from polymers of ethylene oxides are resistant to biological attack because of their (C-O-C) bonds. The ions being smaller, remain less affected by the filtering action of soil. The most frequently applied surfactants are sodium salts of high molecular weight such as alkyl sulphates or sulphonates (LAS or linear C12 alkyl- benzene sulphonate). Surfactants generally have high biodegradability and have a moderate toxicity for fish. The threshold value which can impair aquatic life is 3–12 mg/l for anionic detergent, 3–38 mg/l for non-ionic detergent, and 20mg/l for cationic detergent. In addition to affecting aquatic life, surfactants affect oxygen-turnover of water and reduce sedimentation process, and thus delaying water purification, particularly during aeration of waste water. Surfactants are also called methylene-blue-active substances (MBAS) because they produce colour change in aqueous solution of methylene blue dye.

The most widely used compound in detergent industry is sodium tri-polyphosphate (STP). Phosphates present in

STP create deleterious effect on environment. Increased amount of phosphate is responsible for formation of large amount of algae in water. Common sewage treatment processes applied in municipal and industrial water cannot completely remove phosphates and nitrates. The appearance of anion active material in water may be an indication of potential viral pollution.

Pesticides are important input to modern agriculture and also used in public health in controlling communicable disease. During the last couple of decades, the use of pesticides has dramatically increased in India. However, the average pesticide consumption in India is still one of the lowest in the world at 0.5 kg/hectare against 10.7 kg in Japan and 4.5 kg in the US, mainly because of poor awareness among farmers and high cost of pesticides (Associated Indian Chamber of Commerce and Industry, Mint news, June 2008). The production of pesticides has increased from 5,000 to 85,000 metric tons between the period 1958 and 2004 [1]. The toxicity of these compounds poses risk to human health, environment and to the organisms which may not be targeted by pesticides. The effect of pesticides and their mobility depend upon their chemical and physical properties, soil characteristics, groundwater infiltrations and vadose zone behaviour, vegetation and local weather conditions. They resist degradation by chemical, physical or biological means. The degradation of DDT in soil is 75 to 100% in 4 to 30 years [2].

Organochlorine pesticides or OCPs are susceptible for fixation through food chain and can significantly magnify the original concentration to end-user. OCPs are lipid soluble, and hence cumulative bio-accumulation in the body fat of mammals might pose potential health hazard in the long run [3]. Chronic exposure to OCPs may lead to several dysfunctions of human system like, leukaemia, cancer, damage of lever and reproductive system [4,5]. Though the OCPs are banned in developed countries, in several developing countries they are still in use, like DDT and HCH were used until recently in India for agriculture as well as sanitary purposes. Groundwater contamination by pesticides is an issue of grave concern, particularly where drinking water supply is dependent on aquifers. It is estimated that annually 260 million litres of industrial wastes, run off from the 6 million tons of fertilizers and 9000 tons of pesticides used in agriculture within the Ganga Basin enters into the river [6].

Studies on OCPs in the ground and surface waters of the alluvial plain of upper-and mid-Ganga basin though available [2,6–10], little is known from the delta region specially in and around Kolkata, a large metropolis, known for numerous manufacturing industries, and a hinterland for paddy and cash crop cultivation in the Eastern India. The present investigation aims to make a quantitative evaluation of the anionic surfactants and OCP residues in surface water and groundwater sources, viz., the river Hugli and its tributary, ponds, lakes, dug wells, hand pumps and bore wells, from Kolkata urban and its surrounding areas. The data presents an account of the level of concentration of the twin scourge of man made chemical hazard in a large metropolitan town and its neighbouring area along the river Hugli.

2. Study Area

The study area covers 1246 sq. km of Kolkata Metropolitan District (KMD) and adjoining Howrah, Hugli and 24 Paraganas (North & South) districts, located on either side of the river Hugli and a few moribund tributaries like Saraswati (Figure 1). The population of Kolkata metropolitan area is 13.2 million (Govt. of India 2001). Situated at 130 km up the estuary of the river Hugli, the KMD is in the midst of intense agricultural activity thriving on the fertile tract of western part of the Ganga Delta in West Bengal state in India. The area represents a typical riverine tract surrounded by marshes, tidal creeks, mangrove, swamps and wetlands. The easterly flowing river Ganga swerves southward around the hill ranges of Rajmahal Flow (basalts, Lower Cretaceous) and bifurcates into two streams (Figure 1, inset), the south-easterly flowing Padma enters into Bangladesh and southerly flowing Bhagirathi flows down the Indian territory. The lower tidal reaches of the Bhagirathi is known as the Hugli River, which forms the life-line of KMD. The area receives an annual average rainfall of 1633.6 mm, 75% of which is contributed by southwest monsoon between June and September. Paddy is the main crop followed by potato and vegetables. Three crops are grown in the region, viz., monsoon (June to September), winter (October to February) and summer (March to May), with a cropping intensity of 162 % (Govt of West Bengal 2008).

The study area forms a part of Lower Deltaic Plain of the Ganga river system, lying on both sides of the river Hugli (Figure 1, inset). Fluviatile sediments of Quaternary age made up of a succession of clay, sandy clay, silt and silty clay with occasional gravels underlies KMD [11–13]. The lithological sequence of the Kolkata Metropolitan Area and eastern part of Howrah district reveals a laterally persistent clay/sandy clay bed at the top of the sequence, having a thickness of 13.5 to 54.0 m (Figure 2) [14]. Thin fine sand lenses often interrupt the top clay/sandy clay sequence. Another prominent clay bed occurs between 300 m and 415 m below ground level (bgl). The sequence between the top and the basal clay is marked predominantly by sand of various size grades with occasional gravel and clay beds. Groundwater in this part occurs under semi-confined condition. The
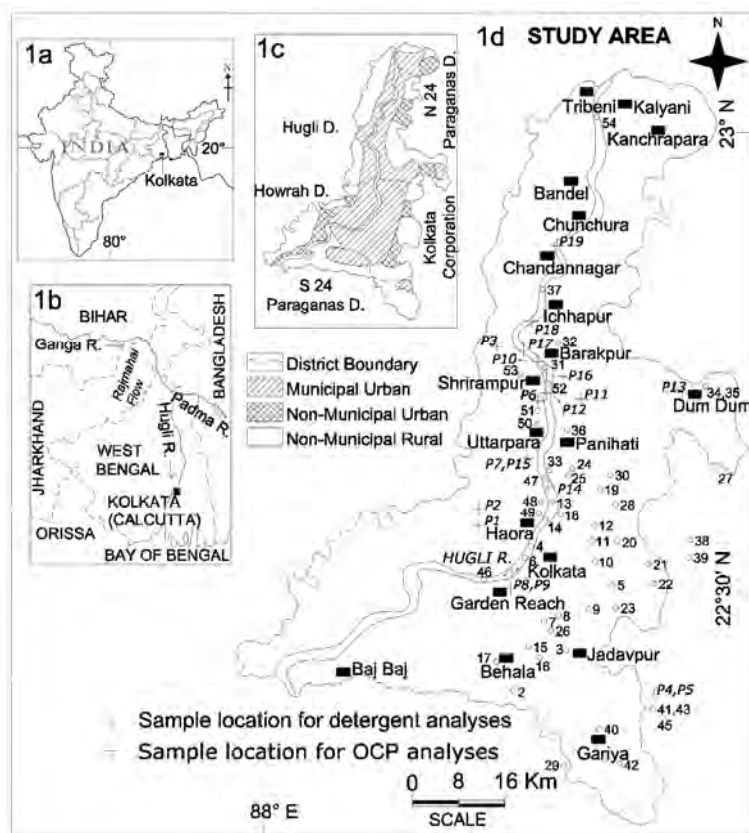
Figure 1. Location map of the study area. a) India, showing the location of West Bengal State. b) Bifurcation of the Ganga to southerly flowing Hugli River in India and easterly flowing Padma River in Bangladesh. c) Municipal and non-municipal areas showing the parts of the districts (Hugli, Howrah, North & South 24 paraganas, Nadia) and Kolkata Corporation falling in KMD. d) Sample stations for organochlorine pesticides (cross) and anionic surfactants (circle) in KMD.
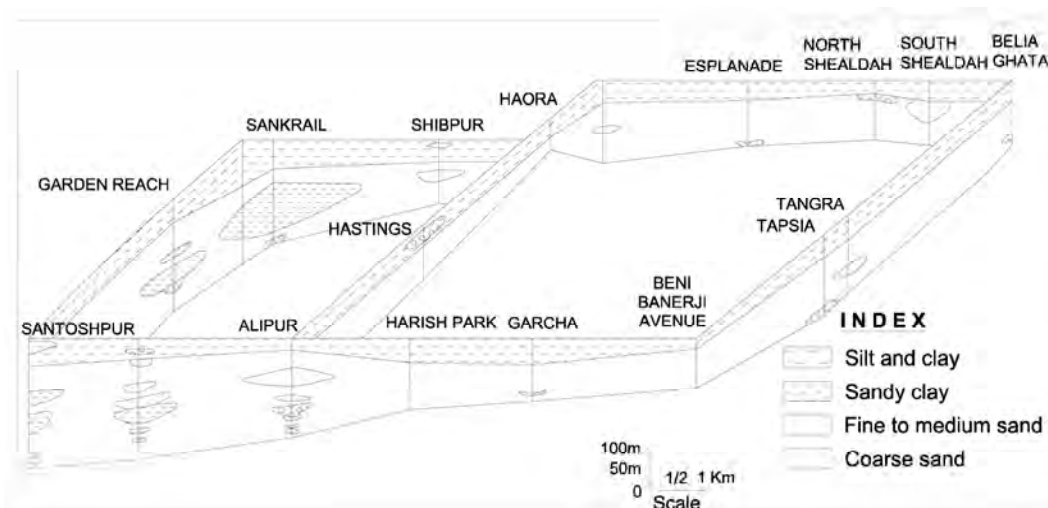

Figure 2. Fence diagram showing aquifer distribution of Kolkata urban area (after Biswas [14]).

principal productive zones usually tapped for municipal water supply ranges from 80 m to 160 m bgl. The hydraulic head of this aquifer varies from 0.5-1.0 m above mean sea level in the northern part of KMD which gradually goes deeper towards south. A groundwater trough is formed below the Kolkata metropolitan area, where the

hydraulic head lies 10 m below msl as a result of overdraft to the tune of 73.5 million litre/day [13].

3. Chemical Quality of Groundwater

Wide variation in chemical quality of groundwater is observed in KMD within the studied depth of 200 m bgl. Analysis of chemical quality of groundwater was beyond the scope of this research. Published literature reveals that groundwater in greater Kolkata is mildly alkaline (pH 6.9-9.0), with total dissolved solids ranging from 368 to 3200 mg/l, with an average of 1130 mg/l [15]. The anion chemistry is dominated by Cl and HCO_3, both showing wide variation between 21–1320 mg/l and 210–666 mg/l, respectively. Sulphate ranges between 0.2 and 140.7 mg/l. Among cations, Na shows wider variation (42–640 mg/l) than Ca (27–269 mg/l). Analyses of groundwater quality through Piper diagram (Figure 3) [13] show; 1) equal dominance of strong (Cl, SO_4) and weak (HCO_3) acids, and 2) marginal dominance of alkalis (Na, K) over alkaline earth (Ca, Mg). A study involving detailed analyses of some toxic trace elements, viz. Cu, Pb, Zn, Cd, As, Hg and Se in groundwater of KMD [15], indicated that the level of concentration of these elements are less in deeper aquifer in comparison to the shallow aquifer. In general, the concentrations remain within the permissible limits for drinking use [16], except a few localised pockets where Pb, Cu, Cd and As have exceeded the limits because of infiltration from industrial effluents.
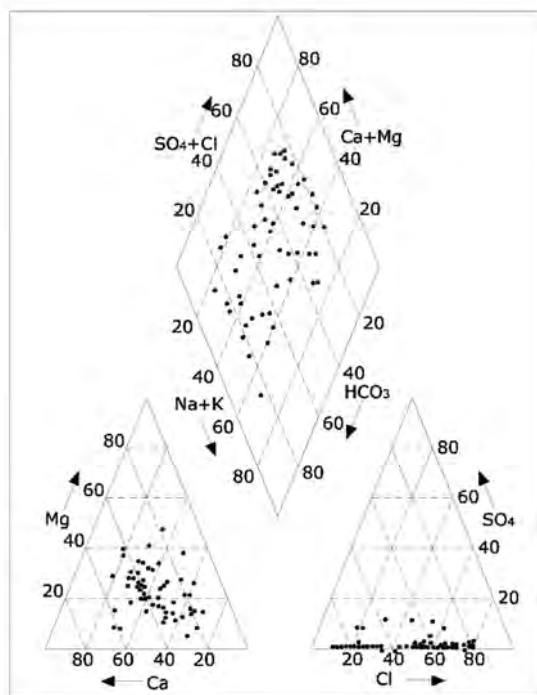

Figure 3. Piper diagram showing groundwater quality in Kolkata Municipal area (after Sikdar *et al*. 2001).

4. Sample Collection

Water samples have been collected from different sources representing both from surface water and groundwater sources. The groundwater samples are collected from hand pumps and tube wells tapping aquifers between 40 m and 180 m bgl. The sample have been collected from the outlets after flushing water for 10 minutes in case of hand pump, and 5 minutes in case of bore well, in order to obtain fresh aquifer water.

For anionic surfactant analysis, 54 samples have been collected (groundwater-27, tanks and other surface water accumulations-16, and river-11) during November (post-monsoon period) (Figure 1, Table 3). Samples for organochlorine pesticides or OCPs have been collected separately from 19 localities (Figure 1, Table 4). To study the seasonal variation in OCP concentrations, repeat samplings are made (except at Palta and Konnagar) in the month of May (pre-monsoon), August (monsoon) and post-monsoon (November) periods. Out of 52 samples collected for OCP investigations, 23 samples are from Hugli River between Chandannagar and Garden Reach, a stretch of about 40 km, representing intense industrial activity (e.g. jute, chemical, automobile, steel, ammunition etc.) on either side of the river (Figure 1). Rest of the water samples have been collected from tanks, treated water from effluent treatment plant, a tributary of Hugli (Saraswati) and groundwater (collected from hand pumps).

For pesticide residue analysis sampling bottles made up of high quality dark glass with teflon stopper are used. Plastic or polyethylene containers are avoided as the pesticides present in water samples is likely to be adsorbed on inner walls of the bottles. Similar containers are used for synthetic detergent analysis as well. The unfiltered water samples for OCP analysis are processed following the standard method [17,18]. Locations of samples are indicated in Figure 1.

5. Analytical Methods

5.1. Anionic Synthetic Detergent

Methylene blue, a redox indicator forms a blue salt or ion pair when methylene blue, a cationic dye, reacts with any anionic surfactant, including linear alkyl sulphonate (LAS). The "Methylene blue" complex is extracted with chloroform and the intensity of the blue colour complex is measured at 652 nm using Varian Spectrophotometer, model DMS (Table 1). The reagents used are 1) stock linear alkyl-benzene sulphonate- 1ml = 1000 µg of the solution, 2) standard solution-0.01 mg/l prepared by diluting 10 ml stock solution (1000 mg/l) to 1:l water, 3) chloroform AR, 4) methylene blue solution (0.1%) AR, 5) phenolphthalein, and 6) concentrated sulphuric acid.

Table 1. Methods adopted, instruments used and detection limits for surfactants and OCP analysis.

Sl No	Parameters	Method	Instruments used	Detection limits (mg/l/µg/l)
1	Anionic surfactants	Ion-Pair method	Spectrophotometer	0.01 mg/l
2	Aldrin	Extraction method with n-Hexane	GLC	0.05 µg/l
3	Dieldrin	-do-	-do-	1.0 µg/l
4	Haptachlor	-do-	-do-	0.05 µg/l
5	P,P'-DDE:DDT	-do-	-do-	0.1 µg/l
6	P,P'-TDD (total)	-do-	-do-	0.1 µg/l
7	P,P'-DDT (isomer)	-do-	-do-	0.1 µg/l
8	HCH (lindane)	-do-	-do-	0.1 µg/l

The intensity of the colour is proportional to the quantity of 'MBAS' (methylene blue active substance) present in the sample, the concentration of which in water is calculated from the calibration curve [17]. Sensitivity-0.025 mg MBAS/litre calculated as LAS. The optimal conditions of analytical method and detection limits are given in Table 1.

5.2. Organochlorine Pesticides

OCP residues are extracted from water samples after treating with acetonitrile. Resulting solution has been extracted several times with n-hexane. The hexane extract is filtered through anhydrous sodium sulphate and subjected to Gas Liquid Chromatography (GLC, model 5700, Nucon) analysis [19]. All reagents used are of analytical grade. Nitrogen gas is employed as the carrier gas (flow rate 50 ml/min) and makeup gas, and the injection technique has been in split mode. Analysis has been done at the linearity region of the detector for particular constituent. The GLC conditions adopted in the laboratory are–1) oven temperature-195°C, 2) injector temperature-235°C, and 3) detector temperature-245°C. Detection limits of different OCPs are given in Table 1 and their retention time in Table 2.

6. Results and Discussions

6.1. Synthetic Detergents

Higher values of surfactant cause skin irritation [20]. The threshold value that can impair aquatic life is 3-12 mg/l. The range and average (parenthesis) values of MBAS, calculated as linear alkyle sulfonate, for surface and groundwater are, 0.025-0.425 (0.149) mg/l and 0.015-0.084 (0.032) mg/l (Table 3). Sector-wise, the surfactant values in the groundwater and surface waters are 0.015-0.052 (0.29) mg/l and 0.25-0.425 (0.148) mg/l for Kolkata (urban); 0.15-0.84 (0.42) mg/l and 0.028-0.075 (0.059) mg/l for 24 Paraganas (North and South) districts in the south (representing semi-urban and rural); and 0.018-0.035 (0.025) mg/l and 0.07-0.125

Table 2. Retention time of various pesticide residue.

Pesticides	Retention time (minute)
ά–HCH	1.31
β–HCH	2.07
γ–HCH (lindane)	1.72
S–HCH	2.33
pp'–DDE	6.82
pp–DDT: DDT	13.08
pp'–TDE: (total)	10.55
pp'–DDT: (isomers)	12.77
Op'–DDT:	9.68
Aldrin	2.88
op'–Dicofol	4.02
pp'–Dicofol	4.08
Heptachlore	4.08

(0.90) mg/l for Howrah and Hugli districts in the north (semi-urban) respectively (Figure 1, Table 3).

Highest concentration of surfactants is noted in surface water from the Hugli River, near Howrah Bridge (0.425 mg/l), and lowest in the groundwater at Chetla in central Kolkata (0.015 mg/l), drawn from a hand pump reaching to a depth of 75m (Table 3). As expected, groundwater in general, shows lower concentration of surfactants in comparison to surface water. Maximum concentration of surfactant in groundwater is recorded at Mathurapur (0.084 mg/l) from a rural area in the southernmost part of South 24 Paraganas (Table 3, Figure 1). The study reveals a range of surfactant value from 0.013 to 0.425 (0.118 mg/l) in the river Hugli, and 0.017 to 0.250 (0.09) mg/l, in the ponds and tanks. A desirable limit of 0.2 mg/l and maximum permissible limit as 1.0 mg/l of surfactant in water have been adopted in India (Bureau of Indian Standards 1991). The anionic surfactant values in surface and groundwater of Calcutta Metropolitan District (CMD) exceed the desirable limit at some places; however, they are well within the maximum permissible limit for drinking use. Lower concentration of anionic detergent in groundwater (av. 0.035 mg/l) in comparison to river waters or tanks may possibly be due to low hydraulic conductivity of the top clay/sandy clay sequence, which is regionally behaving as an aquitard.

Table 3. Synthetic detergent concentration (mg/l) of surface water and groundwater in Greater kolkata.

Sl No.	Sample locality	Water source	Surfactant concentration (mg/l)
1	Rash Behari Avenue	Groundwater[1]	0.018
2	Thakur Pukur	Tank water[2]	0.250
3	Jadavpur	Tank water[2]	0.028
4	Near Howrah bridge	Hugli River water[3]	0.425
5	Subash Sarobar, Beleghata	Tank water[2]	0.205
6	Babu ghat (Central Kolkata)	Hugli River water[3]	0.185
7	Rabindra Sarobar, south Kolkata	Tank water[2]	0.200
8	Kalighat	Tank water[2]	0.150
9	Bondal Road	Tank water[2]	0.020
10	Park Street	Groundwater[1]	0.018
11	College Square	Tank water[2]	0.105
12	Hedua, near Beedon Street	Tank water[2]	0.094
13	Beniatola Ghat	Hugli River water[3]	0.025
14	Nimtola Ghat (north Kolkata)	Hugli River water[3]	0.034
15	Tollyganj	Groundwater[1]	0.035
16	Lake Gardens	Groundwater[1]	0.027
17	Behala	Groundwater[1]	0.025
18	Bag Bazar (Kasi Mitra Ghat)	Hugli River water[3]	0.165
19	Belgachia	Groundwater[1]	0.022
20	Chitpur	Groundwater[1]	0.022
21	Tiljola	Groundwater[1]	0.022
22	Dhapa (site of municipal waste disposal)	Groundwater[2]	0.052
23	Park Circus	Groundwater[1]	0.028
24	Bowbazar	Groundwater[1]	0.039
25	Beniapukur	Groundwater[1]	0.020
26	Chetla	Groundwater[1]	0.015
27	Baguihati	Tank water[2]	0.017
28	Raja Bajar	Groundwater[1]	0.045
29	Bansdroni	Groundwater[1]	0.045
30	Coshipur	Groundwater[1]	0.032
31	Barrackpur	Hugli River water[3]	0.053
32	Palta	Canal water[2]	0.073
33	Dakhineswar	Tank water[2]	0.064
34	Dum Dum	Tank water[2]	0.075
35	Dum Dum	Groundwater[1]	0.043
36	Belgharia (near Texmaco)	Tank water[2]	0.038
37	Naihati	Hugli River water[3]	0.075
38	Salt Lake City (Sech Bhawan)	Groundwater[1]	0.015
39	Salt Lake City (Tank No.13)	Groundwater[1]	0.025
40	Garia	Groundwater[1]	0.028
41	Sonarpur	Groundwater[1]	0.065
42	Narendrapur (R.K. Mission)	Tank water[2]	0.028
43	Sonarpur	Tank water[2]	0.060
44	Mathurapur	Groundwater[1]	0.084
45	Sonarpur	Groundwater[1]	0.058
46	Garden Reach	Hugli River water[3]	0.034
47	Balikhal	Tributary of Hugli River (carries domestic sewage)	0.080
48	Belur	Groundwater[1]	0.022
49	Lilua	Groundwater[1]	0.018
50	Uttrapara	Groundwater[1]	0.070
51	Rishra	Groundwater[1]	0.035
52	Srirampur	Hugli River water[3]	0.085
53	Seoraphuli	Groundwater[1]	0.025
54	Bansberia	Hugli River water[3]	0.013

[1]Drinking use, [2]Community use other than drinking, [3]Used for drinking after treatment. Analyst: T. K. Chatterjee

Various proposals have been made to replace phosphates in detergents by other substances, viz., citric acid, nitrilotriacetic acid (NTA), EDTA, zeolite (sodium alumino-silicate) etc. Although toxicological data for NTA are incomplete, they indicate a potential human hazard because NTA alters the toxicity of metals by affecting their entry in body, as well as their distribution and concentration in the tissues [21]. Pending further toxicological evaluation, the US government has recommended that NTA detergents should not be used.

6.2. Organochlorine Pesticide

The OCPs used in agriculture or in urban areas are transported from their target site and enter into aquatic environment via infiltration, air-drift and surface run-off, affecting the eco-systems [22]. The end destination of OCPs in aquatic system is groundwater, through percolation through the vedose zone, where their transformation products may remain for years [23]. The recommended total pesticide level for drinking water to be less than 0.5µg/l, and individual pesticide not more than 0.1µg/l [24]. The analytical results of the presence of OCP both in surface water and groundwater in the study area are given in Table 4. The pesticide residues detected are lindane, other isomers of HCH, aldrin and dieldrine, dicofel, heptachlor and DDT (total isomers). Among the various pesticide groups-lindane, HCH, aldrin and DDT are detected in the Hugli River stretching between Chandannagar and Garden Reach. Similar accumulation of pesticide residues was noticed in other surface water bodies like tanks, lakes and in a tributary (Saraswati river). Interestingly, heptachlor is not detected in the Hugli River. Only lindane is detected in surface water from Baksara and Andul, whereas at Sonarpur and Uttarpara a wide range of pesticide residues has been recorded (Table 4). Groundwater samples collected from two localities, viz., Sonarpur and Palta, revealed presence of all the pesticide groups under investigation, but in lesser quantity.

γ-HCH, also called as lindane, is found to be most commonly detected pesticide in all types of water sources studied. Presence of lindane indicates its widespread use in agriculture, because of its effectiveness, long-lasting impact, and its use for human vector control. Production of lindane is banned in many countries because of its potential health hazards, but China, Romania and India is still producing [25]. In India, 40 Metric Ton of lindane was produced in 1996-97 [26]. The agricultural use of lindane is diminishing, but no authentic data is available on present level of production. Higher incidence of lindane residue from the groundwater has been reported from the upper part of the Ganga basin [2,7,9]. Heptachlor has been detected rarely, indicating its limited application.

The tolerance limit of some individual pesticide residue for human consumption is: γ-HCH (lindane)-2.0 µg/l, aldrin and dieldrin-0.03 µg/l, heptachlor/ heptachlor epoxide-0.03 µg/l and DDT (total isomers) -2.0 µg/l [21]. The concentration of lindane in surface water or groundwater always remained within tolerable limit. The concentration of aldrin and dieldrin are recorded beyond the permissible limit in the surface waters from the Hugli River at Seoraphuli and Barrackpur (serial nos.10, 17 Table 4).

DDT is widely detected pesticide from different types of sources after lindane. Bioaccumulation potential of DDT is known for its high fat solubility. Its presence in lower levels passes into food chain (soil-water-plant-man). DDT concentration has not exceeded the permissible limit [21], highest concentration being 1.4 µg/l, is found at Sonarpur, a rural area in the south 24 Paraganas district, in winter season. The reason may be accumulation of surface run-off into the tank (pond) from the adjoining localities. Aldrin and dieldrine remain within permissible limit of 0.03 µg/l, except at the Hugli River water at Seoraphuli (sample no 17). Heptachlor and dicofel have been detected in a few localities. In canal water sample at Palta (Sample no 11) heptachlor has exceeded the limit for drinking use. The Hugli River water has been found to be free from these two pesticides.

The water supply in the study area is largely dependent on treated surface water from the Hugli River. Groundwater drawn by deep tube wells and hand pumps are also used for drinking, particularly the outskirts of Kolkata, Hugli and Howra districts, without treatment. The groundwater samples analysed essentially represent drinking water source, except sample no 22, which is a hand pump used other than drinking (Table 3). The tanks are for community used for ablution and drinking for cattle. No water source used for drinking was found to be contaminated.

In surface waters, the pesticide concentrations are found maximum in winter due to its greater application, and minimum in monsoon (rainy season) due to its limited use and dilution. Again their abundance showed marginally higher in summer (May-June) than in the monsoon (June-September). In contrast, the seasonal variation of OCPs in the groundwater showed highest concentration during monsoon and lowest in the summer in conformity with the observations made elsewhere (viz. Kanpur and Unnao) from the upper Ganga basin [2,9]. This feature may be related to infiltration of surface water charged with pesticides to aquifer system during monsoon. Detection of lindane, HCH, eldrine and dieldrine, heptachlor and DDT in the groundwater supports the above contention. These observations are in contrast from the findings of toxic trace elements (viz. Cu, Pb, Zn, Cd, As, Hg and Se) in the groundwater of Kolkata urban area, where the level of concentrations are maximum in

Table 4. Range of pesticide concentration of water in summer, winter and rainy seasons in Greater Kolkata (µg/l). (Figures in brackets indicate mean value).

Sl No	Location	No. of sample	Source	Lindane	Other isomer of HCH	Aldrin and dieldrin	Heptachlor	Dicofel	DDT (total isomers)
1	Baksara, Howrah	3	TW	0.28-0.3 (0.29)	-nd-	-nd-	-nd-	-nd-	-nd-
2	Andul, Howrah	3	TW	0.35-0.37 (0.36)	-nd-	-nd-	-nd-	-nd-	-nd-
3	Saraswati river	3	RW	-nd-	-nd-	-nd-	-nd-	0.02-0.03(.02)	-nd-
4	Sonarpur	3	GW	-nd-	-nd-	0.01-0.03 (0.02)	-nd-	0.02-0.03 (.02)	-nd-
5	Sonarpur	3	TW	0.05-0.1 (0.08)	2.1-9.9 (5.5)	-nd-	-nd-	3.03-14.03 (8.2)	0.8-1.4 (1.07)
6	Konnagar, Hugli	1	TW		0.18	-nd-	-nd-	37.42	0.01
7	Balikhal, Howrah	3	RW	0.04-0.05 (0.045)	0.02-0.04 (0.03)	0.02-0.03 (0.02)	-nd-	-nd-	0.04-.08 (0.06)
8	Garden Reach	3	RW		0.12-0.2 (0.15)	0.01-0.03 (0.02)	-nd-	-nd-	0.03-0.1 (0.07)
9	Garden Reach	3	TW	0.01-0.07 (0.43)	0.07-0.14 (0.1)	0.01-0.01 (0.01)	-nd-	-nd-	0.04-0.12 (0.08)
10	Barackpur	3	RW	0.22-0.35 (0.3)	5.4-6.65 (6.01)	0.7-0.9 (0.8)	-nd-	-nd-	0.05-0.12 (0.09)
11	Palta	1	CW	0.43	7.82	-nd-	0.05	-nd-	0.11
12	Palta	2	GW	0.1-0.3 (0.2)	-nd-	-nd-	0.01-0.01 (0-01)	-nd-	0.3-0.5 (0.02)
13	Dumdum	3	TW	-nd-	-nd-	0.01-0.03 (0.02)	-nd-	-nd-	-nd-
14	Dakhineswar	3	RW	0.05-0.1 (0.077)	0.1-0.2 (0.15)	0.01-0.03 (0.02)	-nd-	-nd-	0.5-0.65 (0.56)
15	Uttarpara	3	RW	0.03-0.08 (0.06)	0.02-0.06 (0.04)	0.01-0.02 (0.015)	-nd-	-nd-	0.2-0.5 (0.33)
16	Srirampur	3	RW	0.02-0.05 (0.033)	0.02-0.05 (0.033)	0.01-0.03 (0.021)	-nd-	-nd-	0.2-0.4 (0.3)
17	Seoraphuli	3	RW	0.25-0.5 (0.38)	4.2-5.5 (4.9)	0.02-0.04 (0.03)	-nd-	-nd-	0.1-0.2 (0.15)
18	Kamarhati	3	RW	0.01-0.04 (0.027)	-nd-	0.01-0.025 (0.018)	-nd-	-nd-	0.01-0.2 (0.18)
19	Chandannagar	3	RW	0.02-0.05 (0.033)	0.2-0.3 (0.25)	0.01-0.02 (0.018)	-nd-	-nd-	0.3-0.6 (0.47)

TW–Tank water, RW–River water, CW–Canal water, GW- Groundwater, TW–Treated water of effluent plant, nd- Not detected

summer and minimum in monsoon due to dilution [15].

7. Conclusions and Recommendations

Anionic synthetic detergent is detected in all surface water and groundwater samples. In no samples, however, it has exceeded the guideline for drinking use (1.0 mg/l) prescribed by the Bureau of Indian Standards (1991). Relatively higher load in the Hugli River (0.013-0.425 mg/l) indicates that the river receives untreated domestic sewage from the urban centres located along the banks. The tanks and ponds are showing higher values than groundwater as they are used for ablution and washing of clothes.

The study reveals that Lindane (0.01-0.37 µg/l) is the most commonly detected pesticides in all types of sources, followed by DDT (0.01-1.4 µg/l) indicating their wide use for agriculture and human vector control. Nowhere the value exceeded the guidelines for drinking use prescribed by the World Health Organisation [21]. Aldrin and di-aldrin are detected both in the surface water and groundwater. The values remained beyond the limit prescribed for drinking use from the Hugli River at

Seoraphuli and Barrackpore. These two urban centres face each other across the river, 20 km north of Kolkata, dotted with a number of chemical, jute and liquor factories. The toxic effect of pesticides even present in traces on prolonged consumption is easily concentrated through the food chain, which should not be underestimated. The level of concentration of OCPs in water bodies in most of the area surveyed though remained within the limits prescribed by the World Health Organisation [21], their use should be controlled and replaced by suitable formulation of short-lived pesticides like organophosphates and carbamates that are relatively expensive, and regularly monitored as a measure for preventing health problems.

Groundwater in Greater Kolkata is safe considering the synthetic anionic detergents and OCPs. Relatively high load of synthetic detergent and OCPs like aldrin and dieldrine in patches of the Hugli River indicates that optimum care should be taken for treatment of the river water before supplying. Detection of these constituents in a few hand pump samples indicate seepage from surface sources through the top fine grained layer where it is sandy or silty, rendering localised higher vertical per

meability.

9. References

[1] P. K. Gupta, "Pesticide Exposure–Indian Scene," El-Sevier Ireland Ltd, 2004.

[2] N. Sankaramakrishnan, A. K. Sharma and R. Sanghi, "Organochlorine and organophosphorous pesticides residues in groundwater and surface waters of Kanpur," Uttar Pradesh, India. Environment International, Vol. 31, pp. 113–120, 2005.

[3] IARC, "Occupational exposure in insecticide application, and some pesticides," International Agency for Research on Cancer, Lyon, (IARC monographs on the evaluation of Carcinogenic Risks to humans, v-53), 1991.

[4] V. K. Dua, R. Kumari, V. P. Sharma and S. K. Subbarao, "Organochlorine residues in human blood from Nainital (UP)," India. Bull Environ Contam Toxicol, Vol. 67, pp. 42–45, 2001.

[5] UNEP, "Global report on regionally based assessment of persistent toxic substances," UNEP Chemicals. Geneva, Switzarland, 2003.

[6] K. P. Singh, A. Malik, D. Mohan and S. Sinha, "Persistant organochlorine pesticide residue in alluvial groundwater aquifers of Ganga Plain," India. Bull Env Cont Toxico, 2005.

[7] S. P. Mohapatra, M. Kumar, V. T. Gajbhiye and N. P. Agnihotri, "Groundwater contamination by organochlorine insecticide residues in a rural area in the Indo-Gangetic Plain," Environ Mon Assess, Vol. 35, pp. 155–164, 1995.

[8] S. Kumar, K. P. Singh and K. Gopal, "Organochlorine residues in rural drinking water sources of Northern and North Eastern India," J Envirnon Sci Health, Vol. 30, pp. 1211–1222, 1995.

[9] R. Sanghi and K. S. Sasi, "Pesticides and heavy metals in agricultural soil of Kanpur," India. Bull Environ Contam Toxicol, Vol. 67, pp. 446–454, 2001.

[10] R. P. Singh, "Comparison of organochlorine pesticide levels in soil and groundwater of Agra," India. Bull Envirno Contam Toxicol, Vol. 67, pp. 126–132, 2001.

[11] G. C. Chatterjee, A. B. Biswas, S. Basu and B. N. Niyogi, "Geology and groundwater resources of the greater Calcutta Metropolitan area," West Bengal, Bull Geol Surv India, Ser B No21, pp.150, 1964.

[12] A. B. Biswas and A. K. Saha, "Environmental hazards of the recession of piezometric surface of groundwater under Calcutta," Proc. Ind Nat Sc Aca, Vol. 51, No. 3, pp. 610–621, 1985.

[13] P. K Sikdar, "Geology of the Quaternary aquifers of the twin city of Calcutta-Howra," Jour Geol Soc Ind, Vol. 56, pp. 169–181, 2001.

[14] A. B. Biswas, "Water supply in Calcutta 'Calcutta, the Live City' v.2, ed. Sukanata Choudhury," Oxford University Press, Kolkata, pp. 160–166, 1990.

[15] N. C Ghose, T. K. Chatterjee, A. Gupta and Saha. Dipankar "Heavy metal concentration in groundwater of Greater Calcutta (Kolkata)," West Bengal, India. Indian Jour. Geol. Vol. 73, pp. 55–56, 2001.

[16] BIS, "Drinking water quality standards. Bureau of Indian Standards," No. 10500, New Delhi, India, 1991.

[17] APHA, "Standard method for the examination of water and wastewater," American Public Health Association, New York, 1984.

[18] AOAC, "Official methods of analysis of the association of official analytical chemists. 16th Ed. Cunniff P (ed.)," 1995.

[19] W. Fresenius, K. E. Quentime and W. Schneider, "Water analysis," Springer Verlag, Berlin, pp. 804, 1988.

[20] H. P. Ciuetha and K. T. Dood, "The determination of the irritancy potential of surfactants using various methods of assessment," Drug Chem. Toxocol, Vol. 3, pp. 305–324, 1978.

[21] WHO, "Drinking water standards," World Health Organisation, Geneva, 1993.

[22] G. M. Rand, P.G. Wells and L. S. McLarti, "Introduction to acquatic toxicology," In. Rand GM ed., Tailor & Francis, 1995.

[23] A. C. Belfroid, M. van Drunen, M. A. Beck, S. M. Schrap, C. A. M. van Gestel and B. van Hattum, "Relative risk of transformation products of pesticides for aquatic ecosystem," Sci Total Environ, Vol. 222, pp.167–183, 1998.

[24] EEC directive, Europian Economic Commission directive 3-76/464/EEC; EUROPA, 1980.

[25] M. Dutta and K. S. Schafer, Lindane, International POP Estimation Network," www.ipen.org, 2003.

[26] S. C. Mathur, "Pesticide industry in India," Pestic Inf XXIII, Vol. 4, pp. 17–29, 1998.

Call For Papers

IEEE   EMB   iCBBE

Environmental Pollution and Public Health (EPPH2010)
Special Track within iCBBE

环境污染与人类健康国际学术会议征文

June 21-23, 2010   Chengdu, China
http://www.icbbe.org/epph2010/

The International conference on Environmental Pollution and Public Health (EPPH2010), a special track within iCBBE 2010, will be held from June 21st to 23rd, 2010 in Chengdu, China. You are invited to submit papers in all areas of environmental pollution and related health problems. As we did in EPPH 2009 and 2008, all papers accepted will be included in IEEE Xplore and cited by Ei Compendex and ISTP.

Topics

Water Quality and Public Health

- Purification of drinking-water supplies
- Treatment, disposal and discharge of wastewater
- New wastewater treatment technologies
- Methods of monitoring water quality
- Modeling and measuring of water pollution
- New water purification technologies
- Ground water pollution control
- Water resources and quality assessment
- Water resource protection and sustainable use
- Hydrobiology and water pollution
- Other topics related to water pollution

Air Pollution and Public Health

- Effects of air pollution on public health
- Sources of air pollution
- Air pollution monitoring and modeling
- Air pollution prevention and control
- Urban/indoor air pollution and control
- Air quality measurement and management
- Global climate change and air pollution

Other Related Issues

- Chemical pollutants and its effects on health
- Land pollution and its effects on health
- Radiation safety in atomic industry
- Food and drug safety control
- Hazardous materials management
- Solid waste management
- Environmental toxicology
- Risk assessment of contaminated environments
- Ecosystem restoration
- Global climate changes and human health

Important Dates

- ◆ Paper Submission Due: Oct. 30, 2009
- ◆ Acceptance Notification: Dec. 31, 2009
- ◆ Conference: Jun. 21-23, 2010

Contact Information

Website: http://www.icbbe.org/epph2010/
E-mail: epph@icbbe.org

Journal of Water Resource and Protection (JWARP)
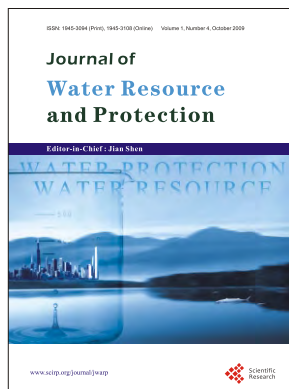
http://www.scirp.org/journal/jwarp

ISSN:1945-3094 (Print), 1945-3108 (Online)

JWARP is an international refereed journal dedicated to the latest advancement of water resource and protection. The goal of this journal is to keep a record of the state-of-the-art research and promote the research work in these fast moving areas.

Editor-in-Chief

Prof. Jian SHEN	College of William and Mary, USA

Editorial Board

Subject Coverage

This journal invites original research and review papers that address the following issues in water resource and protection. Topics of interest include, but are not limited to:

- Water resources and quality assessment
- Rivers, lakes and estuary systems
- Wastewater treatment and sludge biotreatment
- Water purification and water supply
- Water source protection and sustainable use
- Modeling, measuring and prediction of water pollution
- Ground water pollution control
- Reactions and degradation of wastewater contaminants
- Other topics about water pollution

We are also interested in short papers (letters) that clearly address a specific problem, and short survey or position papers that sketch the results or problems on a specific topic. Authors of selected short papers would be invited to write a regular paper on the same topic for future issues of the *JWARP*.

Notes for Intending Authors

Submitted papers should not have been previously published nor be currently under consideration for publication elsewhere. Paper submission will be handled electronically through the website. All papers are refereed through a peer review process. For more details about the submissions, please access the website.

Website and E-Mail

http://www.scirp.org/journal/jwarp   Email: jwarp@scirp.org

TABLE OF CONTENTS

Volume 1   Number 4   **October 2009**

9771945309004 04